2016

Degradation of Hexachlorobenzene, Pentachlorophenol and Pentachloroanisole using Activated Magnesium in an Acidified Ethanol/Ethyl Lactate Cosolvent System

Amel Garbou
University of Central Florida

DEGRADATION OF HEXACHLOROBENZENE, PENTACHLOROPHENOL AND PENTACHLOROANISOLE USING ACTIVATED MAGNESIUM IN AN ACIDIFIED ETHANOL/ETHYL LACTATE COSOLVENT SYSTEM

by

AMEL GARBOU
B.S. Garyounis University, Benghazi, Libya 1999
M.S. Garyounis University, Benghazi, Libya 2006
M.S. Florida Institute of Technology, Melbourne, Florida 2013

A dissertation submitted in partial fulfillment of the requirements
for the degree of the Doctor of Philosophy
in the Department of Chemistry
in the College of Sciences
at the University of Central Florida
Orlando, Florida

Fall Term
2016

Major Professor: Cherie L. Yestrebsky

ABSTRACT

For many centuries, chemists have dedicated many labor-intensive hours to improving the quality of life for mankind by developing synthetic methods for the production of compounds which fulfill the needs and meet the demands of society. However, the innovation of such compounds has frequently come at the cost of detrimental side-effects that do not always present themselves until many years, or even decades, following their initial application. Many compounds in this category come in the form of globally-distributed halogenated molecules which are toxic to many living organisms, susceptible to bioaccumulation and resistant to biodegradation processes. Such compounds are classified as persistent organic pollutants (POPs), and require safe, sustainable and economically viable remediation techniques due to their destructive effects on organisms and the environment In the work done for this dissertation study, three particular POPs, which can be further classified as Polychlorinated Aromatic Hydrocarbons (PCAHs), were studied: pentachlorophenol (PCP), hexachlorobenzene (HCB) and pentachloroanisole (PCA).

Chlorophenols are highly toxic compounds, usually found in soils, water, and effluents resulting from industrial activities. These environmentally-persistent compounds have been found to exhibit probable carcinogenic properties by the United States Environmental Protection Agency and the International Agency for Research on Cancer. The most toxic chlorophenol is PCP, which has a regulated maximum contaminant level (MCL) of 0.03 mg/L in water. Due to the high toxicity of PCP, it is necessary to treat water and soils that have tested positive for concentrations above the MCL. The aim of this work is to demonstrate the capabilities of using ball-milled zero-valent magnesium powder with various amendments, such as acetic acid (as an activator) and ethanol for the dechlorination of PCP. The dechlorination processes of these various combinations were

compared in an attempt to determine the most effective system for the degradation of PCP to phenol. Three systems with powerful capabilities of treatment were studied: ball-milled magnesium powder, ball-milled magnesium carbon (Mg/C), and mechanically alloyed magnesium with palladium. The results of these studies indicate that the most rapid and complete PCP dechlorination is achieved using mechanically alloyed Mg/Pd and a matrix consisting of at least 0.02 g Mg^0/mL of ethanol and 10 µL acetic acid/mL of ethanol, in which case 20 ng/µL of PCP was dechlorinated to phenol in approximately 15 min. with a carbon mass balance of 94.89%.

Hexachlorobenzene (HCB), like many chlorinated organic compounds, has accumulated in the environment from agricultural and industrial activity. After its introduction as a fungicide in 1945, the extensive use of this toxic chemical has instigated its infiltration into all food types. Prohibition from commercial use was enforced in the United States in 1966 due to animal, and possible human, carcinogenic effects. Because of the health risks and the adverse impact on various ecosystems, remediation of this contaminant is of vital concern. The objective of this study is to evaluate the proficiency of activated-magnesium metal in a protic solvent system to enhance the reductive dechlorination of HCB. Experimental results were compared with those predicted by quantum chemical calculations based on Density Functional Theory (DFT). Multivariate analysis detected complete degradation of HCB within 30 minutes, having a rate constant of 0.222 min^{-1}, at room temperature. Dechlorination was hypothesized to proceed via an ionic mechanism, and the main dechlorination pathways of HCB in 1:1 ethanol/ethyl lactate were HCB → PCBz → 1,2,4,5-TCB; 1,3,4,5-TCB → 1,2,4-TriCB; 1,3,5-TriCB → 1,4-DiCB; 1,3-DiCB. The direct relationship between the decreasing number of Cl substituents and dechlorination reaction kinetics agrees with the ΔG values predicted by the computational model. Therefore, the lowest energy pathway for C-

Cl bond dissociation predicted computationally agrees with the experimentally determined kinetic data. The experimental results from these studies have helped to improve our understanding of the dechlorination mechanisms, thereby offering insight into the most efficient pathways for remediation in the environment. This methodology shows promise for the development of an economic and sustainable field application for the treatment of other chlorinated aromatic compounds. In further work, developments will be made in the modification of the system to allow for the implemetation of field-scale applications.

Chloroanisoles are compounds that have similar properties to chlorophenols, but have a higher tendency to bioaccumulate and resist degradation because of their lipophilicity. They are not manufactured for commercial use, but exist in equilibrium with chlorophenols in the environment through biological transformation. Due to the toxicity of both compounds, a strategy for remediation is highly sought after. This study has served to develop an approach to meet the needs for this treatment, based on the successful treatment of PCPs using zero-valent magnesium (ZVMg) discussed in Chapter 1. The results of the method, which makes use of ZVMg/C in acidified ethanol, are compared for both target analytes. Both substrates were degraded to less-chlorinated byproducts within the first four hours; however PCP vanished at a faster rate with no detection at seven minutes. The more heavily-chlorinated byproducts showed faster degradation rates for both compounds, which also had 2,4-dichlorinated congeners in common as major byproducts. The mole balances of PCA and PCP were 92.6% and 94.8%, respectively. Further studies were done to enhance degradation kinetics by re-spiking with acetic acid after two weeks. Although complete degradation was still not achieved, a slight improvement was observed for both

compounds, more so with respect to PCP. Kinetic data followed pseudo first-order trends for the degradation of both PCA and PCP.

To my husband, Fawzi
Thank you so much for believing in me and supporting me through my journey as a chemistry Ph.D. student. I love you.

To my kids, Fatma, Saad and Mohamed
Thank you for your patience and understanding. You are a gift to me.

To my parents
Although you are far away now, the love you gave me and the lessons that I grew up with continue to guide me through life.

ACKNOWLEDGMENTS

Words cannot express the gratitude I have for Dr. Cherie Yestrebsky and Dr. Christian Clausen for giving me the opportunity to learn and develop my skills as a chemist in their group. I was searching for a new direction, after going through hardships at my previous institution. Thankfully, my scholarship allowed a transfer to a much better life at the University of Central Florida, where I was faced with a difficult decision between which faculty advisor I wanted to work for. After reviewing the type of work done in several different laboratories at UCF, I made a decision to work with Dr. Yestrebsky; a decision which turned out to be the best one. Dr. Y believed in me enough to provide financial support for my education when my country was going through political turmoil, resulting in the termination of my scholarship, which was what allowed me to be here in the first place. Not only did Dr. Y understand my situation, but she and Dr. Clausen spent hours helping me through the apprehension and anxiety of having to present my candidacy and seminar presentations in my second language. The pleasantly unexpected success of my academic presentations allowed me to achieve the dream of presenting my research at a national level, when my mentor provided me with the opportunity to present at two conferences, representing the Environmental Division of the American Chemical Society, with the honor of participating in the illustrious SciMix event. Furthermore, the work that I accomplished with my mentor is in the process of becoming reviewed for a publication in the Chemosphere Journal, of the Elsevier publishing house. With the friendship, and mentorship of Dr. Yestrebsky and Dr. Clausen, accomplishments beyond my wildest dreams became a reality.

In addition to my primary faculty advisors, I would also like to extend my gratitude to my committee members, Dr. Andrew Randall, Dr. Karin Chumbimuni-Torres and Dr. Shengli Zou.

Thank you for taking time out of your research to be a part of my committee by reviewing my dissertation and offer valuable suggestions from your years of infinite wisdom. Those to whom I owe an honorable mention are Dr. Shengli Zou and his graduate student Muqiong Liu (for their computational expertise and the work that they accomplished for this project), Dr. Matthew Rex (for always being around to offer training and troubleshooting, and fix any malfunctioning instrument), Nikia Toomey (for being a good friend in the Chemistry Building) and Dr. Pedro Patino, as well as the Chemistry Stockroom staff for always being friendly and helpful. Others who are deserving of my appreciation and gratitude, for being around to help me and show me kindness, are my colleagues from the Industrial Laboratory at the University of Central Florida: Dr. Simone Novaes-Card, Dr. Carolina Franco, Anthony "Tony" Pastore, Ashlyn Hale, Matt Rollando, Adibah Almutairi, Nicole Lapeyrouse, Dr. Fiona Zullo, Amal Mogharbel, Roaa Mogharbel, Charles Lewis and Thomas Shaw. And I would also like to give very special thanks to Patrick Cole, for spending significant time during his semesters to help me with my English, and making corrections to my writing. Finally, I would like to thank my wonderful family, including my husband Fawzi Almadani for standing by me during my education, and for helping me raise the children to whom I am also grateful for giving joy and meaning to my life. And last, but not least, I would to like extend my most heartfelt thanks to my parents, my brothers and my sisters in Libya for believing in me, and sending thoughtful wishes to me from overseas, in the midst of a tragic war, in which they fear for their lives every single day. You are very brave, and I cannot wait to see you again.

TABLE OF CONTENTS

LIST OF FIGURES xiv

LIST OF TABLES xviii

LIST OF ACRONYMS/ABBREVIATIONS xix

CHAPTER ONE: THREE MAGNESIUM TREATMENT SYSTEMS FOR THE DEGRADATION OF PENTACHLOROPHENOL 1

Introduction 1

Past and Current Remediation Options 3

Biodegradation 3

Reductive Dechlorination by Zero-valent Metals (ZVM) 4

Bimetallic Systems 5

ZVMg for Reductive Dechlorination 6

Ball-milling Procedure 7

Materials and Methods 8

Ball-milling Procedure 9

Experimental Procedure 9

Analysis 10

Dissertation Objectives 11

Results and Discussion 12

Degradation of PCP with ball-milled Mg, Mg/C, and mechanically alloyed Mg/Pd 12

Concentration of Dechlorination Byproducts and Mole Balance over Time..... 14

Previous Study for the Analysis of the Magnesium Particle Surface 17

Effect of the Addition of Acetic Acid on the Dechlorination Reaction..... 18

Degradation Kinetics 19

Conclusion 22

CHAPTER TWO: COMPUTATIONAL AND EXPERIMENTAL METHODS FOR THE DECHLORINATION OF HEXACHLOROBENZENE 24

Introduction..... 24

Regulatory History of HCB 24

Current Treatment for HCB Contaminated Materials..... 25

Degradation with Zero- valent Metal..... 26

Theoretical Modeling for the Dechlorination of HCB with Mg^0/C..... 29

Methods 29

Materials and Chemicals..... 29

Ball-milling Procedure..... 30

Experimental Procedure..... 31

Analysis..... 31

Computational Method 32

Dissertation Objectives 33
Results and Discussion 33
Degradation of HCB with Ball-milled ZVMg/C 33
Concentration of Dechlorination Byproducts and Mole Balance over Time 34
Degradation Kinetics 36
Prediction of the Degradation Pathways for Daughter Compounds by Quantum Chemical Calculation 37
Proposed Mechanism for Reductive Dechlorination Pathways 40
Conclusion 43
CHAPTER THREE: DEGRADATION COMPARISON OF PENTACHLOROPHENOL VERSUS PENTACHLOROANISOLE 45
Introduction 45
Background 45
Sources of PCA in the environment 46
Current Treatment for PCA Contaminated Materials 47
Results and Discussion 52
Degradation rate of PCA compared to PCP with ball-milled ZVMg/C 52
Concentration and mole balance for daughter compounds of PCP and PCA over time 52

Dechlorination of PCA by ball-milled ZVMg/C in acidified ethanol with periodic addition of acetic acid 56

Degradation of PCA with ZVMg/Pd system based on prior work with PCP 57

Degradation kinetics and suggested effect on the reaction mechanism 58

Conclusion 60

CHAPER FOUR: CONCLUSIONS 63

APPENDIX A: SUPPORTING INFORMATION FOR CHAPTER ONE 67

APPENDIX B: SUPPORTING INFORMATION FOR CHAPTER TWO 78

REFERENCES 98

LIST OF FIGURES

Figure 1: Respective degradation of PCP with the activated Mg, Mg/C, and mechanically alloyed Mg/Pd systems after 15 min of treatment in acidified ethanol. 13

Figure 2: Dechlorination of PCP with the activated (a) Mg, (b) Mg/C, (c) mechanically alloyed Mg/Pd reducing systems. Each data point represents the mean ± error calculated from duplicate samples. 15

Figure 3: Mole balance and percent chlorinated byproducts plus phenol for PCP/Mg systems after six days of degradation. No CPs were detected for Mg/Pd system. 16

Figure 4: Degradation of PCP by ball-milled ZVMg/C in acidified ethanol with addition of acetic acid after two weeks. 19

Figure 5: Pseudo-first-order kinetics plot for PCP degradation with activated magnesium reducing systems in ethanol. 21

Figure 6: Pseudo-first-order kinetics plot for phenol formation from dechlorination of CPs with activated magnesium reducing systems in ethanol. 22

Figure 7: Data corresponding to the degradation of HCB with the activated Mg/C system after 1 hr of treatment in 1:1 acidified ethanol:ethyl lactate. 34

Figure 8: Experimentally observed degradation byproducts of HCB with the activated Mg/C reducing system in 1:1 ethanol/ethyl lactate solvent. Each data point represents the mean±error calculated from duplicate samples. 35

Figure 9: Pseudo-first-order kinetics plot for HCB degradation with activated magnesium reducing systems in 1:1 ethanol/ethyl lactate co-solvent system. 37

Figure 10: Distribution of HCB and the degradation products with ZVMg/C in 1:1 ethanol:ethyl lactate solvent at room temperature. 39
Figure 11: Proposed hydrodechlorination mechanism for HCB by ZVMg/C in 1:1 ethanol:ethyl lactate solvent. 42
Figure 12: Energy scheme of the ionic mechanism for HCB dechlorination. 43
Figure 13: Examples of several sources of PCP in the environment. 47
Figure 14: PCA and PCP degradation with the activated ZVMg/C system after 6 hours of treatment in acidified ethanol. 54
Figure 15: Experimentally observed degradation byproducts of (a) PCA after two weeks of treatment, and (b) PCP after six days of treatment with the activated ZVMg/C reduction system in acidified ethanol. 55
Figure 16: Degradation of PCA and PCP by ball-milled ZVMg/C in acidified ethanol with addition of acetic acid after two weeks. 57
Figure 17: One week study for the degradation of PCA and PCP by ball-milled ZVMg/Pd in acidified ethanol. 58
Figure 18: Pseudo-first-order kinetics plot for PCA and PCP degradation with activated magnesium reducing systems in acidified ethanol. 59
Figure 19: Comparison studies of PCB-151 degradation using ball-milled ZVMg powder vs. ZVMg powder as received. The ball-milling procedure is a beneficial activation process for the ZVMg powder since it significantly increases the rate of dechlorination of PCBs.* 68
Figure 20: Calibration curves for PCP and its chlorinated byproducts. 69

Figure 21: SEM images of a) unmilled ZVMg powder b) ball-milled ZVMg powder and c) ball-milled ZVMg/C powder.* 71
Figure 22: Chromatograms from GCMS of PCP degradation at different time points, for all three reaction systems in acidified ethanol and Ball-milled a) ZVMg, b) ZVMg/C, and c) mechanically alloyed ZVMg/Pd (11.9min is PCP peak). 72
Figure 23: Chromatograms from GCMS of PCP degradation byproducts after 1 hr in acidified ethanol and Ball-milled a) ZVMg, b) ZVMg/C, and c) mechanically alloyed ZVMg/Pd (2.89min Phenol, 6.41-7.17min DiCP, 8.21-9.12min TriCP, 9.93-10.6min TCP and 16.5min PCB-153; internal standard). 73
Figure 24: Dechlorination of PCP with the activated (a) Mg, (b) Mg/C, (c) mechanically alloyed Mg/Pd reducing systems. Each data point represents the mean ± error calculated from duplicate samples. 74
Figure 25: SEM images of ball-milled ZVMg particles a) before dechlorination and b) after dechlorination.* 75
Figure 26: Calibration curves for HCB and its chlorinated byproducts. 79
Figure 27: Chromatograms from GCMS of HCB degradation at different time points within 1 hr in 1:1 acidified ethanol/ethyl lactate and Ball-milled ZVMg/C, (19.71 min is HCB peak, 15.67 min is 1,2,3,4-TCB, 14.99 min is 1,2,4,5-TCB, 12.79 min is 1,2,4-TriCB, 12.08 is 1,3,5-TriCB and 25.36 min is PCB-153; internal standard). 81
Figure 28: Minimum energy conformation of benzene. 85
Figure 29: Minimum energy conformation of chlorobenzene. 86
Figure 30: Minimum energy conformation of 1,3-DiCB 87

Figure 31: Minimum energy conformation of 1,2-DiCB..... 88

Figure 32: Minimum energy conformation of 1,4-DiCB..... 89

Figure 33: Minimum energy conformation of 1,2,3-TriCB..... 90

Figure 34: Minimum energy conformation of 1,2,4-TriCB..... 91

Figure 35: Minimum energy conformation of 1,3,5-TriCB..... 92

Figure 36: Minimum energy conformation of 1,2,3,4-TCB. 93

Figure 37: Minimum energy conformation of 1,2,3, 5-TCB. 94

Figure 38: Minimum energy conformation of 1,2,4,5-TCB. 95

Figure 39: Minimum energy conformation of PCBz. 96

Figure 40: Minimum energy conformation of HCB. 97

LIST OF TABLES

Table 1: Mass Spectrometry (MS) Selected Ion Monitoring parameters for the degradation of PCP in ethanol and acetic acid. 70

Table 2: Data of the pseudo-first order PCP degradation duplicate runs of the reaction of 66.72 μM of PCP with 2.08×10^{6} μM ZVMg in 5 ml acidified ethanol. 76

Table 3: Data of the pseudo-first order phenol formation of dechlorination of chlorinated phenols with activated magnesium reducing systems in ethanol and acetic acid. 77

Table 4: Mass Spectrometry (MS) Selected Ion Monitoring parameters for the degradation of HCB in 1:1 ethanol/ethyl lactate solvent and acetic acid. 80

Table 5: Data of the pseudo-first order PCP degradation duplicate runs of the reaction of 66.72 μM of PCP with 2.08×106 μM ZVMg in 5 ml acidified ethanol. 82

Table 6: ΔG data of the reaction calculated with Gaussian 09 software with B3LYP method for each chlorinated position in HCB and its degradation products. 83

Table 7: Activation energies data of the reaction calculated with Gaussian 09 software with B3LYP method for each chlorinated position in HCB and its degradation products. 84

LIST OF ACRONYMS/ABBREVIATIONS

CA	Chloroanisole
CAs	Chlorinated anisoles
CBz	Chlorobenzene
CP	Chlorophenol
CPs	Chlorinated phenols
DDT	Dichlorodiphenyltrichloroethane
DFT	Density Functional Theory
DiCA	Dichloroanisole
DiCB	Dichlorobenzene
DiCP	Dichlorophenol
DLS	Dynamic light scattering
ECD	Electron capture detector
EPA	Environmental Protection Agency
GC	Gas chromatogram
GC/MS	Gas chromatogram-mass spectrometry
HCB	Hexachlorobenzene
K_{ow}	Octanol-water partition coefficient
LOD	Limit of detection
LOQ	Limit of quantification
MCL	Maximum contaminant level
MCLG	Maximum contaminant level goal

MS	Mass spectrometry
MVOC	Microbial volatile organic compound
NIST	National Institute of Standards and Technology
OCDD	Octachlorinated dibenzo-*p*-dioxin
OCP	Organochlorine pesticide
PCA	Pentachloroanisole
PCAHs	Polychlorinated Aromatic Hydrocarbons
PCB	Polychlorinated biphenyl
PCBz	Pentachlorobenzene
PCDD	Polychlorinated dibenzo-*p*-dioxin
PCDF	Polychlorinated dibenzofuran
PCM	Polarizable Continuum Model
PCNB	pentachloronitrobenzene
PCP	Pentachlorophenol
POPs	Persistent organic pollutants
SEM	Scanning electron microscopy
SHE	Standard hydrogen electrode
SIM	Selected ion monitoring
TCA	Tetrachloroanisole
TCB	Tetrachlorobenzene
TCP	Tetrachlorophenol
TriCA	Trichloroanisole

TriCB	Trichlorobenzene
TriCP	Trichlorophenol
UCF	University of Central Florida
USEPA	United States Environmental Protection Agency
ZVI	Zero-valent iron
ZVM	Zero-valent metal
ZVMg	Zero-valent magnesium
ZVZ	Zero-valent zinc

CHAPTER ONE: THREE MAGNESIUM TREATMENT SYSTEMS FOR THE DEGRADATION OF PENTACHLOROPHENOL

Some of the contents of this chapter are reproduced from our published work:

A.M. Garbou, C.A. Clausen C.L. Yestrebsky, Chemosphere, 2017, 166, pgs.267– 274.

Introduction

Chlorinated phenols (CPs) are produced in large quantities; annual global production is estimated to be around 150,000 tons. CPs have a variety of different applications, mainly in wood preservation. They are also found in fungicides, bactericides, herbicides, insecticides, mold inhibitors, antiseptics and disinfectants. CPs have seen use as starting materials for certain pesticides as well as dyes and pigments, and are formed as byproducts during the bleaching of pulp with chlorine, in municipal chlorination of drinking water and in incomplete incineration.**(Trapido, Hirvonen et al. 1997)** Improper management of industrial wastes, accidental spills, leakages, runoff, domestic sewage, and liberal use of pesticides in crops has resulted in the prevalence of CPs in natural waters and soil (the MCL for total CPs is 0.01 mg/L).**(Cass, Freitas et al. 2000)** Even at low concentrations, CPs present difficulties in maintaining water quality for human consumption.**(Hwang, Hodson et al. 1986, Cass, Freitas et al. 2000, Torres, Hernandez et al. 2010)** This is because highly toxic organic compounds, such as polychlorinated dibenzo-p-dioxin and polychlorinated dibenzofuran (PCDD/ PCDF), are generated when PCP undergoes a photochemical reaction.**(Kim and Carraway 2003, Chen,**

Huang et al. 2007) Since the toxicity of CPs increases with the number of chloro groups substituted on the ring, pentachlorophenol (PCP) is the most problematic of the CPs.**(Kim and Carraway 2003)** The persistence and toxicity of CPs have incited public awareness and desire to remediate polluted sites, thereby preventing further risks to ecosystems.**(Trapido, Hirvonen et al. 1997, Cass, Freitas et al. 2000)**

Chlorinated phenols are harmful to plant and animal life. Since the toxicity of chlorophenols increases with the number of chloro groups substituted on the ring and there are five positions on a phenol ring which allow for substitution, pentachlorophenol (PCP) is the most problematic of the chlorinated phenols.**(Doyle, Miles et al. 1998)** In addition to their 1980 **(Doyle, Miles et al. 1998)** suspension in the United States, PCP has been banned contemporarily in most European countries. This is due to the high toxicity of their xenobiotic daughter compounds which are normally found in the industrial effluents of pulp, paper, oil, petrochemicals, synthetic plastics, timber, and other aforementioned products.**(Torres, Hernandez et al. 2010)** In other countries, however, chlorophenols still see steady production. For example, Mexico has an important oil and petrochemical industry which refines around 10,000 barrels of crude oil annually, yielding nearly 100 kg of phenols.**(Torres, Hernandez et al. 2010)** Contamination persists even around abandoned facilities such as an old PCP factory found in Taiwan.**(Chen, Huang et al. 2007)**

Chemical and physical properties control the environmental behavior of each individual CP. As the number of substituted chloro groups increases, there is an increase in melting/boiling point and a decrease in water solubility. Since CPs are weak acids, there is a direct relationship between increasing pH and water solubility.**(Kim and Carraway 2003, Chen, Huang et al. 2007)** For instance PCP, which is fully chlorinated, has a pKa of 4.60 and is less soluble than 4-

chlorophenol, which has a pKa of 9.5.**(Kim and Carraway 2003)** The acidic properties of the phenolic hydroxyl group of PCP (pKa = 4.60) **(Buhr, Genning et al. 2000)** contribute to its adsorption to wooden surfaces by the chemical bonding of functional group coupling, as in the case of lignins.**(Buhr, Genning et al. 2000)** Physical properties also have an effect on the environmental behavior of CPs. With a high vapor pressure of 1.1×10^{-2} Pa (at 20 °C), PCP can volatize from the treated material, thereby contaminating indoor environments .**(Buhr, Genning et al. 2000)** Due to the risk of these compounds to marine life and human health, they have been included on the list of the eleven priority phenol derivatives compiled by the United States Environmental Protection Agency.**(Solanki and Murthy 2011)**

Past and Current Remediation Options

Biodegradation

CPs are persistent, toxic, and omnipresent in the environment. Furthermore, the ever-increasing discharge of these compounds has caused various problems in water and wastewater treatment systems.**(Solanki and Murthy 2011)** Because of their carcinogenic potential, and bioaccumulation, remediation of these pollutants is of great importance.**(Buhr, Genning et al. 2000)** In recent developments, physical-chemical and biological systems have been put into place for the degradation of CPs that are present in aquatic ecosystems. Work has been done to study the biodegradation of 4-chlorophenol by the bacterium *Pseudomonas putida*,**(Li and Loh 2007)** the biodegradability of 2,4-dichlorophenol in an upflow anaerobic sludge bed bioreactor**(Chen, Huang et al. 2005)** and the treatment of wastewater containing 2,4,6-trichlorophenol in a hybrid-loop bio-reactor scheme .**(Eker and Kargi 2007)** Although ample research has been done on the

biodegradation of CPs, traditional treatment technologies are insufficient,**(Cass, Freitas et al. 2000)** mainly because highly CPs are always xenobiotic and toxic to microorganisms, and also due to the inability of the bacteria to function under standard conditions.**(Kim and Carraway 2003)**

Reductive Dechlorination by Zero-valent Metals (ZVM)

In the last 20 years, the use of zero-valent metals (ZVM) such as iron, zinc and magnesium has shown great promise for *in situ* remediation of chlorinated aromatic hydrocarbons such as PCP.**(Grittini 1997, Kim and Carraway 2000, Kim and Carraway 2003, Chen, Huang et al. 2007)** Although rapid PCP dechlorination was observed in a study conducted by Ravary and Lipczynska-Kochany **(Kim and Carraway 2003)** using zero-valent iron (ZVI), the results may be at least partially due to loss of the analyte from adsorption. In a series of batch experiments performed by Kim and Carraway **(Kim and Carraway 2003)** reductive dechlorination of penta-, tetra-, and trichlorophenol by zero-valent zinc (ZVZ), begot less-chlorinated reduction products of their respective phenols. However, the experiment showed no further dechlorination for the remainder of the 25-day period. Kinetic research evaluating the efficiency and mechanism of PCP degradation utilizing nanoscale zero-valent iron (ZVI) has been accomplished successfully by Chen, et al.**(Chen, Huang et al. 2007)** Further studies have confirmed ZVZ to be better suited than ZVI for PCP removal due to its greater reduction potential.**(Kim and Carraway 2003)** Despite the much higher reactivity of ZVZ than ZVI towards CPs, limited work has been made of ZVZ on account of the discharge of toxic Zn species released from zinc particles. These species may present a risk to the environment.**(Kim and Carraway 2003)**

Bimetallic Systems

Although reductive dechlorination is possible with single metallic reaction systems, bimetallic systems can be much more efficient even at normal temperature and pressure. Bimetallic systems consist of two metals, one of which has negative reduction potential due to its zero-valent form (e.g. Fe^0, Zn^0 and Mg^0). This component of the system has the potential to give off hydrogen when water activates corrosion from the anode. The great positive reduction potential of the other component of the bimetallic system (e.g. Pd^{4+}-Pd^0, Ag^+-Ag^0) offers catalytic hydrogenation, as well as reduction of the target analyte by forming a metal hydride (M-H) from the hydrogen produced by the anodic corrosion.**(Solanki and Murthy 2011)** In work done by Grittini,**(Grittini 1997)** such degradation byproducts as phenol, 2,4,6-triCP and 2,3,4,5-tetraCP were observed using a Pd-Fe bimetallic system. Trends have been observed in the success of bimetallic systems which rely on the great negative reduction potential of zero-valent magnesium (ZVMg) to give off hydrogen for reductive dechlorination.**(Coutts, Devor et al. 2011)** Successful synthesis of a magnesium nanocatalyst and Mg-Ag

bimetallic catalyst systems have been accomplished in research performed by Jignasa, et al.**(Solanki and Murthy 2011)** After analyzing the results using scanning electron microscopy (SEM) and dynamic light scattering (DLS), optimal success was achieved with the Mg-Ag bimetallic nanocatalyst.

One advantage of using magnesium over iron is its reactivity under aerobic conditions. To prevent the formation of oxide layers on the surface of iron, studies must be performed in an anaerobic environment.**(De Vor, Carvalho-Knighton et al. 2009)** This is due to the slightly water-soluble limiting oxide shell that forms on its surface. When zero-valent iron comes into

contact with oxygen, an insoluble oxide layer forms on the surface of the iron that prevents electrons from being released in solution to reductively dechlorinate the substrate.**(Maloney, DeVor et al. 2011)** This necessitates an anaerobic environment under which ZVI studies must be conducted. Magnesium, however, can be used freely under normal atmospheric conditions. **(Doyle, Miles et al. 1998)** Furthermore, the great negative reduction potential of magnesium offers more free-energy to drive the reaction than iron or zinc, as shown in the standard reduction potential equations below**(Maloney, DeVor et al. 2011)**:

$Mg^{2+} + 2e^{-} \rightarrow Mg^{0}$, $E^{0} = -2.37$ V

$Fe^{2+} + 2e^{-} \rightarrow Fe^{0}$, $E^{0} = -0.44$ V

$Zn^{2+} + 2e^{-} \rightarrow Zn^{0}$, $E^{0} = -0.76$ V

ZVMg for Reductive Dechlorination

Due to the advantages of magnesium as an electron-donating zero-valent metal, magnesium has been made use of to great effect in polychlorinated biphenyl (PCB) degradation studies. Kinetic studies on the hydrodehalogenation degradation of PCB-151 performed by Maloney and associates **(Maloney, DeVor et al. 2011)** determined the ideal reaction conditions with magnesium powder and alcohol solvents using a variety of carboxylic acids. These studies have concluded that the best results for rapid dechlorination of PCB-151 are accomplished with a ratio of 0.02 g of Mg per one mL of ethanol and 10 µL of acetic acid per one mL of ethanol. The results showed an approximate degradation rate of 1.25 $ng\mu L^{-1}min^{-1}$ for 50 ng/µL of PCB-151.**(Maloney, DeVor et al. 2011)** In another study done by Doyle et al.,**(Doyle, Miles et al. 1998)** complete hydrodehalogenation of a mixture of PCB congeners (Aroclor 1221) to biphenyl was

achieved utilizing a Mg/Pd bimetal system. Additionally, other halogenated analytes such as DDT (1,1-bis(4-chlorophenyl)-2,2,2-trichloroethane) and a variety of chlorophenols, naphthalenes and polychlorinated dibenzo-p-dioxins have seen successful degradation using Mg/Pd in different solvent systems.**(Engelmann, Doyle et al. 2001, Hadnagy, Rauch et al. 2007, Patel and Suresh 2007)** In recent work, Dr. Christian Clausen, Dr. Cherie Geiger and co-workers **(DeVor, Carvalho-Knighton et al. 2008, De Vor, Carvalho-Knighton et al. 2009, Coutts, Devor et al. 2011)** of the Industrial Chemistry Laboratory (University of Central Florida) proved a bimetallic system of mechanically alloyed magnesium and palladium (1% on graphite) to be effective in degrading PCBs. This leads the research of the Industrial Chemistry Laboratory in the direction of a pentachlorophenol degradation investigation.

Ball-milling Procedure

Ball-milling offers a preparation method for catalyzed bimetallic systems to be able to function in aqueous solvent systems with minimal oxidation. Previous preparation methods have involved *in situ* synthesis of the bimetallic system through a spontaneous oxidation process between Pd^{4+} and zero-valent metal, followed by immediate application. **(Morales, Hutcheson et al. 2002, Patel and Suresh 2007)** However, these procedures must be performed at the time of treatment, and do not allow for convenient long-term storage of the reactants. Additionally, oxidation on the surface of the un-altered metal leads to rapid formation of insoluble oxides which decrease reactivity. Research done by Huot et al. and Soave et al.

(Huot, Liang et al. 2001) has shown that the ball-milling process enhances the reactivity of zero-valent magnesium metal by cracking the superficial hydroxide/oxide layer, which changes the

microstructure creating more surface defects. Figure 19 in Appendix A illustrates a drastic decrease in the concentration of PCB 151 by degradation with ball-milled ZVMg over time, compared to the changes observed with unmilled ZVMg. **(Maloney, DeVor et al. 2011)** The proven efficacy of the novel technique of ball-milling has offered promising leads in the advancement of degradation technology, and serves as an influence to the pentachlorophenol degradation investigation covered in this paper.

Materials and Methods

Neat PCP standards were obtained from Accustandard and standard solutions were prepared by diluting the neat standards to their desired concentration with absolute ethanol from Pharmco-AAPER. Inc. Absolute ethanol, Optima® grade hexane, toluene, potassium carbonate and acetic anhydride were obtained from Fisher Scientific (Ottawa, ON.). Glacial acetic acid (≥99.8%) was acquired from Acros Organics through Fisher Scientific. Micro-scale unmilled magnesium (~4 μm) was obtained from Heart Metals, Inc (Tamaqua, PA). Palladium on graphite (5 wt.%) and sodium sulfate were obtained from Sigma-Aldrich Chemicals. Helium gas, for gas chromatography-mass spectrometry (GC/MS) analysis, was purchased from Air Gas (Atlanta, GA). All chemicals were high purity (≥98%) and ACS reagent, analytical grade. All chemicals were used in the form in which they were received unless otherwise noted. A precision microscale analytical balance (Model AE 260-S from Mettler-Toledo AG, Greifensee, Switzerland) was used to measure the different Mg loadings.

Ball-milling Procedure

Magnesium activity is increased through ball-milling, a process in which the passivated hydroxide/oxide surface layer is cracked, thereby creating more surface defects which change the microstructure.**(Maloney, DeVor et al. 2011)** In this study magnesium powder, magnesium carbon (Mg/C), and ZVMg mechanically alloyed with palladium on carbon, were ball-milled under optimized conditions. The ball-milling was performed using a Red Devil 5400 series paint shaker fitted with custom plates to hold milling canisters, which provided 670 rpm for ball milling of the metal.**(Coutts, Devor et al. 2011)** The canister and balls are made of stainless steel. Magnesium powder (85 g) was introduced into the canister with 16 steel balls of 1.5 cm diameter having a total mass of 261.15 g, corresponding to a ball/powder mass ratio of 3:1. The canister was sealed under argon atmosphere. The milling duration was 45 minutes. Additionally, to obtain ~10 wt% ball-milled magnesium/carbon, 76.5 g Mg powder and 8.5 g of graphite (C) were introduced into the canister. The material was ball-milled for 30 minutes using the aforementioned paint mixer. Finally, a ~0.1 wt% palladium on magnesium powder mixture was prepared in a similar fashion by ball-milling 83.2 g Mg with 1.8 g of 5% palladium on carbon in a stainless steel canister for 30 minutes using the aforementioned paint mixer.

Experimental Procedure

Experiments were conducted in 20 mL clear glass vials. Ball-milled Mg (0.25 g) and 5 mL of a 20 ng/μL (75.09 μM) PCP in absolute ethanol solution were added. Next, glacial acetic acid (50 μL) was added, and the vials were then placed on a Thermo Scientific MaxQ 4000 orbital shaker table operated at 200 rpm, at room temperature (~26 °C) for the appropriate amount of time.

At designated time points, the glass vials were taken off of the shaker table and sonicated for 5 minutes. Then 5 mL samples of the solution were centrifuged for 10 minutes and filtered using a nylon syringe filters with 0.45 µm pores. Due to the relative polarity, chemical reactivity and low vapor-pressure of PCP, it was necessary to prepare a derivative in which the hydroxyl group was substituted with an acetate group by treating PCP with acetic anhydride.**(Buhr, Genning et al. 2000)** This was done in order to minimize adsorption and prevent tailing of the chromatographic peaks.**(Zuin, Da Silva Airoldi et al. 1999)** The organic phase, containing the derivatized PCP, was separated, dried over Na_2SO_4 for 5 minutes and transferred to a clean 4 mL screw-cap vial. Then 2 mL were pipetted into a GC-vial for analysis.

Analysis

All of the experiments were conducted in duplicate. The toluene/hexane extracts were analyzed for residual PCP and its degradation byproducts on an Agilent 6850 series II GC/MS equipped with an autosampler and an Agilent 5975 mass spectrometer. An Rxi®-5HT capillary column (30 m × 0.25 mm i.d.; 0.25 µm film thickness) was used with helium as a carrier gas, with a flow rate of 2.0 mL/min and a gas velocity of 53 cm/s. The instrument parameters were as follows: after an initial temperature of 100 ˚C was held for 2 minutes, the column was ramped at 10 ˚C/min to 250 ˚C and then held for 2 minutes prior to cool down. The temperature of injector and detector were maintained at 250 and 280 ˚C respectively. Injection volumes were set at 2 µL and were performed in splitless mode. The limit of detection (LOD= $3S_b/m$), and the limit of quantitation (LOQ= $10S_b/m$) were calculated in order to determine the minimum concentration which is detectable at a known confidence, and the lowest concentration of analyte which can be measured by the instrument, respectively. These calculations are vital for validating the efficacy

of the method, with lower values indicating better accuracy. A calibration plot for PCP and its chlorinated phenol byproducts was prepared in the concentration range of interest and was found to be linear with correlation coefficient values at >0.99. This plot is shown in Figure 20 (Appendix A). Eluted compounds were identified by comparing sample mass spectra to reference spectra catalogued by the National Institute of Standards and Technology (NIST). PCB-153 (2,2',4,4',5,5'-hexachlorobiphenyl) was used as an internal standard for the analyses. Degradation was measured by disappearance of the PCP peak and confirmed (as opposed to adsorption to the Mg) by the appearance of lower chlorinated congeners. Selected ion monitoring (SIM) parameters are shown in Appendix A (Table 1). Separate analyses were conducted to monitor the changes in pH of all three ZVMg reaction systems over the duration of one week. For this study, 1 mL aliquots of the ethanol solution were collected from the samples, at chosen time points, and then transferred into vials where they were diluted 9:1 with deionized water. The pH of each of the solutions was then measured using an Accumet Research AR15 pH meter. Back-calculations of the hydrogen ion concentrations in the non-aqueous solvents were then conducted to understand the reaction conditions based on the observed change in pH.

Dissertation Objectives

The objective of this research is to compare the dechlorination processes of ZVMg systems to establish a technology for use as an *ex situ* application for the remediation of PCP. This research focuses on three systems with great capabilities of treatment: ball-milled magnesium powder, ball-milled magnesium carbon (Mg/C), and mechanically alloyed ZVMg with a catalyst, in this case

palladium, creating a bimetallic system capable of dechlorinating PCP very rapidly to less toxic CPs.

Results and Discussion

Degradation of PCP with ball-milled Mg, Mg/C, and mechanically alloyed Mg/Pd

A kinetic study of these treatment systems was performed in an ethanol solvent system with an initial PCP concentration of 66.72 µM, closed in a vial with acetic acid, (to keep the surface of the ball-milled ZVMg clean from the formation of thick oxide/hydroxide layers, so that the ethanol can establish contact), **(Elie, Clausen et al. 2012)** at room temperature. The data on the time-dependent concentration of PCP from these studies, in each metal system, are illustrated in Figure 1. The LOD and LOQ were determined to be 2.14 µM and 7.14 µM, respectively. The plot below illustrates a rapid decrease in the concentration of PCP, with no detection of PCP after 30 min for any of the magnesium systems. After 4 min, reduction in PCP concentration showed that the percent degradation for PCP with ball-milled ZVMg, ZVMg/C, and mechanically alloyed ZVMg/Pd was 17.19%, 68.29% and 33.32%, respectively. After 15 min of treatment, PCP concentrations decreased by an average of 36.6% and 62.4% when treated with ZVMg and ZVMg/Pd, respectively. However, no PCP was detected after treatment with ZVMg/C. In previous studies, **(Elie, Clausen et al. 2012)** faster reaction kinetics were observed using ball-milled ZVMg/C than either milled or unmilled ZVMg. This is due to the protection offered by the layers of graphite on the metal surface which prevent an oxide layer from forming, as confirmed by Scanning Electron Microscopy (SEM) **(Elie, Clausen et al. 2012)** (Figure 21 in Appendix A). These results are in agreement with the observations made by Bouaricha et al. **(Bouaricha,**

Dodelet et al. 2001) This protection, combined with the added cleaning effect of the glacial acetic acid on the ball-milled metal after exposure to air, afforded maximum reactivity for the surface of the metal to accomplish the degradation. **(Elie, 2012)** Another explanation for the enhanced reaction kinetics of ZVMg/C is the difference in its particle diameter compared to the unmilled and ball-milled ZVMg (9 μm versus 18 and 14 μm, respectively). **(Elie, 2012)**

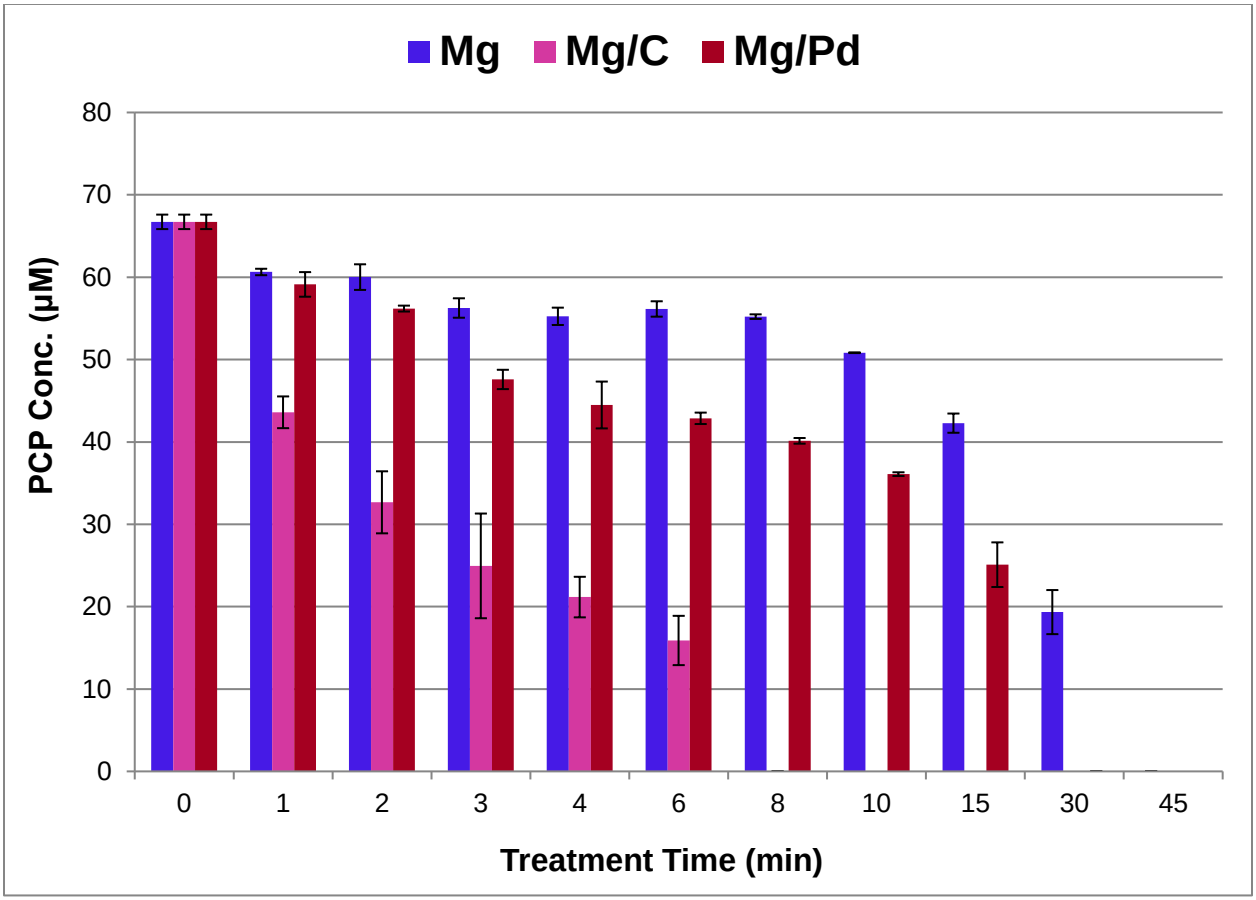

Figure 1: Respective degradation of PCP with the activated Mg, Mg/C, and mechanically alloyed Mg/Pd systems after 15 min of treatment in acidified ethanol.

The chromatographic data showing reduction of the analyte peak at different time points,

for all three reaction systems, can be found in Appendix A (Figure 22). Additional chromatograms showing the formation of dechlorination byproducts for each system over the course of one hour can also be found in Appendix A (Figure 23).

Concentration of Dechlorination Byproducts and Mole Balance over Time

The appearance of many degradation byproducts of PCP became evident in the mass spectra of the sample taken at different time points over a six day study on the three magnesium systems. As presented in Figure 2, the reductive dechlorination of the PCP by ZVMg and the production of tetra-, tri-, di-, mono-chlorinated phenols and phenol itself were observed. The graphic data detailing the formation of the minor byproducts is presented in the Appendix A (Figure 24). Results from the ZVMg/Pd system (Figure 24-C) showed that the degradation of PCP yielded 12 different congeners of dechlorination byproducts including 2 isomers of tetra-, 4 isomers of tri-, 3 isomers of di-, 2 isomers of mono chlorinated phenols and phenol. Similar trends were observed for ZVMg and ZVMg/C systems (Figure 24-A,B). However, two notable byproducts observed from the dechlorination of PCP in ZVMg system were 3,5-DiCP and 3-CP. ZVMg/C system showed the same degradation byproducts as ZVMg with the exclusion of 2,3,4-TriCP.

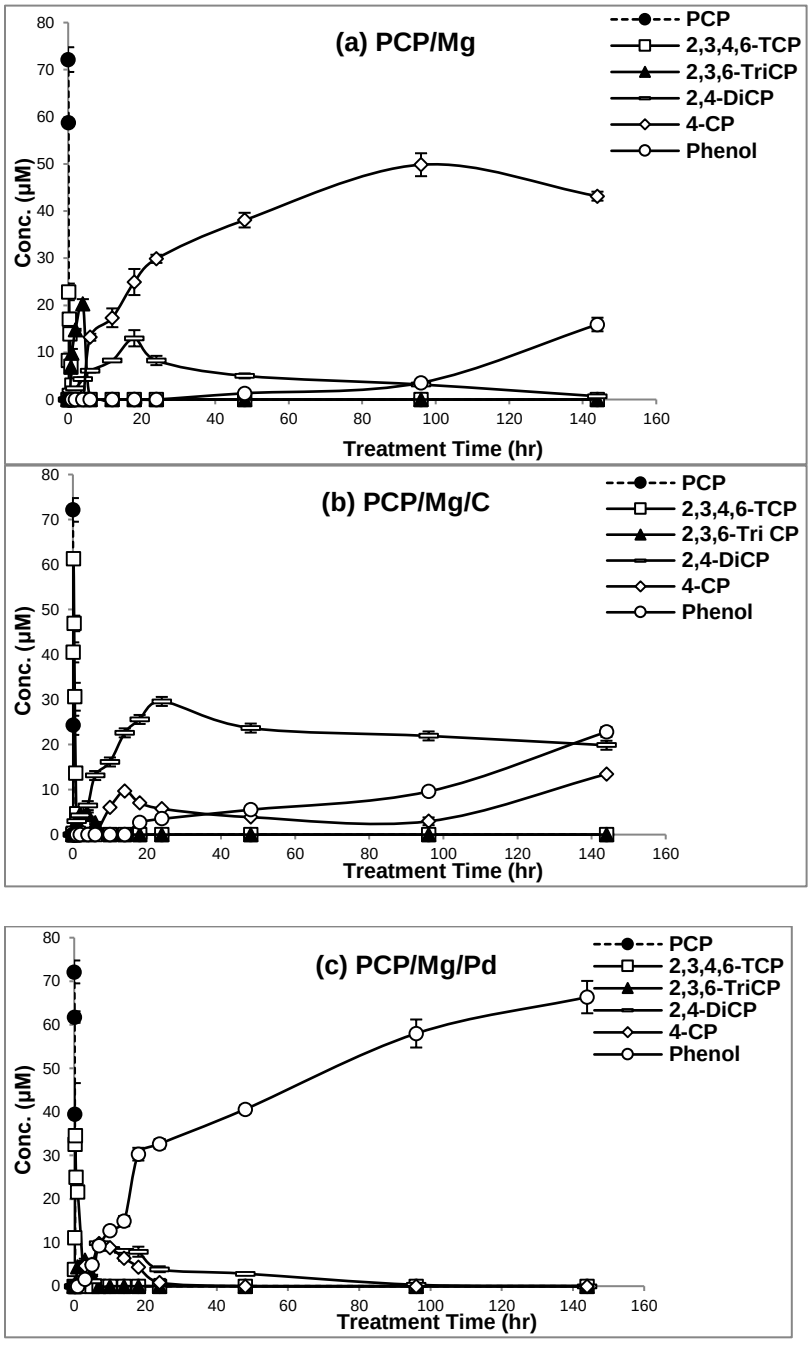

Figure 2: Dechlorination of PCP with the activated (a) Mg, (b) Mg/C, (c) mechanically alloyed Mg/Pd reducing systems. Each data point represents the mean ± error calculated from duplicate samples.

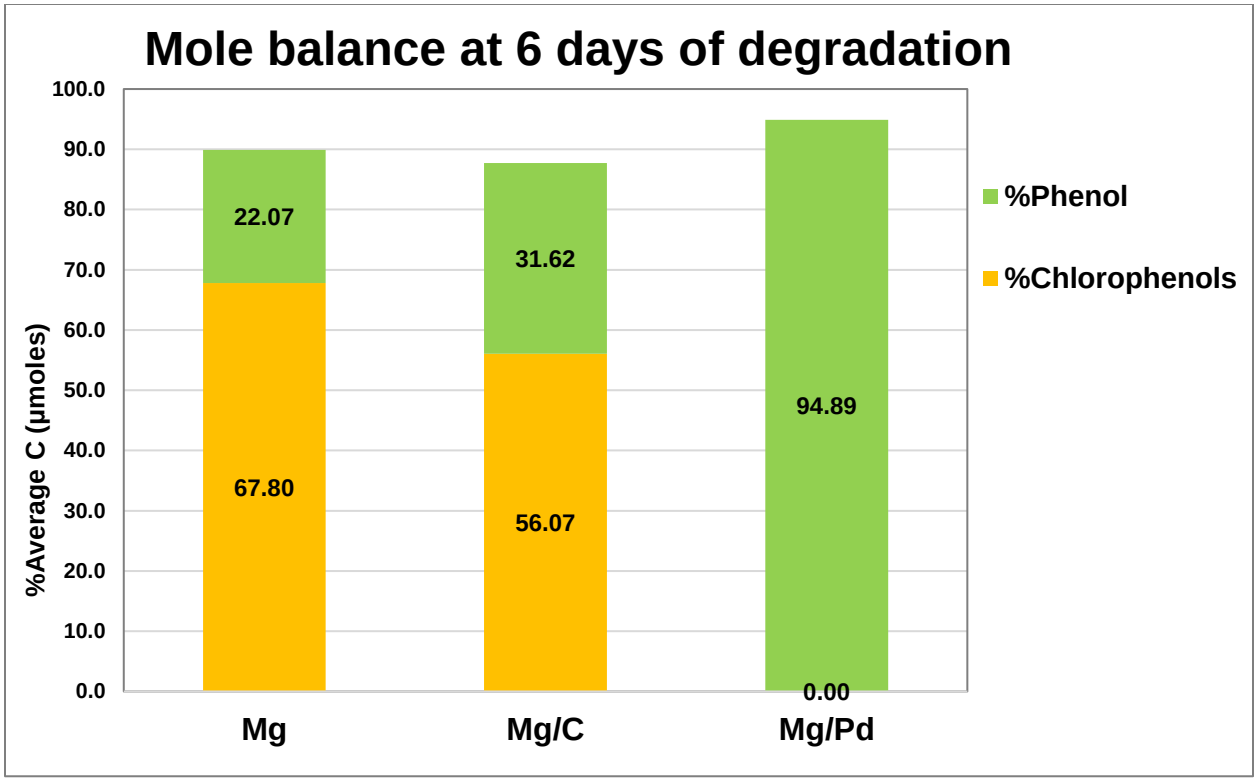

Figure 3: Mole balance and percent chlorinated byproducts plus phenol for PCP/Mg systems after six days of degradation. No CPs were detected for Mg/Pd system.

Dechlorination kinetics were faster for higher-chlorinated chlorophenol congeners. The dechlorination kinetics showed an increasing trend in the order of ZVMg < ZVMg/C < ZVMg/Pd. The majority of the PCP degradation occurred within the first four minutes with ball-milled ZVMg/C, while little degradation occurred from the ZVMg and ZVMg/Pd systems, as indicated in Figure 1. Despite the early success of the ZVMg/C system, the difference in concentration throughout the variety of different possible congeners which formed as byproducts fell within the range of 0-30 µM with no particular preference for phenol formation. In the ZVMg/Pd alloyed system, however, phenol formation increased rapidly in proportion with the disappearance of the

lower CPs, concluding with a 94.89% phenol formation at six days of degradation, showing the highest mole balance for all three systems, as illustrated in Figure 3.

Previous Study for the Analysis of the Magnesium Particle Surface

One of the challenges to using Mg in an ethanol solvent system is the formation of magnesium ethoxide, $Mg(OCH_2CH_3)_2$. According to the results of the pH study, the basicity of the solutions increased over the duration of one week after adding ZVMg to the reaction vials. The solutions from the zero-hour time point were all acidic, each having a pH of 4.4. The back-calculations of the solutions for all ZVMg systems was alkaline beyond the thirty minute time point, with a pH range of 10.5 – 11.1. This lends merit to the idea that there is a build-up of the solid white ethoxide precipitate which prevents the PCP reactant from absorbing to the active sites on the surface of the magnesium metal. In previous SEM studies conducted in the Industrial Chemistry Laboratory at UCF, **(Novaes-Card, 2013)** particles of unused ball-milled magnesium were compared with particles used in the degradation of PCBs. The images from this study were able to confirm signs of corrosion and pitting from the oxidation of the magnesium surface. In addition to this corrosion, clumpy aggregates of smooth material, which is conjectured to be a combination of both $Mg(OH)_2$ and $Mg(OH)(OCH_2CH_3)$, were found on the surface (see Figure 25 in Appendix A).

The poor ethanol solubility of $Mg(OH)_2$ leads to a significant reduction in the degradation rate of the analyte over time **(Cass, Freitas et al. 2000)**. This occurrence is suspected to contribute to declining dechlorination rates observed after approximately 24 hours. In the same study, **(Novaes-Card, 2013)** Energy Dispersive Spectroscopy (EDS) was used to

help characterize the identity of the smooth and pitted areas on the surface of the used ball-milled magnesium particles. This confirmed the presence of $Mg(OH)_2$ on the pitted areas; the smooth areas, however, contained an excess of oxygen and carbon compared to magnesium indicating the likelihood of $Mg(OH)(OCH_2CH_3)$. **(Novaes-Card, 2013).**

Effect of the Addition of Acetic Acid on the Dechlorination Reaction

In the most recent kinetic study on the degradation of PCP using ZVMg/C, samples were prepared in the same way and left on the shaker table for two weeks before being re-spiked with an additional 50 µL of glacial acetic acid and shaken for two more weeks. The samples were then analyzed for the concentration of PCP and its degradation byproducts on the previously mentioned GC-MS. As illustrated on the graph in Figure 4, there was a slight increase in the concentration of monochlorinated phenols (namely, 2-, 3- and 4-CP [which are ortho, meta and para, respectively]).

However, complete degradation to phenol was still not observed. Therefore, the additional glacial acetic acid was beneficial, but more work needs to be done in order to successfully accomplish complete degradation without the use of a palladium catalyst. SEM imaging needs to be performed on the surface of the metal particles in order to access the adjustments that need to be made to optimize the reaction conditions.

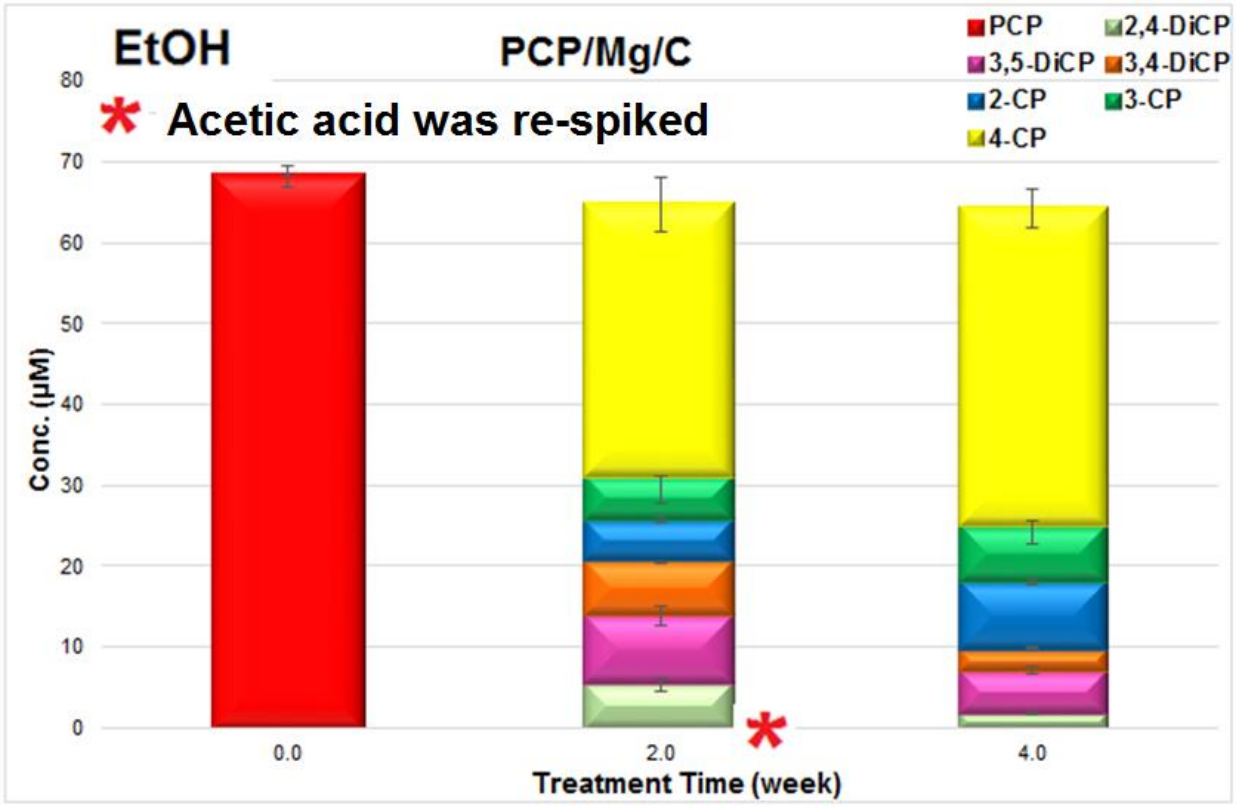

Figure 4: Degradation of PCP by ball-milled ZVMg/C in acidified ethanol with addition of acetic acid after two weeks.

Degradation Kinetics

In previous studies, kinetic data has shown a pseudo-first order trend with respect to the rate of the degradation for the target analyte in the presence of excess ZVM.**(Elie, Clausen et al. 2013)** The results from this particular study were obtained using concentrations of 10.42 mmol of ZVMg and 0.375 mmol of PCP, corresponding to a molar ratio of 28:1 (Mg:PCP).

The pseudo-first-order results have been demonstrated in the kinetic data obtained from studies performed on both PCP degradation and phenol formation with all ZVMg systems. Tables 2 and 3 (in Appendix A) show the natural log of PCP and phenol concentration at each time point.

The data in Figure 5, corresponding to the disappearance of PCP, were plotted following a pseudo-first-order model showing linear correlation coefficients (R^2 values) of 0.9488, 0.9464 and 0.9602 for ball-milled ZVMg, ZVMg/C and mechanically alloyed ZVMg/Pd, respectively. Figure 6 shows the data corresponding to the formation of phenol for ZVMg, ZVMg/C and ZVMg/Pd with the respective linear correlation coefficients of 0.9488, 0.9464 and 0.9602. The values in Figure 5 and 6 indicate that the experimental data is in good agreement with a pseudo-first-order kinetic model. The rate constants were obtained from duplicate measurements in which the natural log of the value of each PCP and phenol concentration (in μM) was taken at its respective time point. Initially, the ZVMg/C system showed the fastest PCP degradation kinetics, as reported in Figure 5. The rate constants for PCP degradation were calculated to be 0.0383, 0.237 and 0.0595 min^{-1} for ZVMg, ZVMg/C and ZVMg/Pd, respectively. However, the rate constants for phenol formation were calculated to be 0.0259, 0.0268 and 0.1652 h^{-1} for ZVMg, ZVMg/C and ZVMg/Pd, respectively, as shown in Fig 6. It follows that the ZVMg/Pd system, which has the highest natural log of its rate constant for phenol formation, shows the fastest kinetics, which agrees with the trend illustrated in the mole balance in Figure 3 as well as the plots shown in Figures 2C and 6. Although the ZVMg/Pd system had the most overall success in degrading PCP, the ZVMg/C system was more effective in the beginning, with diminishing returns after approximately 24 hours. A possible explanation for this observation is the obstruction of the reactive site by the formation of a magnesium hydroxide/ethoxide precipitate when magnesium ionizes and reacts with an anionic species from the solvent system; however future investigations of the metal's surface are necessary to confirm this. Data of the pseudo-first order kinetics for PCP degradation and phenol formation are presented in tables 2 and 3 in Appendix A.

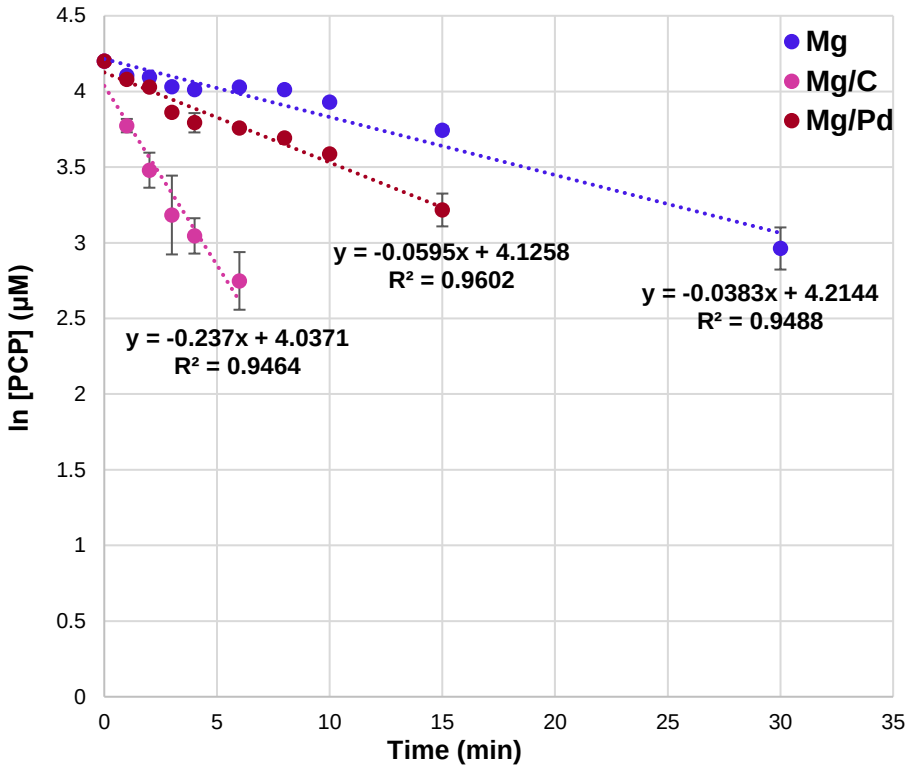

Figure 5: Pseudo-first-order kinetics plot for PCP degradation with activated magnesium reducing systems in ethanol.

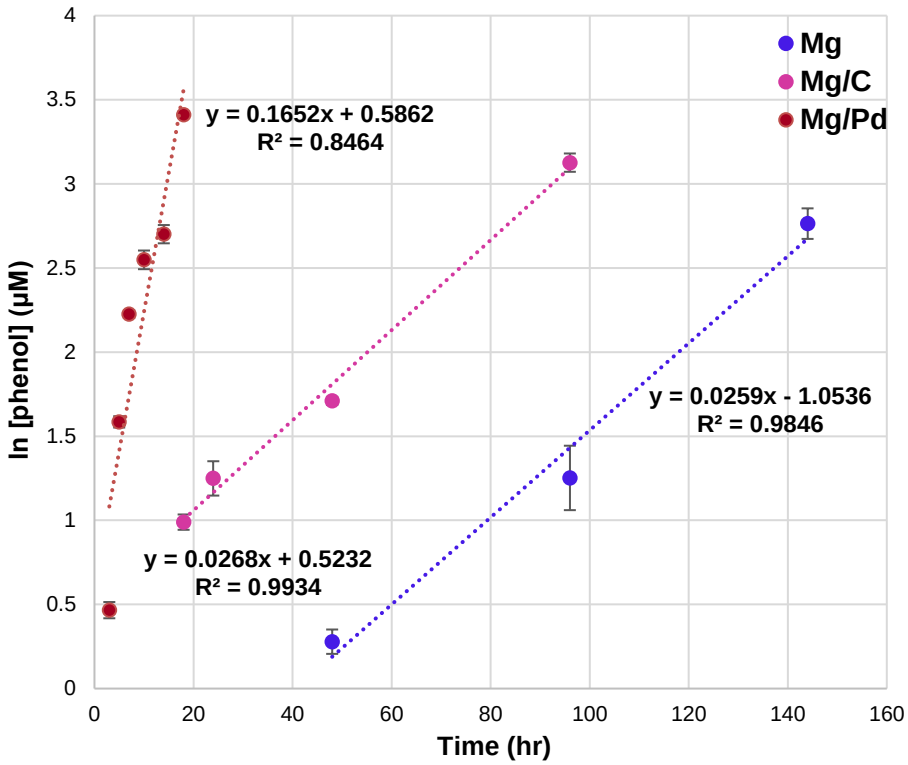

Figure 6: Pseudo-first-order kinetics plot for phenol formation from dechlorination of CPs with activated magnesium reducing systems in ethanol.

Conclusion

From a practical point of view, this study demonstrated that ball-milled magnesium powder with various amendments is an excellent candidate for treatment of CPs. Magnesium has dramatically enhanced reactivity for PCP degradation in comparison with other metals, including iron and zinc. Lower CPs can also be treated by magnesium, although they showed slower reaction rates than PCP. It should be noted that the more chlorine atoms on the phenol ring, the more toxic the CP **(Kim and Carraway 2003),** magnesium has higher reactivity with highly chlorinated CPs; therefore it quickly reduces the concentration of higher chlorinated, more toxic CPs. The results

of these studies indicate that all magnesium systems were powerful for PCP degradation, no PCP was detected after 30 minutes of degradation and the majority of the PCP degradation occurred within the first four minutes with ball-milled ZVMg/C. After 30 minutes, mechanically alloyed Mg/Pd proved to be the most efficient system for the PCP dechlorination with a matrix consisting of at least 0.02 g Mg^0/mL ethanol and 10 µL acetic acid/mL ethanol, in which case 20 ng/µL of PCP was dechlorinated to phenol in approximately 15 minutes with a carbon mass balance of 94.89%. The dechlorination kinetics showed an increasing trend in the order of ZVMg < ZVMg/Pd < ZVMg/C for PCP degradation. However, the increasing trend of kinetics for phenol formation (complete dechlorination) followed the order of ZVMg < ZVMg/C < ZVMg/Pd.

CHAPTER TWO: COMPUTATIONAL AND EXPERIMENTAL METHODS FOR THE DECHLORINATION OF HEXACHLOROBENZENE

Introduction

Regulatory History of HCB

Hexachlorobenzene (HCB) is a highly toxic, degradation-resistant, semi-volatile polychlorinated aromatic compound which has seen widespread contamination in water, air and soil due to its extensive use as a fungicide and wood preservative.**(Beurskens, Dekker et al. 1994, Duan and Adrian 2013, Jiang, Wang et al. 2015, Ren, Kang et al. 2015)** According to the Toxics Release Inventory Database of the U.S. Environmental Protection Agency (EPA), 16,000 kilograms of HCB were released into the environment in 2001 alone from a sample of monitored industries.**(Jiang, Wang et al. 2015)** As a result of its low volatility (vapor pressure 3.4×10^{-4} kPa) and hydrophobic nature (log K_{ow}: 5.73/ aqueous solubility: 0.005 mg/L at 25 °C), HCB is highly toxic to living organisms due to its accumulation in fatty tissue.**(Lin, Hung et al. 2013, Ren, Kang et al. 2015)** It is also carcinogenic to animals, and presents reasonable evidence for posing carcinogenic risks to humans.**(Pavlostathis and Prytula 2000, Brahushi, Doerfler et al. 2004)** According to the EPA, HCB has been classified as a probable human carcinogen, and has been assigned a maximum contaminant level (MCL) of 0.001 mg/L with a maximum contaminant level goal (MCLG) of zero.**(Pavlostathis and Prytula 2000)** Because of its nine-year half-life,**(Zhang, Zheng et al. 2007, Chen, Wang et al. 2015)** ubiquitous application, and tendency to bioaccumulate, HCB is listed as one of twelve Persistent Organic Pollutants (POPs) by the

Stockholm Convention on Persistent Organic Pollution restricting the production and use of POPs, effective May 2004.**(Fennell, Nijenhuis et al. 2004, Kengara, Doerfler et al. 2013, Ren, Li et al. 2014, Zhang, Wang et al. 2014, Jiang, Wang et al. 2015, Yan, Mao et al. 2015)** Despite the prohibition of its production, HCB is still released into the environment as an industrial byproduct from the production of many pesticides and chlorinated solvents, as well as through incomplete combustion.**(Miyoshi, Nishio et al. 2004, Su, Liu et al. 2014)** Residues of HCB have been found in soil, fish, wildlife and food products throughout the world.**(Pavlostathis and Prytula 2000)** Municipal waste incineration has been known to generate HCB and create pollution in waste streams near chloroalkali and wood-preserving plants.**(Pavlostathis and Prytula 2000, Brahushi, Doerfler et al. 2004)** Other evidence of unwanted HCB contamination can be found in pine needles and human tissues in the industrialized region of north-east China.**(Yan, Mao et al. 2015)** Due to the inadvertent continued production and slow degradation of HCB a powerful, sustainable and cost-effective approach for *in situ* remediation technology is necessary.

Current Treatment for HCB Contaminated Materials

The most common practice for HCB treatment in the environment is oxidative remediation through incineration, which is nearly 100% effective at destroying HCB; however it comes at the expense of generating highly carcinogenic compounds such as polychlorinated dibenzo-*p*-furans (PCDFs) and polychlorinated dibenzo-*p*-dioxins (PCDDs).**(Loiselle, Branca et al. 1997, Zhang, Zheng et al. 2007, Xiao, Jiang et al. 2011, Cravotto, Garella et al. 2013, Su, Liu et al. 2013, Ren, Kang et al. 2015)** Other studies have been done using high temperature (~400 ^{o}C) thermal degradation in fly ash via a dechlorination/hydrogenation reaction pathway, however little is known about the interactions of HCB with the calcium oxide in fly ash or its byproducts, since the

concentrations of the dechlorinated products are too low to be studied.**(Yin, Gao et al. 2013)** Certain techniques involving electron beam and γ-irradiation have also been employed for HCB degradation, but these procedures are costly and energetically inefficient.**(Zacheis, Gray et al. 1999, Yin, Wada et al. 2001, Zhang, Zheng et al. 2007)** A more energetically efficient method uses electrode potentials in aqueous solutions, however this technique is not effective due to the poor water solubility (~10^{-8} M) of HCB.**(Merica, Banceu et al. 1998)** In more recent studies certain techniques involving biodegradation and microbial degradation have been employed,**(Beurskens, Dekker et al. 1994, Watanabe and Yoshikawa 2008, Duan and Adrian 2013, Jiang, Wang et al. 2015, Yan, Mao et al. 2015)** however, anaerobic microorganisms are hard to acquire and only incomplete degradation has been accomplished under anaerobic conditions. In addition, not much information is available on the microbial metabolism of HCB in an aerobic environment, and anaerobic microorganisms that can accomplish the dechlorination of penta- or hexachlorobenzene have yet to be isolated, or even identified.**(Wu, Milliken et al. 2002, Yan, Mao et al. 2015)** Furthermore, the toxicity of chlorobenzenes increases with chlorine substitutions, which decreases the efficiency of microbial degradation.**(Zacheis, Gray et al. 2000)** It stands to reason that a novel technique is needed to treat anaerobic environments, where soil, sediments and sewage are contaminated with HCB. One promising technique for the treatment of HCB is reductive dechlorination using zero-valent metals.**(Zheng, Yuan et al. 2009)**

Degradation with Zero- valent Metal

Reductive dechlorination of organic compounds has been studied intensively over the past few decades using zero-valent metals, such as zero-valent iron (ZVI), zero-valent zinc (ZVZ) and zero-valent magnesium (ZVMg), with the support of catalysts such as copper, silver, palladium

and platinum. ZVI has shown promise as an effective reducing agent for the dechlorination of polychlorinated hydrocarbons. Many different contaminants have been the subject of study for remediation using ZVI, particularly nano-scale ZVI due to its increased surface reactivity as a consequence of increased surface area.**(Shih, Hsu et al. 2010, Su, Hsu et al. 2012, Chen, Pan et al. 2014)** In several studies conducted on polychlorinated hydrocarbons, rapid and complete dechlorination was achieved through the reduction potentials of bi-metallic systems including iron/palladium, iron/silver and iron/lead.**(Zheng, Yuan et al. 2009, Coutts, Devor et al. 2011, Nie, Liu et al. 2012, Nie, Liu et al. 2013, Nie, Liu et al. 2013)** Cost -effective dechlorination of HCB was accomplished by using microscale and nanoscale ZVI alloyed with Cu.**(Zheng, Yuan et al. 2009, Zhu, Luan et al. 2010, Su, Hsu et al. 2012)** Most of these metals, particularly Pt, Pd and Ag, have been known to effectively enhance the dechlorination kinetics, however these methods are not economically viable for practical use in large scale remediation projects.**(Xiao and Jiang 2014)** The main disadvantage of using iron is the formation of an insoluble surface oxide layer which prevents the reduction that takes place through the release of electrons in solution.**(De Vor, Carvalho-Knighton et al. 2009)** This disadvantage weakens the efficiency of iron to reductively dechlorinate polychlorinated aromatic hydrocarbons in aerobic environments.**(Zheng, Yuan et al. 2009)**

An alternative zero-valent metal that can be used in the treatment of polychlorinated hydrocarbons is ZVZ, which has higher negative reduction potential ($Zn^{2+} + 2e^{-} \rightarrow Zn^{0}$, $E^{0} = -0.76$ V) than ZVI ($Fe^{2+} + 2e^{-} \rightarrow Fe^{0}$, $E^{0} = -0.44$ V). Despite the higher reactivity of ZVZ towards polychlorinated hydrocarbons than ZVI, limited use has been made of ZVZ because of toxic Zn species released into the environment from zinc particles.**(Kim and Carraway 2003)** Magnesium,

however, has a much higher negative reduction potential ($Mg^{2+} + 2e^{-} \rightarrow Mg^{0}$, $E^{0} = -2.37$ V) than ZVI or ZVZ, making it a more effective reducing agent. In addition, the surface of Mg has a protective layer of magnesium oxide, preventing corrosion under aerobic conditions. However, the formation of magnesium oxides in alcohol solutions can obstruct the dechlorination reaction, thereby retarding the rate at which it takes place.**(Elie, Clausen et al. 2012)** The advantages of magnesium over iron have afforded many electron-donating opportunities in degradation studies involving PCBs. Much work has been done to optimize the ideal reaction conditions for the degradation of PCBs by Maloney and associates.**(Maloney, DeVor et al. 2011)** Kinetic studies performed on PCB-151 using magnesium powder and a variety of alcohols and carboxylic acids have successfully yielded degradation rates of up to 1.25 $ng\mu L^{-1}min^{-1}$.**(Maloney, DeVor et al. 2011)** Complete dechlorination of the variety of PCBs found in Aroclor 1221 was accomplished by Doyle et al.**(Doyle, Miles et al. 1998)** using a Mg/Pd bimetallic system; this alloy had the potential to completely convert every PCB in the mixture to biphenyl. It stands to reason that the catalytic effects of Pd provide a lower energy pathway for rapid dechlorination; however Pd is expensive and impractical for use in field applications. A more practical approach for overcoming the passivation of the magnesium surface formed by a $MgO/Mg(OH)_2$ layer is the ball-milling of magnesium powder with carbon in the form of graphite. This is because the activation of the surface of the magnesium is greatly enhanced by the presence of carbon, thereby improving the reactivity of magnesium.**(Elie, Clausen et al. 2013)** In a study performed by Marc R. Elie,**(Elie, Clausen et al. 2012)** at the Industrial Chemistry Laboratory at the University of Central Florida (UCF), a 94% conversion of benzo[a]pyrene to less toxic hydrogenated cyclic compounds using

activated magnesium powder ball-milled with carbon (i.e. graphite) in acidified ethanol solution,was accomplished within 24 hours.**(Elie, Clausen et al. 2012)**

Theoretical Modeling for the Dechlorination of HCB with Mg^0/C

Degradation of HCB with zero-valent metals has led to the formation of different byproducts, which may or may not be more benign than the original compound. In order to better understand the mechanism of degradation, theoretical modeling can be used for accurate calculations of chemical reactivity. The quantum mechanical calculation type that was used for mechanism and byproduct pathway analysis in this work is called Density Functional Theory (DFT). It is very important to perform both experimental and theoretical studies for the dechlorination of HCB, since the toxicity of byproducts is affected by the way in which they are formed. If experimental studies on the kinetics of the reaction are consistent with the theoretical calculations, then verification of the reliability of the calculation is satisfactory. In previous experiments that were conducted on the photodegradation of HCB, theoretical DFT calculations were used to make accurate predictions for the pathway of degradation.**(Yamada, Naito et al. 2008)**

Methods

Materials and Chemicals

Neat HCB standards were acquired from Accustandard and standard solutions were prepared by diluting the neat standards to the desired concentrations with a 1:1 absolute ethanol/ ethyl lactate solution. Absolute ethanol, ethyl L(-)lactate, 97%, and Optima® grade n-hexane, 95%,

were obtained from Fisher Scientific (Ottawa, ON.). Glacial acetic acid (≥99.8) was obtained from Acros Organics through Fisher Scientific. Sodium sulfate was acquired from Sigma-Aldrich Chemicals. Micro-scale unmilled magnesium (~4 μm) was obtained from Heart Metals, Inc (Tamaqua, PA). PCB-153 (2,2',4,4',5,5'-hexachlorobiphenyl) was used as an internal standard for the analyses, and was purchased from Accustandard. Helium gas, used for gas chromatography-mass spectrometry (GC/MS) analysis, was purchased from Air Gas (Atlanta, GA). All chemicals were of high purity (≥98%) and ACS reagent, analytical grade. All chemicals were used as they were received unless otherwise specified. A precision microscale analytical balance (Model AE 260-S from Mettler-Toledo AG, Greifensee, Switzerland) was utilized in the measurement of the different Mg loadings. 50, 100 and 1000 μL (calibrated) Eppendorf Research® pipettes (from Eppendorf, Hamburg, Germany) were used to dispense the standards and solutions.

Ball-milling Procedure

The activity of the magnesium is enhanced through ball-milling, a process by which the passivated hydroxide/oxide surface layer can be cracked, thus creating more defects in the surface which allow change to the microstructure.**(Maloney, DeVor et al. 2011)** In this study, magnesium carbon (Mg/C) was ball-milled under optimized conditions. The ball-milling was accomplished using a Red Devil 5400 series paint shaker fitted with custom-made plates to support milling canisters, which accommodated a rotation of 670 rpm for the process of ball-milling the metal.**(Coutts, Devor et al. 2011)** The canister and balls are made of stainless steel. To produce ~10 wt% ball-milled magnesium/carbon, 76.5 g Mg powder and 8.5 g of graphite (C) were mixed into the canister with 16 stainless steel balls of 1.5 cm diameter having a total mass of 261.15 g,

corresponding to a 3:1 ball/powder mass ratio. The canister was sealed under an argon atmosphere. The material was ball-milled for 30 minutes using the aforementioned paint mixer.

Experimental Procedure

The reaction was carried out in 20 mL clear glass vials. First, 250 mg of ball-milled Mg/C and 4.95 mL of a 20 ng/µL (70.23 µM) HCB in 1:1 ethanol/ethyl lactate solution were mixed. Next, 50 µL of glacial acetic acid were added, and the vials were then secured on a SK-300 shaker table set to 200 rpm at room temperature (~21 ˚C) for the appropriate amount of time. At the designated time points the reaction vials were removed from the shaker table, and after being extracted in 5 mL of hexane they were placed in the sonicator for 5 minutes. After sonication, samples of the solution were filtered using nylon syringe filters with 0.45 µm pores. The resulting filtered solutions were then added to glass centrifuge tubes with 4 mL of D.I. water and centrifuged for 10 minutes. The organic supernatant containing the HCB was removed, dried over Na_2SO_4 for 5 minutes and then transferred to clean 4 mL glass screw-cap vials. Then 950 µL from each were pipetted into autosampler vials for analysis, along with 50 µL of PCB-153 solution as an internal standard.

Analysis

The samples were run in duplicate. The hexane extracts were analyzed for left over HCB and its degradation byproducts on an Agilent 7820A series II GC-MS furnished with an autosampler and an Agilent 5977E mass spectrometer. The capillary column used was an Rxi®-5ms (30 m × 0.25 mm i.d.; 0.25 µm film thickness) with helium as a carrier gas, a flow rate of 2.0 mL/min, and an average gas velocity of 51.016 cm/s. The oven temperature program was set

according to the following method: after warming up to an initial temperature of 30 ˚C, it was held for 4 minutes, then the column was ramped up at a rate of 10 ˚C/min to 250 ˚C and held for 2 minutes prior to cooling down. The injector and detector temperatures were maintained at 250 and 280 ˚C respectively. Injection volumes were set at 2.5 µL and were executed in pulsed splitless mode. Calibration plots for HCB and its chlorinated benzene byproducts were prepared within the appropriate concentration range and were found to be linear with correlation coefficient values of above 0.998 as shown in Figure 26 (Appendix B). The identity of the eluted compounds were confirmed by running a variety of chlorobenzene standard solutions, and comparing the mass spectra of the samples to mass spectra referenced from the catalog of the National Institute of Standards and Technology (NIST). The degradation rate was measured by the disappearance of the HCB peak and confirmed by the formation of lower chlorinated congeners. Selected ion monitoring (SIM) parameters are presented in Appendix B (Table 4).

Computational Method

All calculations were performed using Gaussian 09 molecular orbital calculation software with B3LYP method to track the degradation pathways. The 6-31+G(d,p) basis set was chosen to conduct geometry optimizations and energy level calculations. In all calculations, the Polarizable Continuum Model (PCM) was applied for solvent calculation to evaluate the effect of the solvent. The static dielectric constant was set to 20.3 and the dynamic dielectric constant was set to 1.93 for the 1:1 mixed ethanol:ethyl lactate solvent in all cases. The dielectric constants were calculated using the volume ratio of the two solvents and their dielectric constants.

Dissertation Objectives

Due to the effectiveness, convenience and environmental benevolence of magnesium, as well as the advancements in ball-milling technology with enhanced kinetics provided by the addition of graphite, a successful approach to the remediation of HCB has been established through the work done in the Industrial Chemistry Laboratory at UCF. The goal of this study is to evaluate the efficacy of activated magnesium metal in a protic co-solvent system of 1:1 ethanol:ethyl lactate and to propose the degradation pathway. This kinetic data will provide a better understanding of the optimal methodology for implementing an application for the *ex situ* remediation of HCB. Agreement of kinetic data with DFT calculations will ensure the accuracy of the research.

Results and Discussion

Degradation of HCB with Ball-milled ZVMg/C

A kinetic study of the degradation of HCB treated with ball-milled ZVMg/C was performed in a solvent system consisting of ethanol and ethyl lactate at an initial analyte concentration of 70.23 µM in a closed vial with glacial acetic acid at room temperature. Figure 7 shows the data for this study; the bars indicate the concentration of HCB as it decreases with time. The graphic representation shows an abrupt decrease in the concentration of HCB after 5 min, with no detection of HCB after 30 min. The GC-MS results for concentration reduction showed that the percent degradation for HCB at the 5 min time point was 57.2%. A greater reduction of HCB concentration was observed after 10 min of treatment, showing an 81.5% decrease. Only a trace amount of HCB was detected at the 30 min time point, with a reduction of 98.5% from the initial concentration.

An overlay of the chromatograms from this study, representing the diminution of the analyte peak as a function of time, is provided in Appendix B (Figure 27).

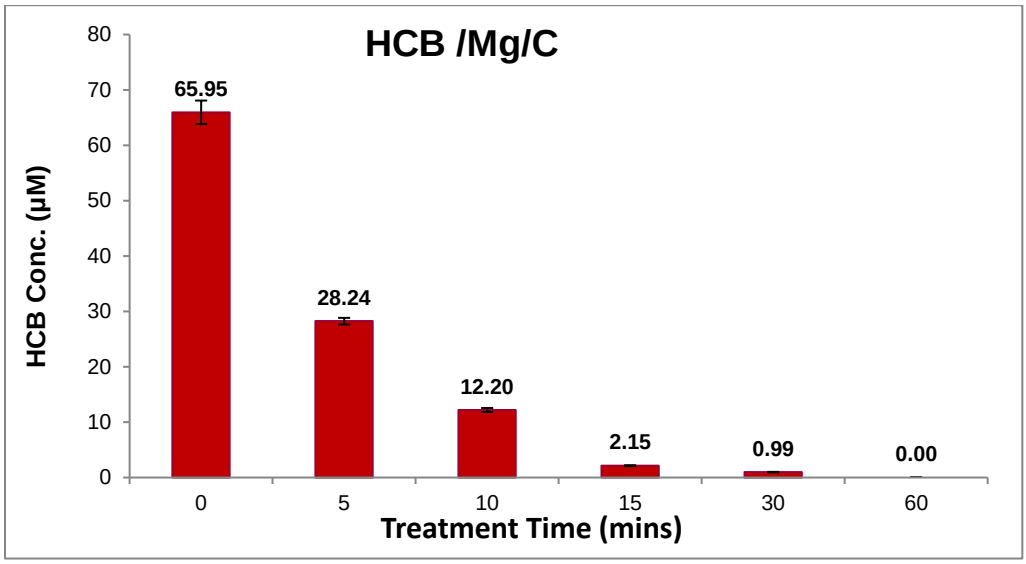

Figure 7: Data corresponding to the degradation of HCB with the activated Mg/C system after 1 hr of treatment in 1:1 acidified ethanol:ethyl lactate.

Concentration of Dechlorination Byproducts and Mole Balance over Time

The formation of dechlorination byproducts of HCB became the subject of study in a nine day time period, over which the mass spectra of the samples were analyzed periodically. The GC analysis indicated that the degradation products of HCB are lower chlorinated benzenes. According to the results, the seven different congeners of byproducts, including penta-, 2 isomers of tetra-, 2 isomers of tri-, and 2 isomers of di-chlorinated benzene rings, that were produced are shown in Figure 8 (which presents the distribution of chlorinated benzenes with respect to reaction time at room temperature). After an abrupt disappearance of HCB, the subsequent removal of chloro groups quickly produced pentachlorobenzene (PCBz), followed by two tetrachlorobenzene

isomers: 1,2,3,5-TCB and 1,2,4,5-TCB. Further dechlorination reduced the concentration of the TCB isomers, replacing them with two trichlorobenzene isomers: 1,2,4- and 1,3,5-trichlorobenzene (TriCB). The dechlorination of the TriCBs, which occurred at a slower rate than that of PCBz and the TCBs, generated two isomers of di-chlorobenzene: 1,3- and 1,4-DiCB. There was no detectable formation of mono-chlorinated or non-chlorinated benzene. The mass balance, which is the sum of the micromoles of HCB and all of its daughter compounds compared to the zero-hour concentration of HCB, was above 80% for the initial degradation time points. A gradual decrease in the mole balance, indicating the presence of other undetected by-products, was then observed. After nine days of degradation a final average mole balance of 79.2% was achieved, as portrayed in Figure 8. The by-product yielding the highest concentration was 1,2,4-trichlorobenzene, which was generated from both isomers of tetrachlorobenzene.

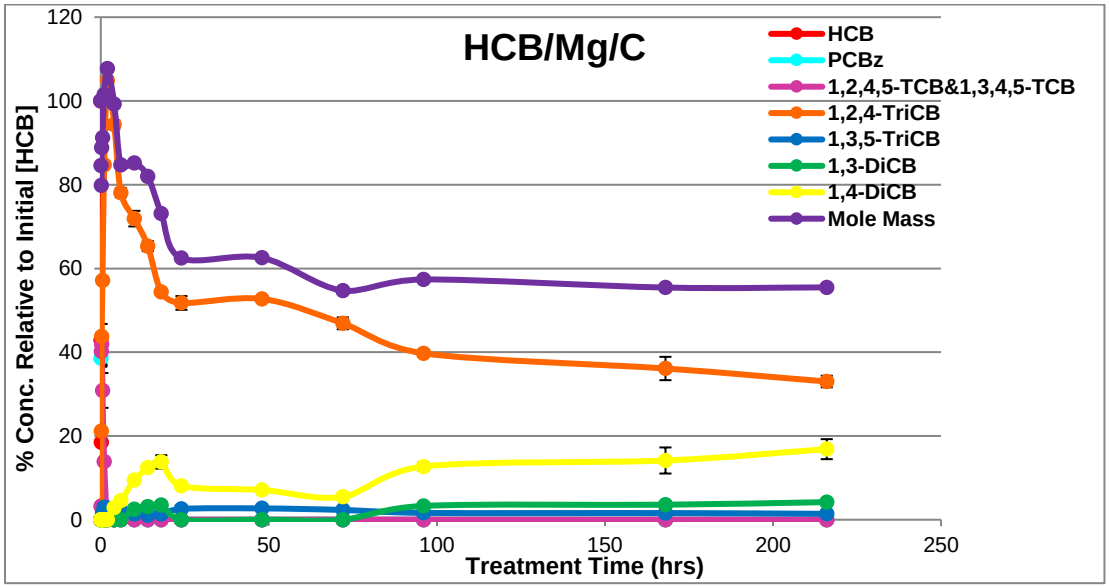

Figure 8: Experimentally observed degradation byproducts of HCB with the activated Mg/C reducing system in 1:1 ethanol/ethyl lactate solvent. Each data point represents the mean±error calculated from duplicate samples.

As the study shows, the kinetics of dechlorination were faster for heavier congeners of chlorobenzene. Figure 7 shows that the vast majority of HCB was degraded within the first ten minutes of the study. The success of the ZVMg/C reaction system was maximal in the early stages of the study as evidenced by the predomination of 1,2,4-TriCB, which has half the chlorine mass of the parent compound. The formation of magnesium ethoxide, $Mg(OCH_2CH_3)_2$, from the reaction of Mg with the ethanol solvent system imposed some limitations on this experiment. The build-up of this solid white ethoxide precipitate prevents the analyte reactant from adsorbing onto the active sites of the magnesium metal surface. Consequently, a significant reduction in the degradation rate of the analyte, and therefore the concentration of lower-chlorinated congeners, is observed after 24 hours.**(Cass, Freitas et al. 2000)** This also creates difficulty in the filtration of the samples. The presence of ethyl lactate in the solvent system controls the pH, keeping it low enough to hinder the formation of hydroxide and/or ethoxide in solution, although this is a temporary remedy.

Degradation Kinetics

Data from previous kinetic studies has shown a pseudo-first order trend for the degradation rate of various target analytes in the presence of excess zero-valent metal.**(Pavlostathis and Prytula 2000, Elie, Clausen et al. 2013)** The UCF Industrial Lab has observed the same results in the kinetic studies performed under the same conditions to collect the data in this project. A pseudo-first-order relationship for the degradation reaction of HCB, with respect to time, in a system using consistent concentrations of ZVMg/C has always been the guaranteed outcome. The kinetic data from this specific project were obtained using concentrations of 10.42 mmol of ZVMg/C and 0.35 mmol of HCB, which correspond to a molar ratio of 30:1 (Mg:HCB). As shown

in Figure 9, the natural log of HCB concentration was plotted against time to show a pseudo-first order decay model with respect to the disappearance of HCB, with a linear correlation coefficient (R^2 value) of 0.9627. Tabulated data corresponding to Figure 9 can be found in Appendix B (Table 5). The rate constant of 0.2223 min^{-1} that was obtained was evaluated from the natural log of four duplicate measurements of each HCB concentration value (in μM).

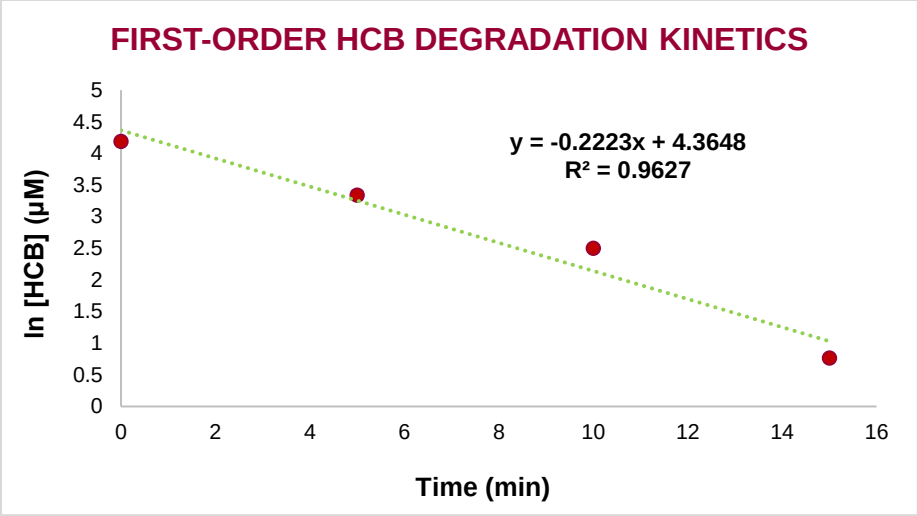

Figure 9: Pseudo-first-order kinetics plot for HCB degradation with activated magnesium reducing systems in 1:1 ethanol/ethyl lactate co-solvent system.

Prediction of the Degradation Pathways for Daughter Compounds by Quantum Chemical Calculation

The free energies (ΔG) of the reaction have been calculated using Gaussian 09 molecular orbital calculation software with B3LYP method to track the degradation pathways.: **xCl–PCBz + H = (x-1)Cl–PCBz + Cl,** where x is the number of Cl substituents in the polychlorinated benzene (PCBz) molecule (not to be confused with the PCBz abbreviation for pentachlorobenzene used throughout this article). Tables 6 and 7 in Appendix B list the ΔG and activation energy data,

respectfully, of the reaction as calculated with Gaussian 09 for each chlorinated position in HCB and its degradation products.

Experimentally, the main products were identified as penta-, tetra-, tri- and di-chlorinated benzene congeners. However, no experimental evidence of the formation of 1,2,3,4-TCB, 1,2,3-TriCB, 1,2-DiCB, monochlorobenzene or benzene was observed. As previously mentioned, the main tetrachlorinated products were 1,2,4,5-TCB and 1,3,4,5-TCB, the main trichlorinated products were 1,2,4-TriCB and 1,3,5-TriCB, and the main dichlorinated products were 1,4-DiCB and 1,3-DiCB. Thus, the main experimental dechlorination pathways are: HCB→ PCBz→ 1,2,4,5-TCB; 1,3,4,5-TCB→ 1,2,4-TriCB; 1,3,5-TriCB→ 1,4-DiCB; 1,3-DiCB, as shown in Figure 8.

In general, the tendency of the dechlorination reaction decreases with decreasing number of Cl substituents in the chlorinated benzene molecules according to the ΔG values. The energy analysis also shows that for each step the ΔG is different, which may explain why specific products were observed during the experiment while others were not. When x=5, the possible products are 1,2,3,4-, 1,2,4,5-, and 1,3,4,5-TCB. Among all the products, the reaction that produces 1,2,4,5-TCB, which is the major product observed from the experiment, has the lowest ΔG value (-30.07 kcal/mol). The minor product, 1,3,4,5-tetrachlorobenze, has a slightly higher ΔG value (-29.69 kcal/mol). The calculated ΔG value for 1,2,3,4-TCB was -27.50 kcal/mol which, being greater than that of the other two isomers, may explain why it was not observed experimentally. When x=4, the possible products are 1,2,3-, 1,2,4- and 1,3,5-trichlorobenze. The 1,2,4-TriCB converted from both TCB reactants is the major product while the 1,3,5-TriCB is the minor product, however there was no yield for 1,2,3-TriCB. When x=3, the major product is 1,4- dichlorobenzene in the experiment, which also agrees with the ΔG data in the table S3 (-26.10 kcal/mol). 1,3-

dichlorobenze from 1,3,5-trichlorobenzene is also found in the reaction mixture. With a theoretical ΔG value of -23.63 kcal/mol, there was no production of 1,2-DiCB from the degradation of the only possible trichlorinated parent, which is 1,2,4-TriCB.

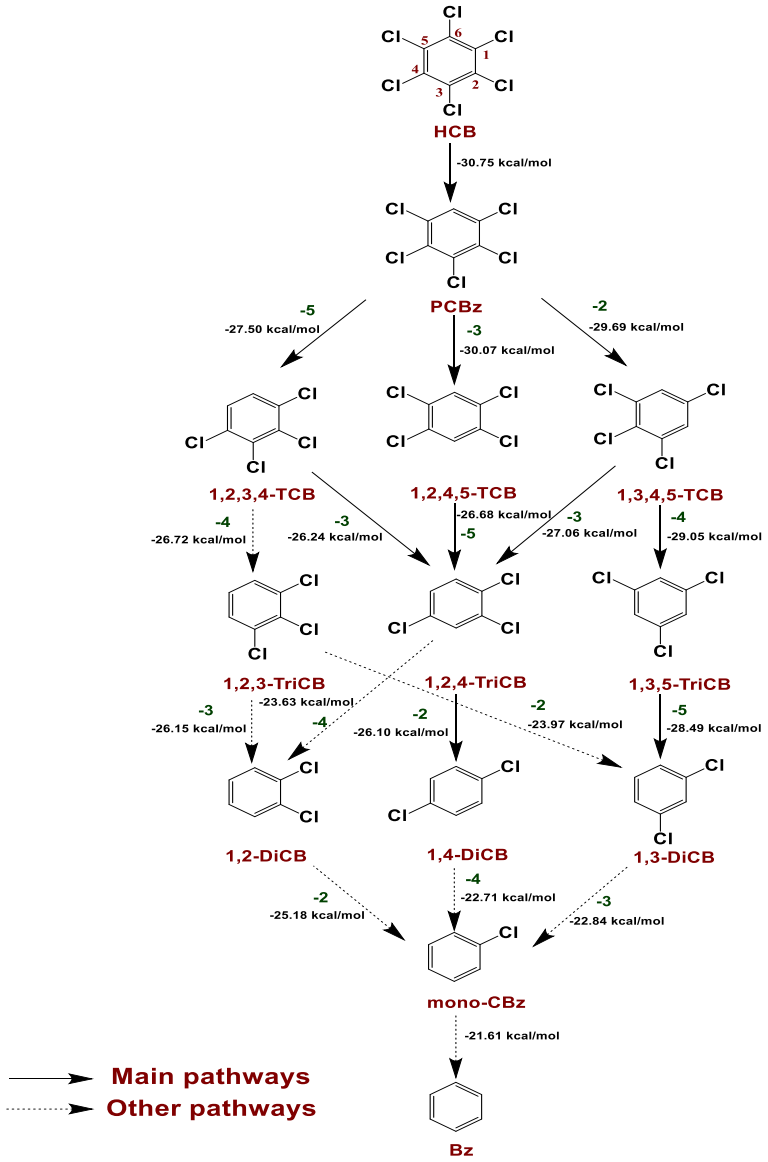

Figure 10: Distribution of HCB and the degradation products with ZVMg/C in 1:1 ethanol:ethyl lactate solvent at room temperature.

The following theoretical main pathways have been predicted by estimation of the compound produced through dechlorination at the lowest free energy position (Figure 10): HCB → PCBz → 1,2,4,5-TCB; 1,3,4,5-TCB → 1,2,4-TriCB; 1,3,5-TriCB → 1,4-DiCB; 1,3-DiCB. These pathways were compared with the experimentally observed pathways shown in Figure 8 and found to be perfectly synchronized. Therefore the experimental degradation pathways of HCB in 1:1 ethanol:ethyl lactate solvent, as well as those of the photodegradation pathways of HCB in hexane, IPA, and methanol solvents,**(Yamada, Naito et al. 2008)** were predicted reliably through the theoretical calculations of the bond dissociation energies with Gaussian 98W using the B3LYP/6-311G method. It is expected that the degradation pathways of various chlorinated aromatic compounds in many solvents can be predicted using this method.

Proposed Mechanism for Reductive Dechlorination Pathways

Reduction of a wide range of functional groups can be accomplished using a system of magnesium in ethanol. This is because the Mg/MeOH system conveniently facilitates a reductive reaction by the transfer of a single electron. It is believed that reduction reactions such as this are likely to take place through the transfer of a hydrogen atom with the help of magnesium.**(Miyoshi, Nishio et al. 2004)** The ionization of small alkali metals, such as iron, zinc and aluminum, can be achieved by hydrogen donors which are slightly acidic, such as hydroxyl or amino groups. When magnesium is introduced into a solution of 1:1 ethanol:ethyl lactate, the magnesium can form a partial bond to a halogen atom on a halide molecule and induce bond cleavage through the formation of a Grignard reagent, followed by the reductive displacement of a hydrogen atom on an ethanol molecule resulting in a dehalogenation via a proton transfer (Figure 11). Due to the

nature of its similarity to the Grignard-Zerewitinoff reaction such reactions are referred to as Grignard-Zerewitinoff-like reactions.**(Wang 2013)**

In the first step of the mechanism, a magnesium atom donates electron density to one of the chlorine atoms on the HCB molecule, forming an ionic intermediate which is stabilized by the protic solvent system. This intermediate then goes on to form a Grignard reagent (TS1), which is the rate-limiting step. A proton transfer then takes place between TS2 and an ethanol (or possibly ethyl lactate) molecule with very small activation energy. The carbon atom is displaced by the hydrogen, leaving behind PCBz and chloroethoxymagnesium, in a similar style to the Zerewitinoff reaction. All of the steps in this reaction are exothermic, and the C-Cl bonding energy is approximately 80 kcal/mol, as confirmed by the computational method with the basis set 6-31+G(d,p). It should be noted that no radical transition states were calculated by the method, which is a reasonable claim since this a reductive dechlorination reaction with ZVMg without UV involved. In previous studies in which a radical mechanism was confirmed using energy calculations, ultraviolet light played a critical role.**(Yamada, Naito et al. 2008)**

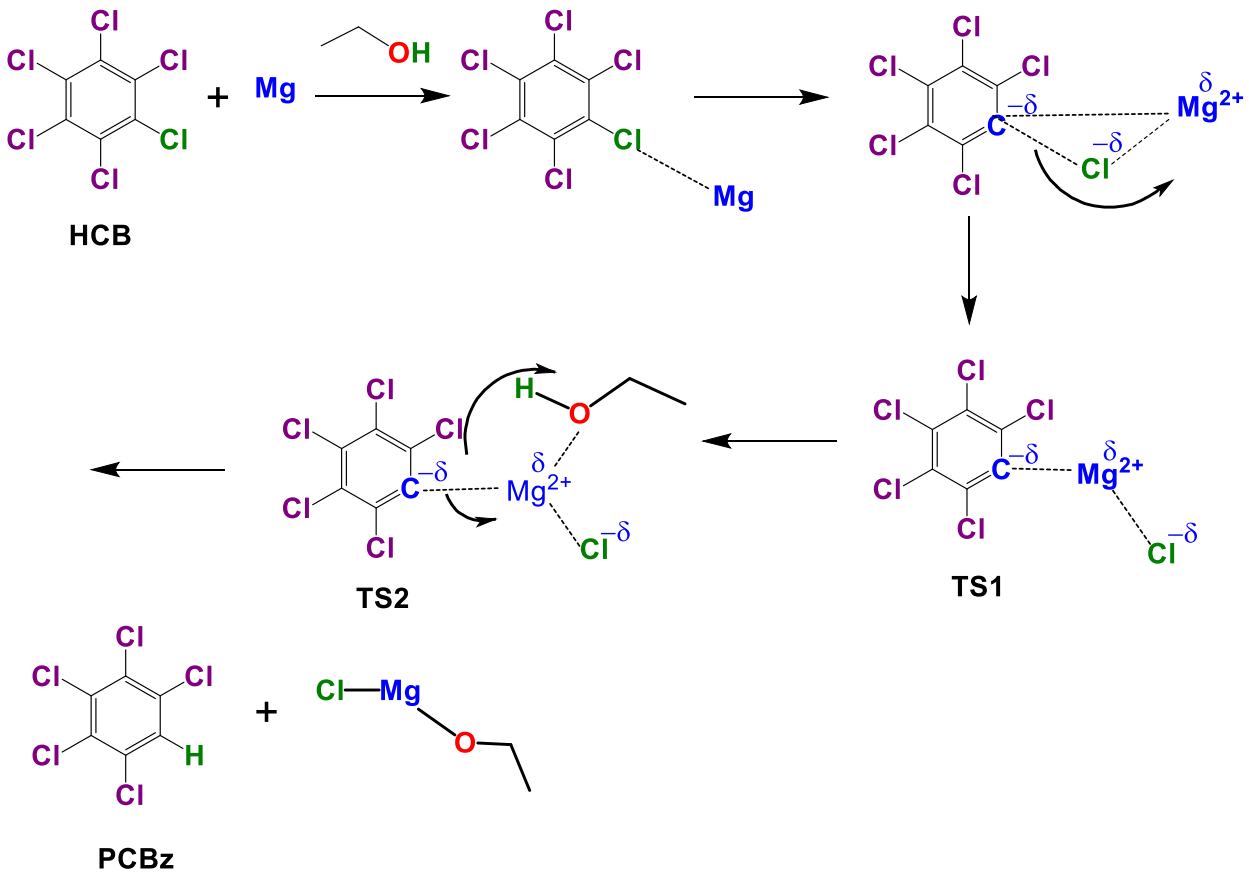

Figure 11: Proposed hydrodechlorination mechanism for HCB by ZVMg/C in 1:1 ethanol:ethyl lactate solvent.

An energy scheme of the ionic channel through which the removal of the first chlorine atom on HCB is removed is shown in Figure 12. The rate limiting step in which TS1 is formed from HCB is represented by the first curve, and then it is shown that TS2 is formed at a much lower energy level, corresponding to its relatively minimal energy of activation. The PCBz product is then formed very rapidly in an exothermic reaction. This process will repeat with the chloro groups that have been removed experimentally, and may persist as long as the metal is still active.

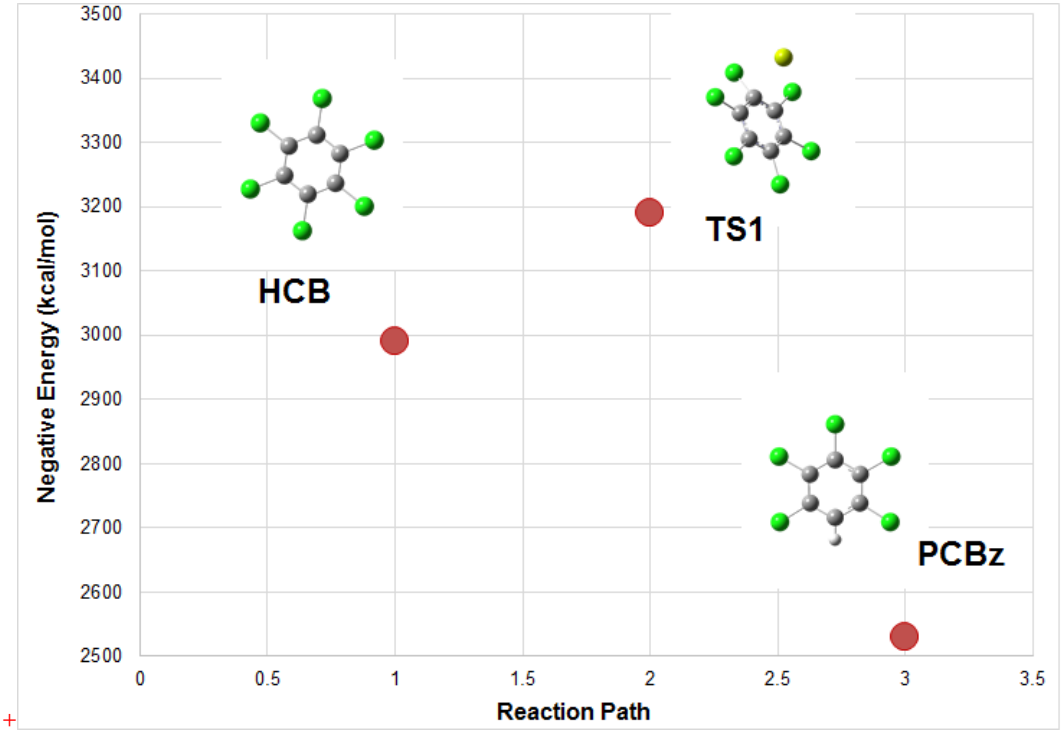

Figure 12: Energy scheme of the ionic mechanism for HCB dechlorination.

Conclusion

In the studies that were performed at ambient conditions, ball-milled ZVMg was proven to be more efficient than iron or zinc as a reagent for the reductive treatment of HCB, and possibly other chlorinated benzenes. Within the detection limits of the GC-MS, nearly 100% of the HCB was found to be degraded within the first 30 min of the study, and the majority of the HCB degradation occurred within the first ten minutes. PCBz, as well as other lower-chlorinated congeners such as tetra-, tri- and dichlorobenzenes, were identified and quantified using GC-MS methodology. However, no monochlorinated benzene or benzene itself were detected. The main dechlorination pathways of HCB in 1:1 ethanol/ethyl lactate were HCB → PCBz → 1,2,4,5-TCB; 1,3,4,5-TCB → 1,2,4-TriCB; 1,3,5-TriCB → 1,4-DiCB; 1,3-DiCB. The reaction kinetics followed

a pseudo-first order trend, and degradation rates were found to be slower for lower-chlorinated congeners. The average mole balance observed over a nine day study was 79.2%. Experimental results were consistent with quantum mechanical calculations showing the same ΔG values for the predicted degradation reaction pathways. Other calculations that were performed were successful in explaining the reaction mechanism and showing that it took place through ionic transition states in a Grignard-Zerewitinoff-like reaction. Ultimately, reductive dechlorination using zero-valent metals in conjunction with bioremediation will provide a safe and effective way to overcome challenges seen in the remediation of lower-chlorinated aromatic compounds, with possible applications for aliphatic halohydrocarbons.

CHAPTER THREE: DEGRADATION COMPARISON OF PENTACHLOROPHENOL VERSUS PENTACHLOROANISOLE

Introduction

Background

Chloroanisoles are extremely toxic, possibly carcinogenic compounds**(Cheng, Ekker et al. 2015)** which have a strong tendency to accumulate in the environment. Compared to chlorophenols, which have a hydroxyl substituent, chloroanisoles are less toxic but have a methoxy substituent which is the source of their lipophilic nature.**(Goswami, Recio et al. 2007)** Because of this lipophilicity, chloroanisoles tend to bioaccumulate in the tissue of living organisms such as rats, mice and certain fish**(Goswami, Recio et al. 2007)**, where they can be converted into much more toxic chlorophenols.**(Campoy, Alvarez-Rodriguez et al. 2009)** In a 2015 publication, an ecotoxicological study**(Cheng, Ekker et al. 2015)** on the effects of PCA on the development of zebrafish has shown morphological deformation and developmental problems with the central nervous system, and an imbalance of hormone levels. For the same reason, chloroanisoles have a tendency to resist biodegradation in soils and humic materials, where they may stay for decades. However, due to the high Henry's Law constant of most chloroanisoles, volatilization from moist soils is possible. If found in aquatic environments, chloroanisoles cannot convert to chlorophenols through hydrolysis, but can accumulate in the atmosphere, with estimated half-lives of 5.7 hours in rivers and 6.9 days in lakes.**(Cserjesi and Johnson 1972)** As chloroanisoles exist as vapors in the atmosphere, they undergo photochemical reactions which produce hydroxyl radicals and have a half-life of 15 days.**(Meylan and Howard 1993)** Their mobilization in aquatic and terrestrial

environments, as well as the atmosphere, has allowed chloroanisoles to find their way into the oils and fats of certain foods and organic constituents in beverages. One chloroanisole in particular, 2,4,6- trichloroanisole (2,4,6-TCA), is responsible for fungi which spoil the aroma of certain beverages such as wine and sake, and foods such as chicken, eggs and dried fruits; this causes great expense to industries, particularly wine making.**(Carasek, Cudjoe et al. 2007, Goswami, Recio et al. 2007, Recio, Alvarez-Rodriguez et al. 2011, Bai, Zhang et al. 2016)**

Sources of PCA in the environment

Although PCA has been used industrially it is not manufactured for commercial use, despite its presence in the environment.**(Yuan, Goehl et al. 1993, Cheng, Ekker et al. 2015)** Compounds that come from pesticides and industrial wastes, such as hexachlorobenzene (HCB), pentachloronitrobenzene (PCNB) and hexachlorocyclohexane (lindane), can be the source of pentachlorophenol (PCP), which exists in equilibrium with pentachloroanisole (PCA) in the environment as shown in Figure 13.**(Marco and Kishimba 2007)** Therefore, the presence of PCA is indicative of PCP and PCNB contamination from a nearby source.**(Marco and Kishimba 2007)** Also, due to the fact that anisoles are less toxic to prokaryotes than to eukaryotes, methylation of PCP to PCA is catalyzed in the environment under aerobic conditions by microorganisms found in soils and sediments.**(Lamar and Dietrich 1990, Marco and Kishimba 2007, Vorkamp and Riget 2014)** This can be dangerous to humans and other eukaryotes since the production of PCA can occur in buildings with moist conditions, where the scent of mold can indicate their presence.**(Lorentzen, Juran et al. 2016)** Since PCA is a microbial volatile organic compound (MVOC), it can propagate through the air and cause adverse health effects to those undergoing exposure.**(Lorentzen, Juran et al. 2016)**

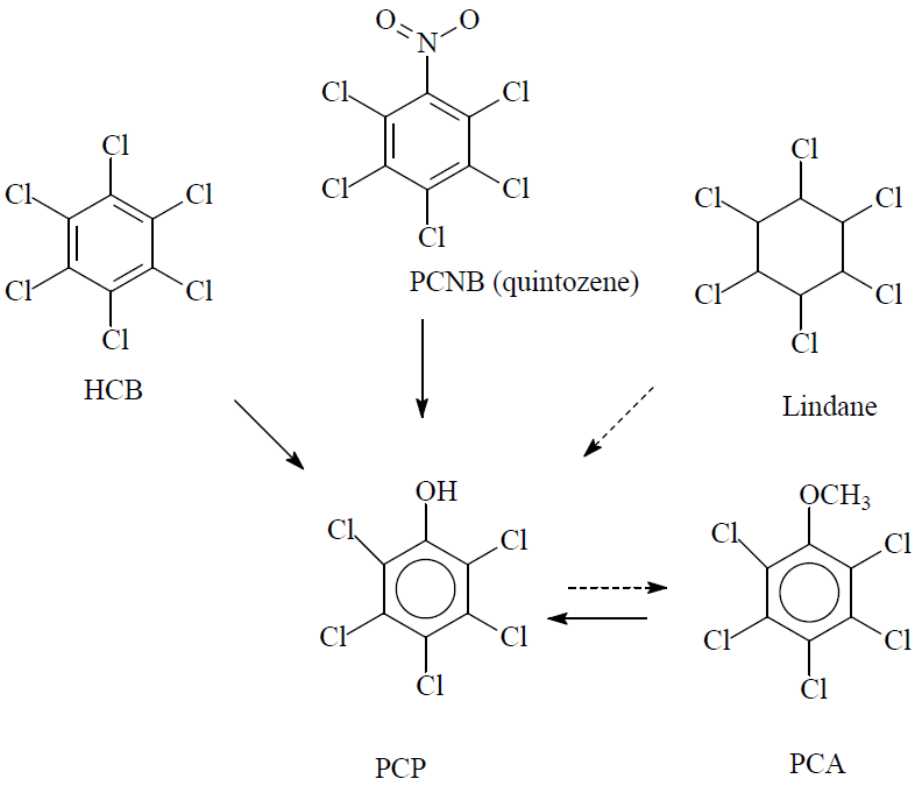

Figure 13: Examples of several sources of PCP in the environment.

Current Treatment for PCA Contaminated Materials

Despite the known toxicological effects of PCA on living organisms and the economic strain it imposes on the food and beverage industries, minimal work has been done on developing a technique for its remediation.**(Goswami, Recio et al. 2007)** Biodegradation studies on trichloroanisoles (TCAs, particularly 2,4,6-TCA) have been conducted using certain strains of bacteria, the most successful being *Xanthomonas retroflexus* INBB4.**(Bai, Zhang et al. 2016)** However, this species was only able to remove one chloro group, transforming the 2,4,6-TCA into 2,6-dichloro-para-hydroquinone (2,6-DCHQ), which was then be mineralized.**(Cheng, Ekker et al. 2015)** Complete dechlorination of 2,4,6-TCA has been accomplished by the same group

through biodegradation using an enzyme from white-rot fungi which produced 1,2,4-trihydroxylbenzene (1,2,4-THB), which mineralized into CO_2, H_2O and Cl^-.**(Campoy, Alvarez-Rodriguez et al. 2009)** Alternatively, chemical methods involving activated peroxides have been found to dechlorinate both TCA and PCA. These methods make use of catalysts such as Cu^{2+}, Co^{2+}, Mn^{2+} or MoO_4^{2-} to activate hydrogen peroxides, forming high-energy hydroxyl or singlet-oxygen radicals which are very destructive to the anisolic compound found in the corks of wine bottles.**(Recio, Alvarez-Rodriguez et al. 2011)** These methods are safe, practical and affordable, but more work needs to be done to optimize their industrial implementation. Treatment of mono-**(Quint, Park et al. 1996, Quint 2006)** and tri-chlorinated**(Careri, Mazzoleni et al. 2001)** anisoles using radiolysis in neutral aqueous media and heptane, respectively, has also been investigated, with successful degradation as monitored by chromatography. However, this technique is expensive and can lead to the formation of high-energy radicals.

Since chlorophenols and chloroanisoles coexist in the environment, the main objective of this research is to compare degradation techniques of chlorophenols to those of chloroanisoles, thereby determining if one can be applied towards the remediation of both. The direction of the research, which has been influenced by remediation technologies involving the redox reactions that occur on the surface of zero-valent metals, will continue in accordance with the success seen using zero-valent magnesium (ZVMg). ZVMg, which has a greater redox potential than that of iron or zinc, in addition to lower oxide obstruction on its surface than that of iron**(De Vor, Carvalho-Knighton et al. 2009)** and lower toxicity than zinc,**(Kim and Carraway 2003)** is the preferred candidate for the zero-valent metal used in this study.**(Doyle, Miles et al. 1998)** Catalysts such as palladium have been used in conjunction with magnesium in the past, and have shown

enhanced reaction kinetics.**(Doyle, Miles et al. 1998)** However, ball-milling with graphite has been proven to improve reactivity at a lower cost by activating of the surface of the magnesium and keeping it clean of oxide layer formation.**(Elie, Clausen et al. 2012, Elie, Clausen et al. 2013)** Systems using the reduction potential of ZVMg ball-milled with graphite to form a homogeneous powder, referred to as ZVMg/C, have been used in previous studies to successfully dechlorinate PCP, as explained in detail in Chapter 1 of this dissertation. In this study the technology being used relies upon the reduction potential of ball-milled ZVMg/C to degrade PCA in an acidified ethanol solvent system. Kinetic studies were performed to test the efficacy of the ZVMg/C reaction system and results were compared to those for PCP.

Methods

Materials and Chemicals

Neat PCA standards were provided from Accustandard and standard solutions were prepared by diluting the neat standard to the required concentrations in absolute ethanol solution. Absolute ethanol and Optima® grade n-hexane, 95%, were supplied from Fisher Scientific (Ottawa, ON.). Glacial acetic acid (≥99.8) was obtained from Acros Organics through Fisher Scientific. Micro-scale unmilled magnesium (~4 µm) was acquired from Heart Metals, Inc. (Tamaqua, PA). PCB-153 (2,2',4,4',5,5'-hexachlorobiphenyl) was purchased from Accustandard and utilized as an internal standard for the analyses. Helium gas, used for gas chromatography-mass spectrometry (GC/MS) analysis, was purchased from Air Gas (Atlanta, GA). All chemicals were of high purity (≥98%) and ACS reagent, analytical grade. All chemicals were used as they were received unless otherwise specified. A precision microscale analytical balance (Model AE 260-S from Mettler-

Toledo AG, Greifensee, Switzerland) was utilized in the measurement of Mg loadings. Standards and solutions were dispensed using 50, 100 and 1000 µL (calibrated) Eppendorf Research® pipettes (from Eppendorf, Hamburg, Germany).

Ball-milling Procedure

The activity of the magnesium is enhanced through ball-milling using the process described in Chapter 1 & 2, by which the passivated hydroxide/oxide surface layer can be cracked, thus creating more defects in the surface which allow change to the microstructure.**(Maloney, DeVor et al. 2011)** In this study, magnesium carbon (Mg/C) was ball-milled under optimized conditions. The ball-milling was accomplished using a Red Devil 5400 series paint shaker fitted with custom-made plates to support milling canisters, which accommodated a rotation of 670 rpm for the process of ball-milling the metal.**(Coutts, Devor et al. 2011)** The canister and balls are made of stainless steel. To prepare ~10 wt% ball-milled magnesium/carbon, 76.5 g Mg powder and 8.5 g of graphite (C) were mixed into the canister with 16 stainless steel balls of 1.5 cm diameter having a total mass of 261.15 g, corresponding to a 3:1 ball/powder mass ratio. The canister was sealed under an argon atmosphere. The material was ball-milled for 30 minutes using the aforementioned paint mixer.

Experimental procedure

The reaction was performed exactly the same as in Chapter 2, using 20 mL clear glass vials with 250 mg of ball-milled Mg/C and 4.95 mL of a 20 ng/µL (71.34 µM) PCA in ethanol solution. Next, 50 µL of glacial acetic acid were added and the vials were secured on a SK-300 shaker table set to 200 rpm at room temperature (~21 °C) for the appropriate amount of time. At the designated time

points, the reaction vials were detached from the shaker table, extracted in 5 mL of hexane and shaken for 2 minutes. After that, samples of the solution were filtered using nylon syringe filters with 0.45 µm pores. The resulting filtered solutions were then added to glass centrifuge tubes with 4 mL of D.I. water and centrifuged for 10 minutes. The organic supernatant containing the PCA was removed then transferred to clean 4 mL glass screw-cap vials. Then 950 µL from each vial were pipetted into autosampler vials for analysis, along with 50 µL of PCB-153 solution as an internal standard.

Analysis

The samples were run in triplicate. The hexane extracts were analyzed for left over PCA and its degradation byproducts on an Agilent 7820A series II GC-MS furnished with an autosampler and an Agilent 5977E mass spectrometer. The capillary column used was an Rxi®-5ms (30 m × 0.25 mm i.d.; 0.25 µm film thickness) with helium as a carrier gas, a flow rate of 2.0 mL/min, and an average gas velocity of 51.016 cm/s. The oven temperature program was set according to the following method: after warming up to an initial temperature of 50 ˚C for 4 minutes, the column was ramped up at a rate of 10 ˚C/min to 250 ˚C and held for 2 minutes prior to cooling down. The injector and detector temperatures were maintained at 250 and 280 ˚C respectively. Injection volumes were set at 3 µL and were executed in pulsed splitless mode. A calibration plot for PCA was prepared within the appropriate concentration range and was found to be linear with a correlation coefficient value of about 0.99. The identities of the eluted compounds were confirmed by running PCA and anisole standard solutions and comparing the mass spectra of the samples to mass spectra referenced from the catalog of the National Institute

of Standards and Technology (NIST). The degradation rate was measured by the disappearance of the PCA peak and confirmed by the formation of lower chlorinated congeners.

Results and Discussion

Degradation rate of PCA compared to PCP with ball-milled ZVMg/C

A kinetic study on PCA degradation using a treatment system of ball-milled ZVMg/C was performed at room temperature using an initial analyte concentration of 71.34 μM in a closed vial with ethanol and glacial acetic acid. The data for this study was compared with that from the PCP study, which is detailed in Chapter 1. Figure 14 shows the comparison of the decrease in concentration of both analytes, as measured by GC-MS, plotted against time. The results for reduction in concentration show that the degradation percentage of PCA at the 2 min time point was 31.7%. An abrupt decrease of 86.2% in PCA concentration took place at approximately 7 min. Between 7 minutes and 4 hours, concentration reduction decreased at a more gradual rate, with just a trace amount of the analyte detected at the 4 hour mark. No PCA was detected at the 6 hour time point. In comparison, the overall degradation rate of PCP was much steadier, however its rate of degradation was much faster than that of PCA.

Concentration and mole balance for daughter compounds of PCP and PCA over time

Over a two-week time period, the formation of degradation byproducts of PCA were analyzed as samples were extracted periodically and run on a GC-MS. As indicated by the results of the GC analysis in Figure 15a, the products of PCA degradation were characterized to be lower chlorinated anisoles. Among the twelve different byproducts observed, there were two tetra- (first

appearing at 5 min.), five tri- (first appearing at 10 minutes), three di- (first appearing at 45 minutes [with 2,4-DiCA appearing in the greatest abundance]), and one monochlorinated anisole (first appearing at 1 day in trace amounts), as well as trace amounts of completely dechlorinated anisole (first appearing at 4 days). Faster rates of degradation occurred with the more highly chlorinated anisoles, such as the two tetrachlorinated congeners which disappeared after 20 minutes. Two of the dichlorinated congeners: 2,4,6-TriCA (previously mentioned to be responsible for the odors found in wine) and 2,3,6-TriCA, were gone after one hour while detection of 3,4,5-, 2,3,5- and 2,4,5-TriCA ceased after two, four and fourteen hours, respectively. All of the dichlorinated, monochlorinated and non-chlorinated anisoles were detected until the end of the study. The observed mole balances for both analytes were satisfactory, with PCA having a 92.6% mole balance and PCP a 94.8% mole balance.

In the six-day time period during which the degradation study for PCP took place, a greater rate of disappearance for the concentration of the analyte was observed in a shorter time than for the PCA study. This agrees with the trend observed in studies which have compared the rate of biodegradation for the two analytes.**(Goswami, Recio et al. 2007)** As seen in Figure 15b, 13 different byproducts were generated during this study including two tetra-, three tri-, four di- and three monochlorinated phenols, as well as phenol. As observed in the degradation study for chloroanisoles, there was an agreement in the faster degradation rate for higher-chlorinated CP congeners, and the major product was also found to be the 2,4-DiCP congener of dichlorophenol, although the overall yield was lower than 2,4-DiCA. In contrast to the PCA study, the dichlorinated congeners all appeared in much smaller concentrations, with the 3,5-DiCP congener being completely removed. The final concentration of phenol was much lower than that of the final

concentration of anisole, indicating that more of the di- and mono-congeners were converted to phenol.

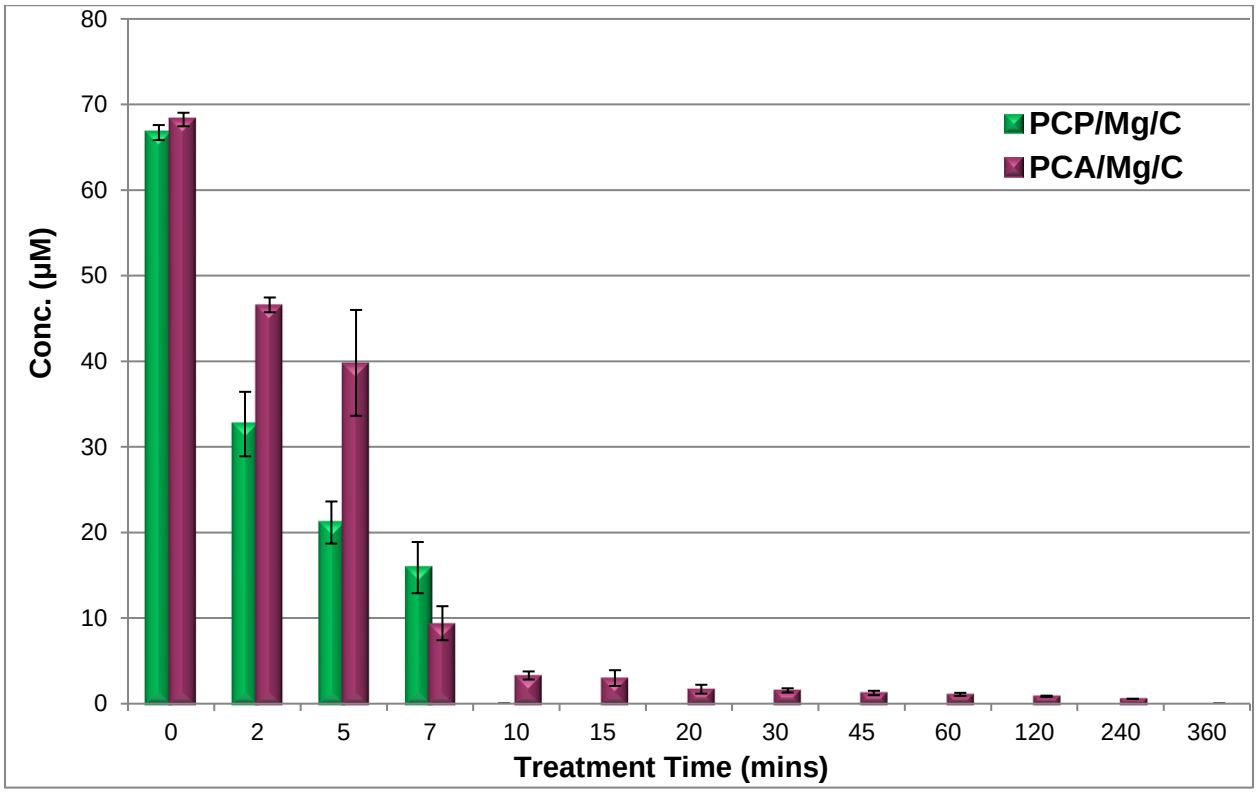

Figure 14: PCA and PCP degradation with the activated ZVMg/C system after 6 hours of treatment in acidified ethanol.

One possible side-reaction that may impose a hindering effect on the degradation of either analyte is the formation of either magnesium hydroxide or magnesium ethoxide ($MgOH/Mg(OCH_2CH_3)_2$) from the ionization of magnesium in the ethanol solvent system.**(Cass, Freitas et al. 2000)** A solid white hydroxide/ethoxide precipitate may adsorb onto the magnesium metal surface, thereby blocking the active sites. This may contribute to a significant reduction in the degradation rate of the analyte, shown by a leveling-off in the rate of decline in concentration

which is observed after approximately 24 hours for both PCA and PCP, however with a more constant plateau for PCA. Possible evidence of this can be perceived in the difficulty experienced while filtering the samples. Further studies have been conducted to optimize the reactivity of this system, and are discussed in the following section.

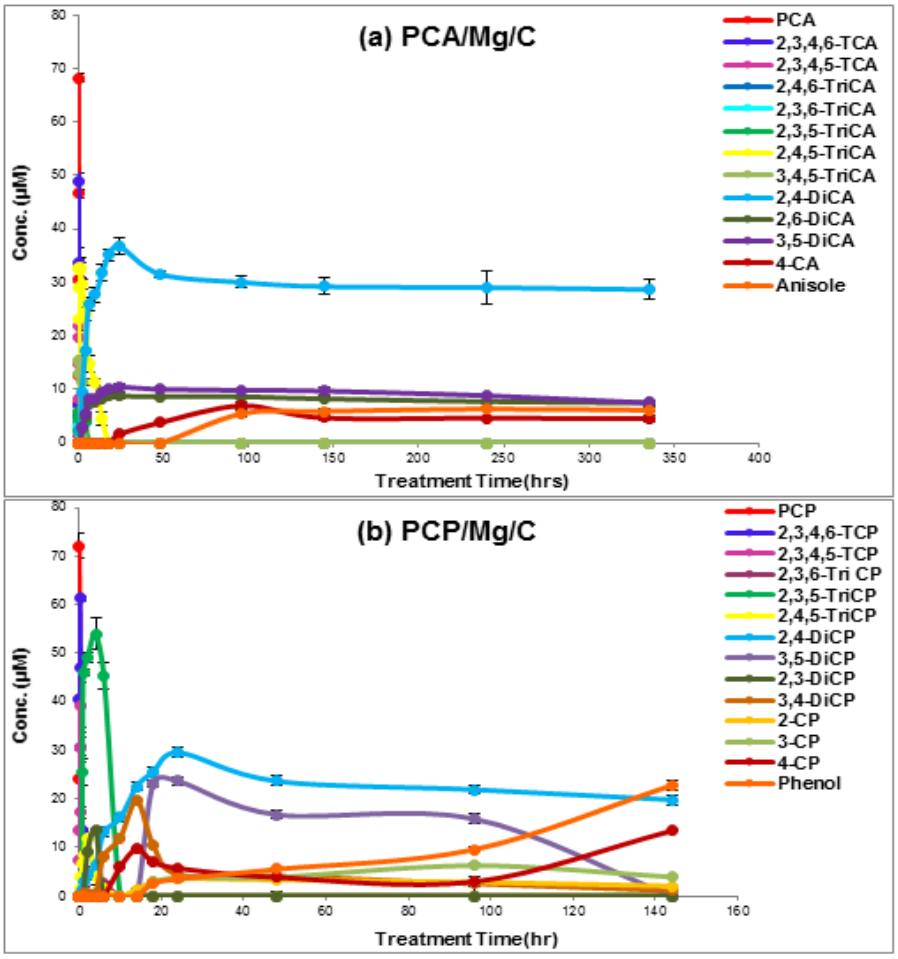

Figure 15: Experimentally observed degradation byproducts of (a) PCA after two weeks of treatment, and (b) PCP after six days of treatment with the activated ZVMg/C reduction system in acidified ethanol.

Dechlorination of PCA by ball-milled ZVMg/C in acidified ethanol with periodic addition of acetic acid

In a more recent kinetic study on the degradation of both PCA and PCP with ZVMg/C, samples were prepared in the same way using an ethanol solution spiked with glacial acetic acid and then attached to the shaker table for two weeks. Instead of a Thermo Scientific MaxQ 4000 shaker table, an SK-300 shaker table was used at ~21 ˚C instead of 26 ˚C. The samples were then detached so that 50 more µL of the glacial acetic acid could be added, and the samples were then shaken for two more weeks. Analysis of the samples for the concentration of both analytes and degradation byproducts was then completed using the same GC-MS. Figure 16 shows a decrease in the variety of congeners observed as byproducts for both analytes, although all of them are relatively low in number of chloro groups substituted. There were three degradation byproducts of PCA: 2,4-DiCA, 3,5-DiCA and 4-CA. PCP yielded six different byproducts: 3,5-DiCP, 2,4-DiCP, 3,4-DiCP, 2-CP, 3-CP and 4-CP. The number of congeners observed as byproducts for each analyte did not change, however there was an increase in the di- and monochlorinated byproducts of both analytes, indicating progress in the reduction of the congeners. The major product observed for PCA degradation was 2,4-DiCA, and that of PCP degradation was 4-CP. Neither anisole nor phenol were produced from this study. The change in reaction conditions may have been responsible for this, either due to the change in the motion of the shaker table (from a rocking motion to an orbital motion), but most likely due to the change in temperature. Further work, including SEM imaging of the metal surface, needs to be done to establish the reason for the incomplete degradation observed.

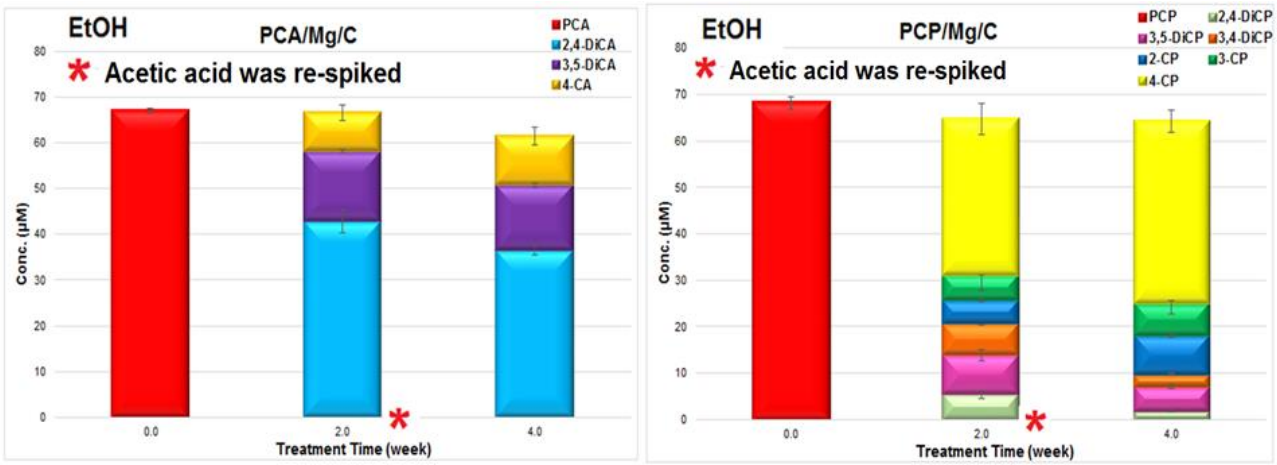

Figure 16: Degradation of PCA and PCP by ball-milled ZVMg/C in acidified ethanol with addition of acetic acid after two weeks.

Degradation of PCA with ZVMg/Pd system based on prior work with PCP

In a previous effort to dechlorinate PCP, a ball-milled mixture of zero-valent magnesium and palladium was used in the aforementioned acidified ethanol solvent system. The results showed that, over one week, complete dechlorination of PCP to phenol was achieved. In order to produce similar success with PCA, a new study was conducted in which a trace amount (~0.1%) of palladium was ball-milled with the zero-valent magnesium and applied to the reaction system. The results in Figure 17 show that the palladium was a success, and that by one week PCA was dechlorinated completely to anisole (left). However, no anisole started to form until 24 hours after the beginning of the reaction; whereas the first trace amounts of phenol were detected within the first four hours of the PCP study (right) on which this PCA study was based. At four hours, there were still trace amounts of PCA present in solution, whereas all PCP was gone by then in the original study. At four days, all of the trichlorinated congeners of PCA byproduct were gone, leave

only 2,4-DiCA and anisole. Similarly, there was only one dichlorinated congener (3,4-DiCP) left with phenol at the four-day time point of the PCP study. Overall, the results proved to be satisfactory for the one-week complete dechlorination of both analytes using the zero-valent magnesium system with support from only trace amounts of palladium. The use of palladium, even at such a low amount, is still impractical for field applications and further experiments will be done to improve the ZVMg/C system.

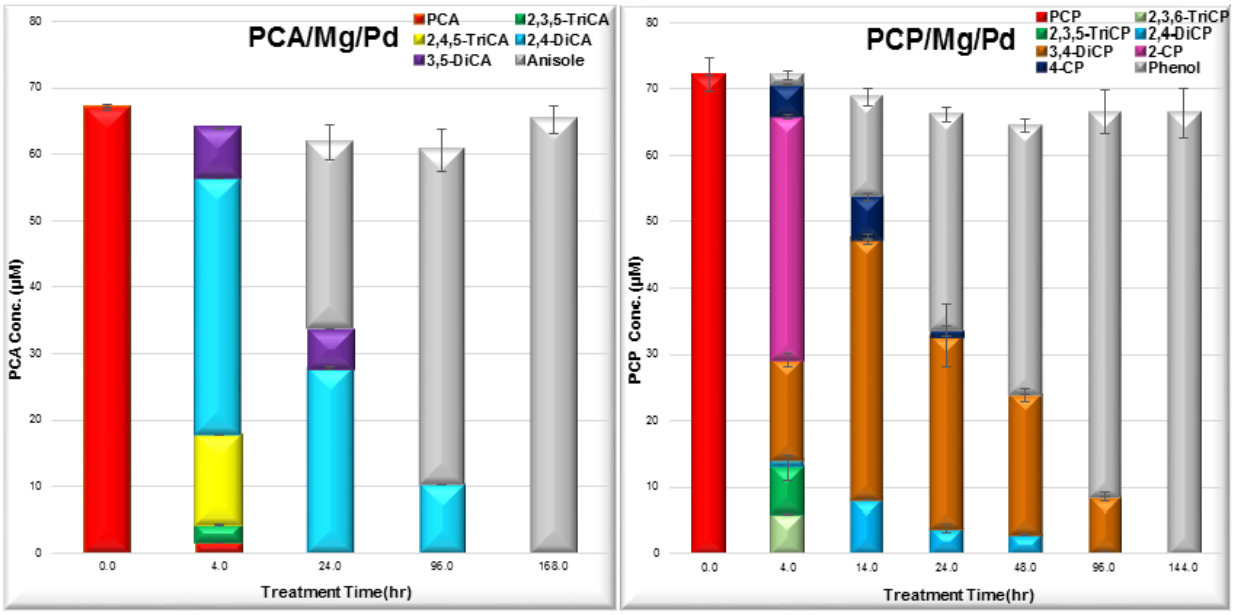

Figure 17: One week study for the degradation of PCA and PCP by ball-milled ZVMg/Pd in acidified ethanol.

Degradation kinetics and suggested effect on the reaction mechanism

In previous kinetic studies, data has been shown to follow a pseudo-first order trend with respect to the rate of analyte degradation in the presence of excess zero-valent metal **(Elie et al.,**

2013). As reported in Chapter 1, results from the PCP degradation kinetic study were obtained using concentrations of 10.42 mmol of ZVMg/C and 0.375 mmol of PCP, corresponding to a molar ratio of 28:1 (Mg:PCP). The data from the results showed an expected trend of pseudo-first order kinetics. Under the same reaction conditions with PCA as the target analyte, a pseudo-first order trend was also confirmed. The data in Figure 18, which corresponds to the decline in PCP and PCA concentrations, were plotted following a pseudo-first order model showing coefficients of determination (R^2 values) of 0.9464 and 0.9793 for PCP and PCA, respectively. As shown in Figure 18, the rate constant of PCP degradation is slightly higher than that of PCA showing that it underwent dechlorination at a marginally faster rate.

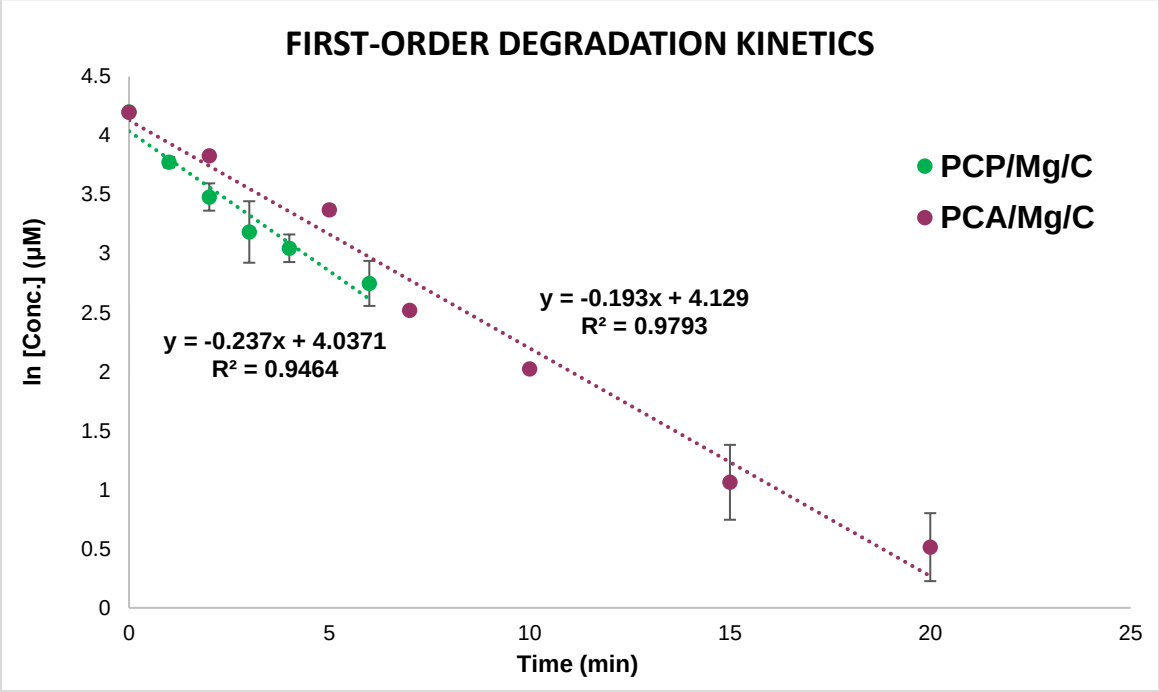

Figure 18: Pseudo-first-order kinetics plot for PCA and PCP degradation with activated magnesium reducing systems in acidified ethanol.

A possible explanation for the difference in reaction kinetics is the difference in the strength of electron withdrawing groups between the substituents. PCA has a methoxy group on the ring, which is electron-withdrawing by induction. However, since the oxygen atom is attached to an aryl group on one side and to a methyl group on the other side, this weakens the inductive effect of the oxygen rendering the chloro substituents on the ring richer in electron density. On the other hand, PCP, which has a hydroxyl substituent, experiences stronger inductive electron withdrawing effects from the oxygen atom due to the lack of electron donation from the hydrogen to which it is bonded. As suggested by the computational data in Chapter 2, the lowest energetic pathway for the dechlorination reaction of hexachlorobenzene in the same reaction solution is through the mechanism of the Grignard-Zerewitinoff-like reaction. If this is also the lowest-energy pathway for the dechlorination of PCP and PCA then the zero-valent magnesium, which has a thermodynamic preference for the ionization to Mg^{2+}, is more attracted to the electron-deficient chloro substituent of the PCP ring, therefore causing the expected PCP Grignard reagent to form at a faster rate.

Conclusion

Chloroanisoles are compounds that exhibit similar properties to and coexist in equilibrium with chlorophenols. Although they are less toxic than chlorophenols, their methoxy substituent makes them more lipophilic and causes them to have higher bioaccumulation and more resistance to biodegradation than chlorophenols. One specific congener, 2,4,6-TCA, is responsible for the contamination of certain foods and beverages, chiefly the tainting of corks used in wine bottles. Chloroanisoles are not manufactured for commercial use; however they can be synthesized in

nature from chlorophenols through biotransformation and biomethylation. Therefore, work needs to be done to develop methods of treatment for both PCA and PCP. Despite the toxicological effects and economic detriment resulting from the presence of PCA in the environment, little work on the remediation of chloroanisoles has been published. This study has served to develop an approach to meet the needs for this treatment based on the approach for the treatment of PCPs discussed in Chapter 1. The results of the method, which makes use of ZVMg/C in acidified ethanol, are compared for both target analytes. As reported from the results that were found within the GC-MS detection limits, complete degradation of PCP to less chlorinated byproducts was achieved within the first seven minutes while PCA degradation was completed within the first four hours, with the majority of the degradation occurring within the first seven minutes. The rate of degradation was higher for the more heavily-chlorinated byproducts, with the 2,4-disubstituted congeners of each substrate favored as major degradation byproducts. There was a satisfactory mole balance observed of 92.6% for PCA and 94.8% for PCP. After ~24 hours, the rate of degradation plateaued for each analyte, with a more consistent trend of stagnation for PCA. A possible explanation for the termination of the reaction is an obstructing effect imposed on the active site of the zero-valent magnesium via the formation of either magnesium hydroxide or magnesium ethoxide ($MgOH/Mg(OCH_2CH_3)_2$). Further studies were done in order to overcome the difficulties presented by the ethoxide formation. In a recent four-week experiment, samples of PCP and PCA were re-spiked with acetic acid after two weeks of degradation in order to facilitate lasting effects of the reaction system. Although complete degradation was still not achieved, even after re-spiking, the kinetic data from both experiments agreed that PCP can be degraded to its major product of 4-CP at a higher rate than PCA can be degraded to its major product of 2,4-DiCA.

One study has shown that complete degradation of either substrate is accomplished through the use of ZVMg/Pd in one week, but this is an impractical approach for environmental remediation. Kinetic data has shown that the reaction rate for the degradation of both PCP and PCA follow a pseudo first-order trend. PCP has a slightly higher rate constant, which may be due to the stronger inductive effects of the hydroxyl substituent. Ultimately, the conditions for the reductive dechlorination reaction of PCA and PCP using ZVMg/C in an acidified ethanol system need to be optimized in order to achieve complete degradation so that this system can be put into practice for large-scale *in situ* remediation of PCA and PCP. SEM analysis on the surface of the metal will be performed before and after ball-milling in order to characterize the barrier imposed upon the reactive site.

CHAPER FOUR: CONCLUSIONS

From a practical point of view, the study from Chapter 1 demonstrated that ball-milled magnesium powder with various amendments can be an excellent candidate for treatment of CPs. Magnesium has dramatically enhanced reactivity for PCP degradation in comparison with other metals, including iron and zinc. Lower CPs can also be treated by magnesium, even if they showed slower reaction rates than PCP. It should be noted that the more chlorine on the phenol ring, the more toxic are the CPs **(Kim and Carraway 2003)** and magnesium has higher reactivity for highly CPs, making the reduction of higher chlorinated, more toxic CPs rapid and favorable. The results of these studies indicate that all magnesium systems were powerful for PCP degradation, no PCP was detected after 30 minutes of degradation and the majority of the PCP degradation occurred within the first four minutes with ball-milled ZVMg/C. After 30 minutes, mechanically alloyed Mg/Pd proved to be the most efficient system for the PCP dechlorination with a matrix consisting of at least 0.02 g Mg^0/mL ethanol and 10 µL acetic acid/mL ethanol, in which case 20 ng/µL of PCP was dechlorinated to phenol in approximately 15 minutes with a carbon mass balance of 94.89%. The dechlorination kinetics showed an increasing trend in the order of ZVMg < ZVMg/Pd < ZVMg/C for the PCP degradation. However, the increasing trend of kinetics for the phenol formation (complete dechlorination) was in the order of ZVMg < ZVMg/C < ZVMg/Pd.

In the studies that were performed, ball-milled ZVMg/C was proven to be more efficient at ambient conditions than iron or zinc as a reagent for the reductive treatment of HCB, and possibly other chlorinated benzenes. Within the detection limits of the GC-MS, nearly 100% of the HCB was found to be degraded within the first 30 min of the study, and the majority of the HCB degradation occurred within the first ten minutes. PCBz, as well as other lower-chlorinated congeners, such as tetra-, tri- and dichlorobenzenes were identified and quantified using GC-MS methodology. However, no monochlorinated benzene or benzene itself were detected. The main dechlorination pathways of HCB in 1:1 ethanol/ethyl lactate were HCB → PCBz → 1,2,4,5-TCB; 1,3,4,5-TCB → 1,2,4-TriCB; 1,3,5-TriCB → 1,4-DiCB; 1,3-DiCB. The reaction kinetics followed a pseudo-first order trend, and degradation rates were found to be slower for lower-chlorinated congeners. The average mole balance observed over a nine day study was determined to be 79.2%. Experimental results were consistent with quantum mechanical calculations showing the same ΔG values for the predicted degradation reaction pathways. Other calculations that were performed were successful in explaining the reaction mechanism and showing that it took place through ionic transition states in a Grignard-Zerewitinoff-like reaction. Ultimately, reductive dechlorination using zero-valent metals in conjunction with bioremediation will provide a safe and effective way to overcome some of the challenges that were seen in the past with the remediation of lower-chlorinated aromatic compounds, with possible application for aliphatic halohydrocarbons.

Chloroanisoles are compounds that exhibit similar properties to and coexist in equilibrium with chlorophenols. Although they are less toxic than chlorophenols, their methoxy substituent makes them more lipophilic and causes them to have higher bioaccumulation and more resistance to biodegradation than chlorophenols. One specific congener, 2,4,6-TCA, is responsible for the

contamination of certain foods and beverages, chiefly the tainting of corks used in wine bottles. Chloroanisoles are not manufactured for commercial use; however they can be synthesized in nature from chlorophenols through biotransformation and biomethylation. Therefore, work needs to be done to develop methods of treatment for both PCA and PCP. Despite the toxicological effects and economic detriment resulting from the presence of PCA in the environment, little work on the remediation of chloroanisoles has been published. This study has served to develop an approach to meet the needs for this treatment based on the approach for the treatment of PCPs discussed in Chapter 1. The results of the method, which makes use of ZVMg/C in acidified ethanol, are compared for both target analytes. As reported from the results that were found within the GC-MS detection limits, complete degration of PCP to less chlorinated byproducts was achieved within the first seven minutes while PCA degradation was completed within the first four hours, with the majority of the degradation occurring within the first seven minutes. The rate of degradation was higher for the more heavily-chlorinated byproducts, with the 2,4-disubstituted congeners of each substrate favored as major degradation byproducts. There was a satisfactory mole balance observed of 92.6% for PCA and 94.8% for PCP. After ~24 hours, the rate of degradation plateaued for each analyte, with a more consistent trend of stagnation for PCA. A possible explanation for the termination of the reaction is an obstructing effect imposed on the active site of the zero-valent magnesium analyte via the formation of either magnesium hydroxide or magnesium ethoxide ($MgOH/Mg(OCH_2CH_3)_2$). Further studies were done in order to overcome the difficulties presented by the ethoxide formation. In a recent four-week experiment, samples of PCP and PCA were re-spiked with acetic acid after two weeks of degradation in order to facilitate lasting effects of the reaction system. Although complete degradation was still not achieved even

after re-spiking, the kinetic data from both experiments agreed that PCP can be degraded to its major product of 4-CP at a higher rate than PCA can be degraded to its major product of 2,4-DiCA. One study has shown that complete degradation of either substrate is accomplished through the use of ZVMg/Pd in one week, but this is an impractical approach for environmental remediation. Kinetic data has shown that the reaction rate for the degradation of both PCP and PCA follow a pseudo first-order trend. PCP has a slightly higher rate constant, which may be due to the stronger inductive effects of the hydroxyl substituent. Ultimately, the conditions for the reductive dechlorination reaction of PCA and PCP using ZVMg/C in an acidified ethanol system need to be optimized in order to achieve complete degradation so that this system can be put into practice for large-scale *in situ* remediation of PCA and PCP. SEM analysis on the surface of the metal surface will be performed before and after ball-milling in order to characterize the barrier imposed upon the reactive site.

APPENDIX A: SUPPORTING INFORMATION FOR CHAPTER ONE

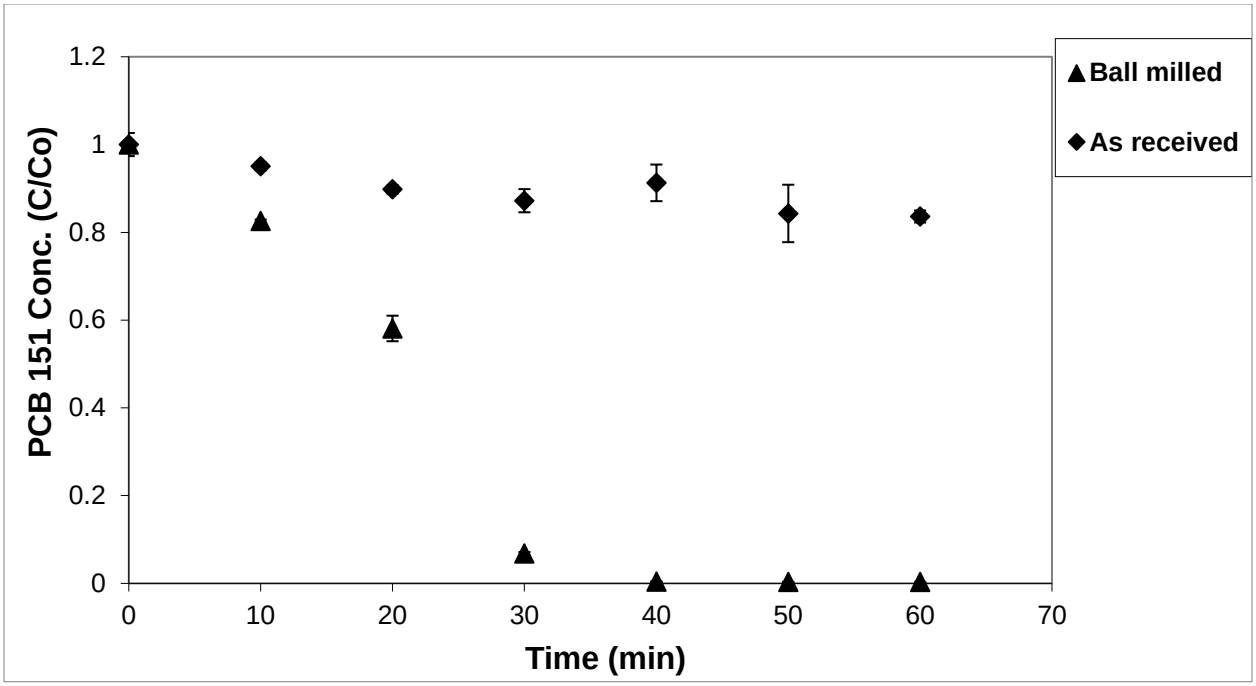

Figure 19: Comparison studies of PCB-151 degradation using ball-milled ZVMg powder vs. ZVMg powder as received. The ball-milling procedure is a beneficial activation process for the ZVMg powder since it significantly increases the rate of dechlorination of PCBs.[*]

([*]Maloney, P.; DeVor, R.; Novaes-Card, S.; Saitta, E.; Quinn, J.; Clausen, C. A.; Geiger, C. L., Dechlorination of polychlorinated biphenyls using magnesium and acidified alcohols. *J. Hazard. Mater.* **2011,** *187*, 235-240)

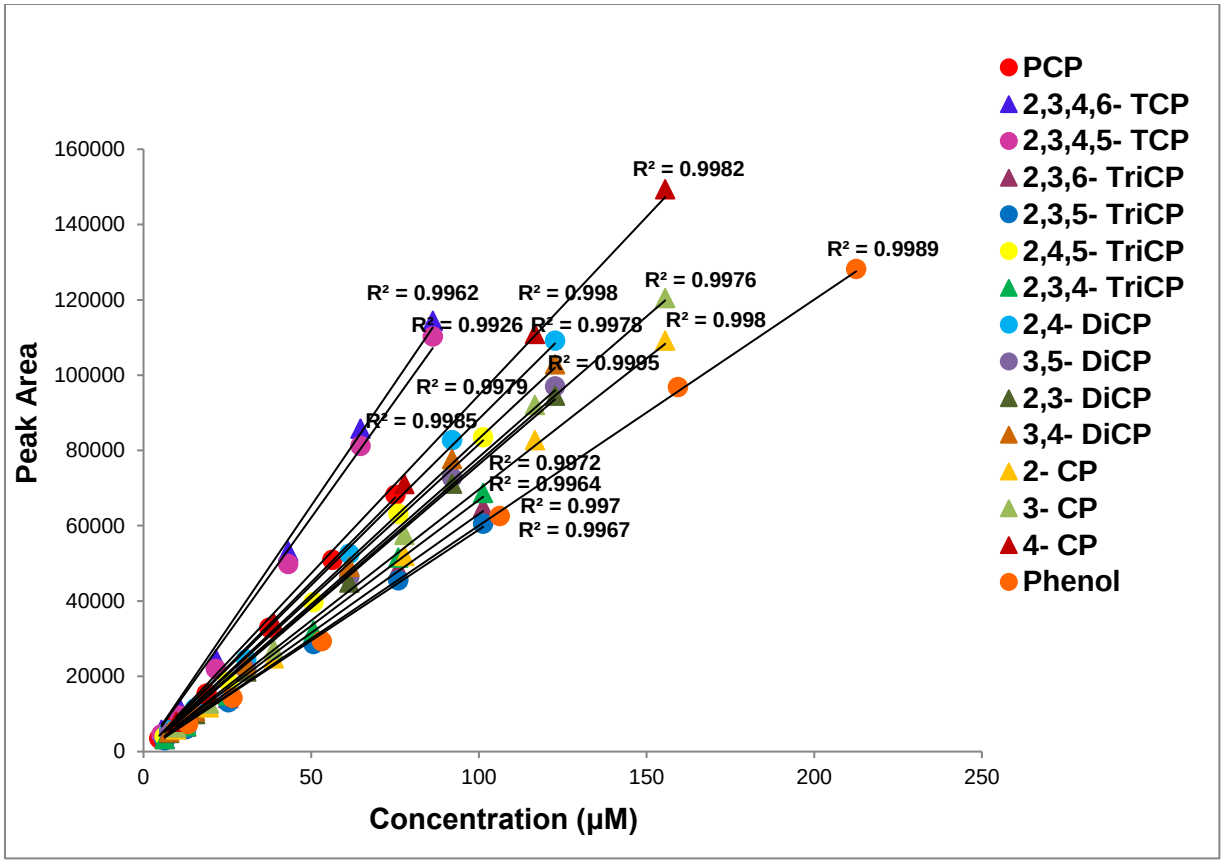

Figure 20: Calibration curves for PCP and its chlorinated byproducts.

Table 1: Mass Spectrometry (MS) Selected Ion Monitoring parameters for the degradation of PCP in ethanol and acetic acid.

Compound	**Retention Time (min)**	**Molecular Ion (m/z)**	**Fragment Ions (m/z)**
Pentachlorophenol (PCP)	11.983	266	264, 178, 152
2,3,4,6-Tetrachlorophenol (TCP)	10.086	232	230, 178, 165
2,3,4,5-TCP	9.928	-	-
2,3,6-Trichlorophenol (TriCP)	8.683	198	196, 165, 152
2,3,5-TriCP	8.187	-	-
2,4,5-TriCP	8.799	-	-
2,3,4-TriCP	8.509	-	-
2,4-Dichlorophenol (DiCP)	7.022	162	160, 146, 126
3,5-DiCP	6.718	-	-
2,3-DiCP	6.929	-	-
3,4-DiCP	6.211	-	-
2-Chlorophenol (CP)	4.641	128	126, 112, 106
3-CP	4.360	-	-
4-CP	4.087	-	-
Phenol	3.054	94	78, 57
PCB-153 (Internal Standard)	16.821	360	358,242

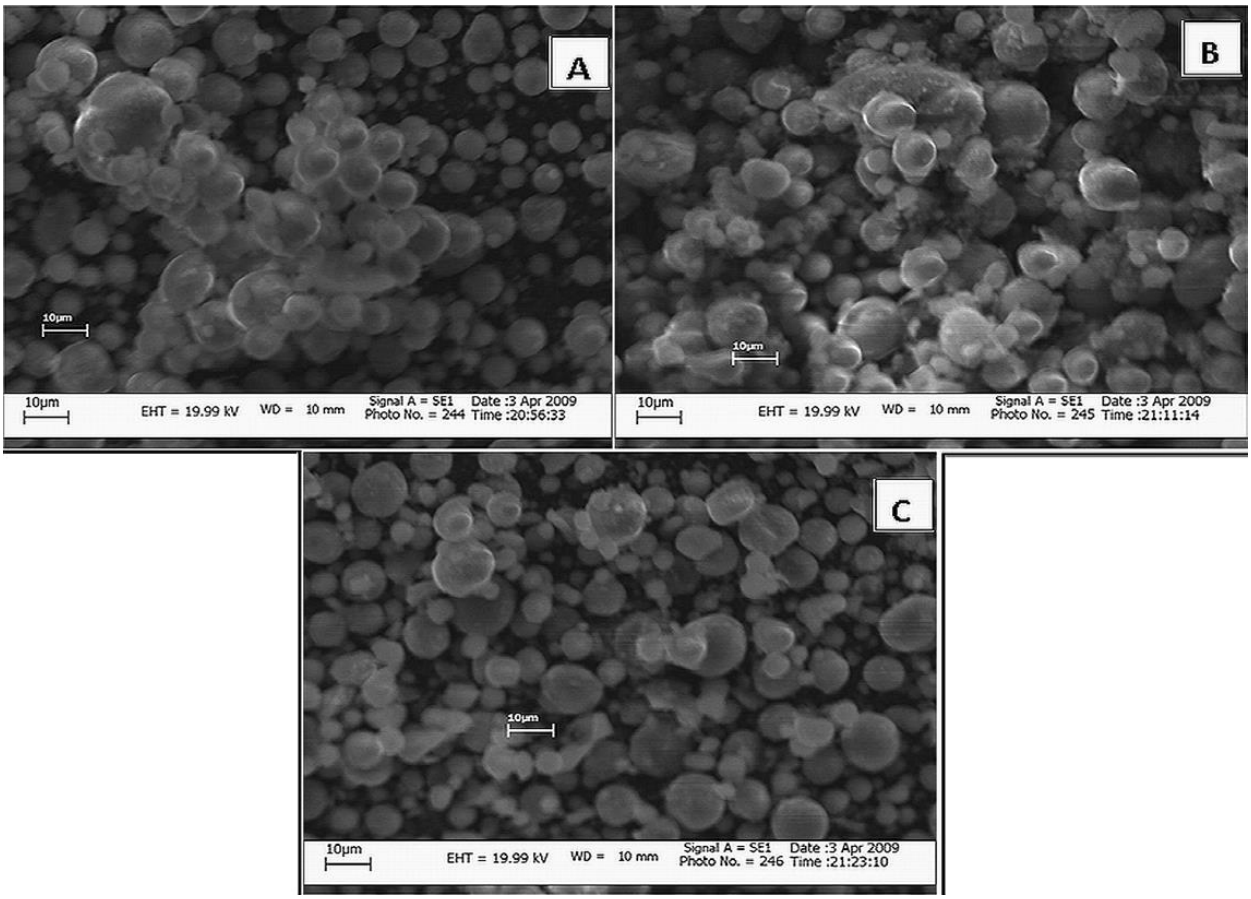

Figure 21: SEM images of a) unmilled ZVMg powder b) ball-milled ZVMg powder and c) ball-milled ZVMg/C powder.*

(*Elie, M. R.; Clausen, C. A.; Geiger, C. L., Reduction of benzo[a]pyrene with acid-activated magnesium metal in ethanol: A possible application for environmental remediation. *J. Hazard. Mater*. **2012,** *203-204*, 77-85)

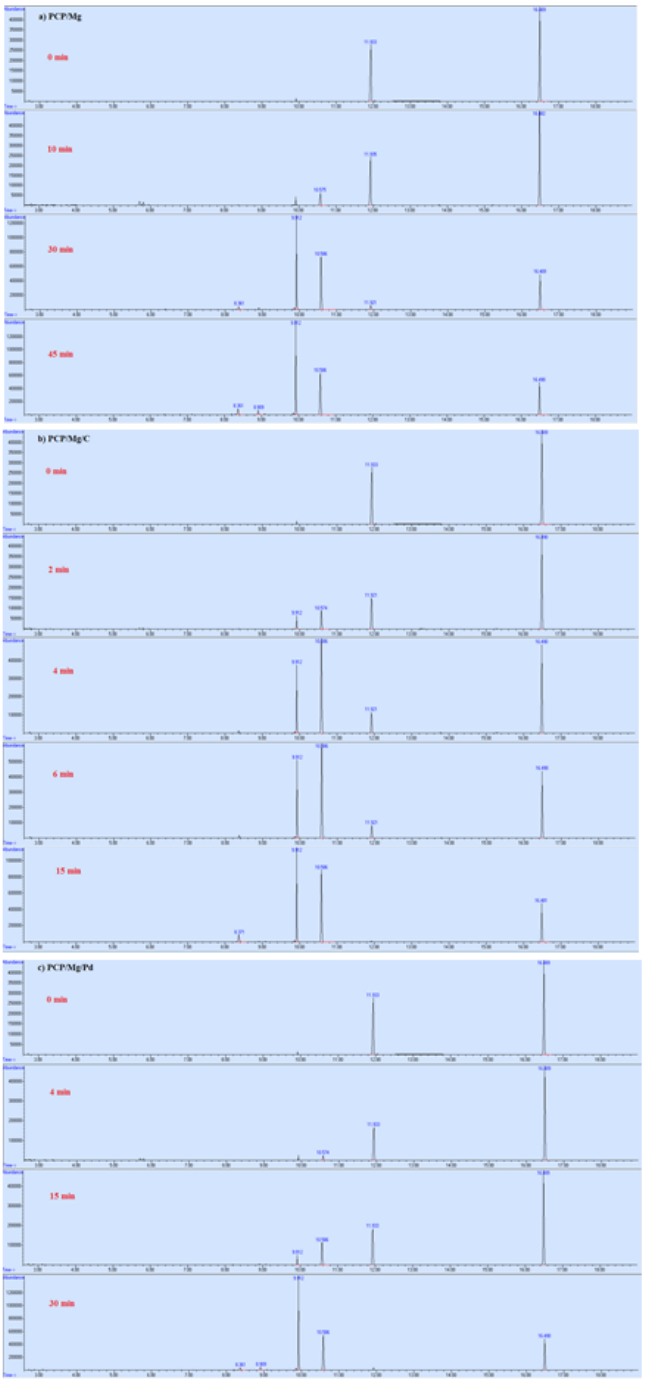

Figure 22: Chromatograms from GCMS of PCP degradation at different time points, for all three reaction systems in acidified ethanol and Ball-milled a) ZVMg, b) ZVMg/C, and c) mechanically alloyed ZVMg/Pd (11.9min is PCP peak).

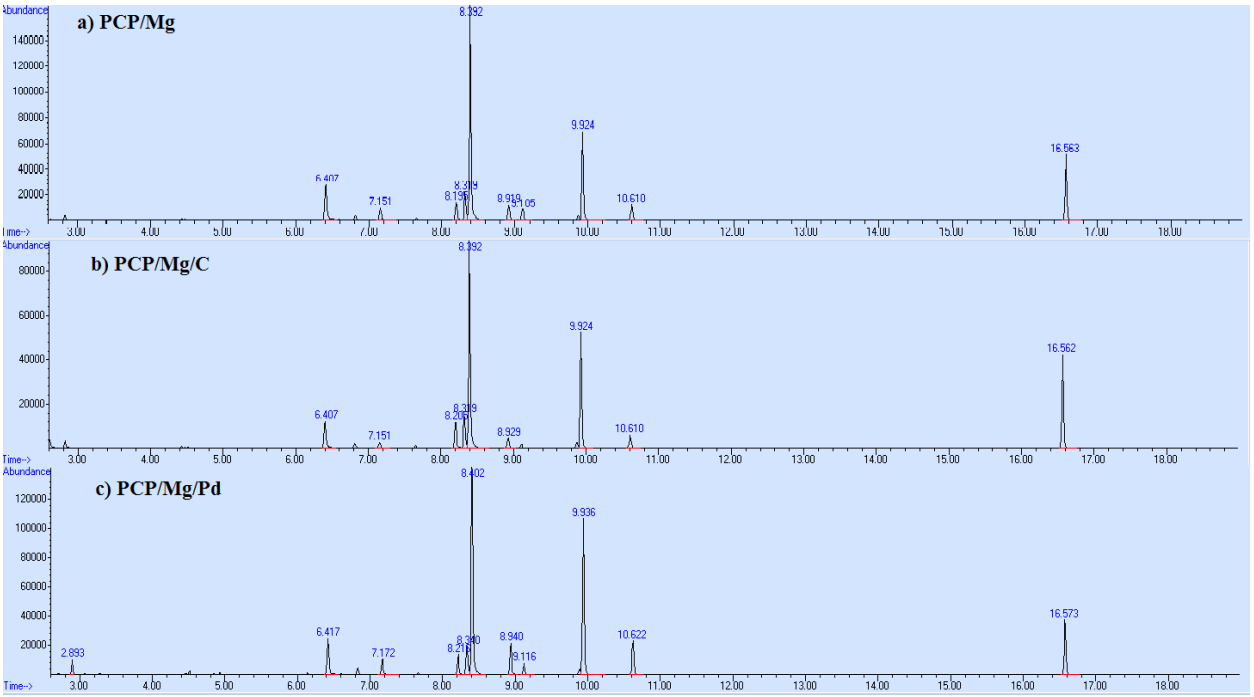

Figure 23: Chromatograms from GCMS of PCP degradation byproducts after 1 hr in acidified ethanol and Ball-milled a) ZVMg, b) ZVMg/C, and c) mechanically alloyed ZVMg/Pd (2.89min Phenol, 6.41-7.17min DiCP, 8.21-9.12min TriCP, 9.93-10.6min TCP and 16.5min PCB-153; internal standard).

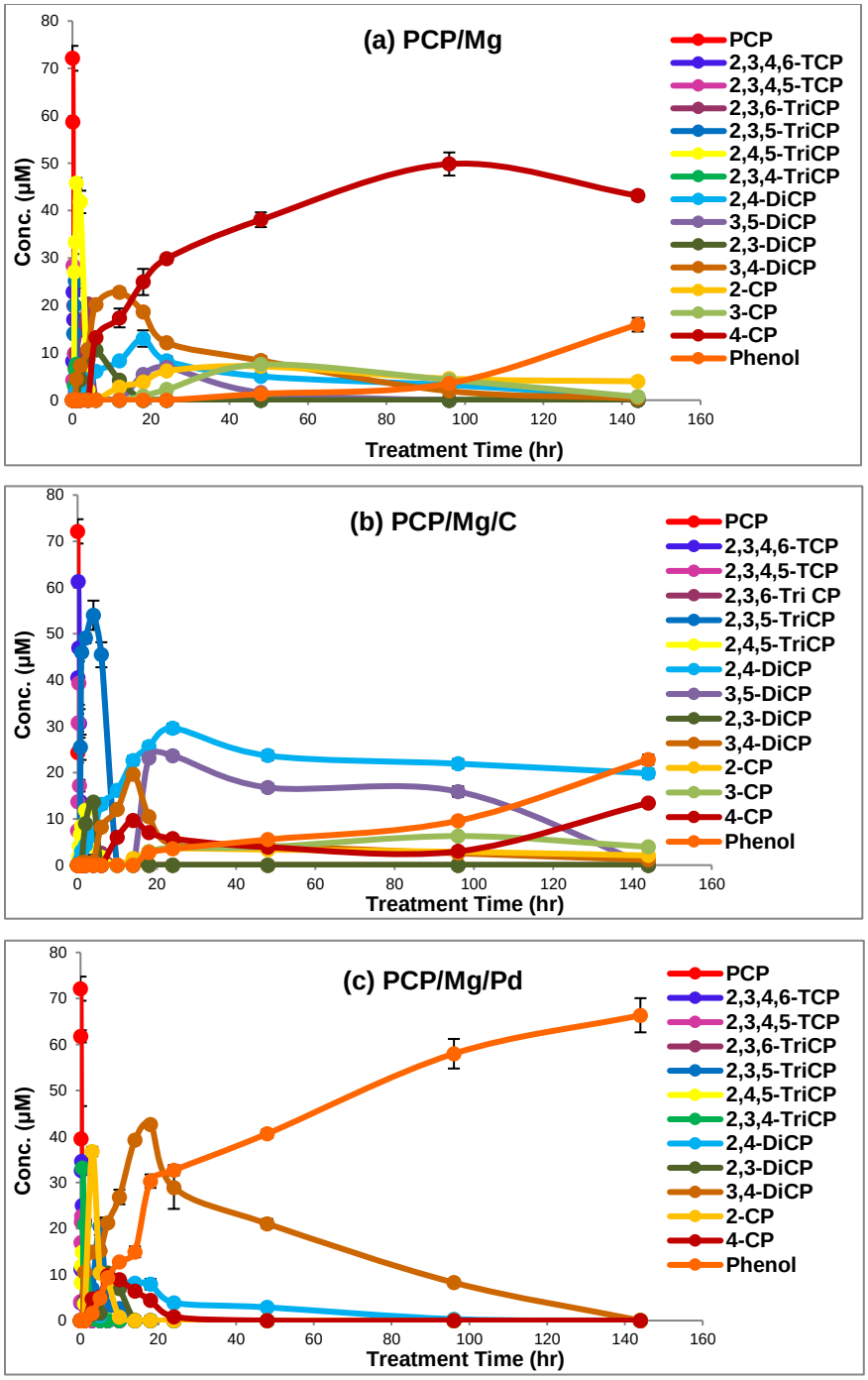

Figure 24: Dechlorination of PCP with the activated (a) Mg, (b) Mg/C, (c) mechanically alloyed Mg/Pd reducing systems. Each data point represents the mean ± error calculated from duplicate samples.

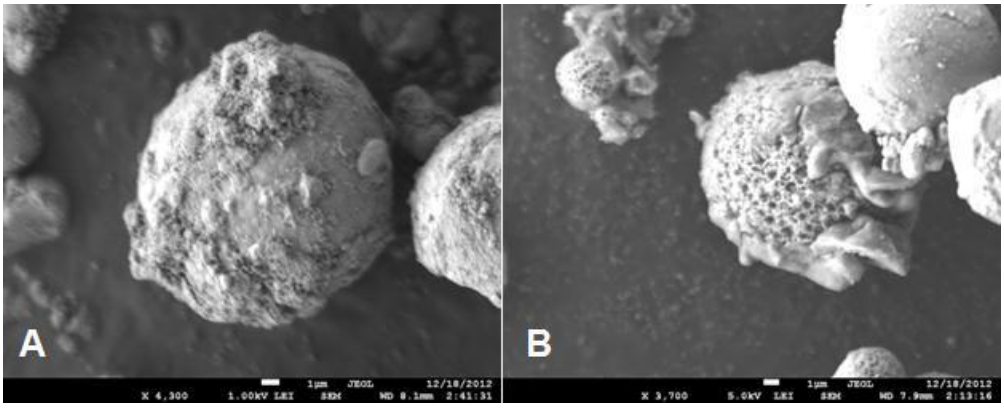

Figure 25: SEM images of ball-milled ZVMg particles a) before dechlorination and b) after dechlorination.[*]

([*]Novaes-Card, S. Magnesium and Acidified Ethanol Based Treatment Systems for Extraction and Dechlorination of Polychlorinated Biphenyls from Contaminated Oils, Paints, and Soils. 2013).

Table 2: Data of the pseudo-first order PCP degradation duplicate runs of the reaction of 66.72 μM of PCP with 2.08×10^6 μM ZVMg in 5 ml acidified ethanol.

Mg		**Mg/C**		**Mg/Pd**	
Time (min)	**ln (PCP) (μM)**	**Time (min)**	**ln (PCP) (μM)**	**Time (min)**	**ln (PCP) (μM)**
0	4.20±0.013	0	4.20±0.013	0	4.20±0.013
1	4.10±0.006	1	3.77±0.044	1	4.08±0.025
2	4.09±0.026	2	3.48±0.116	2	4.03±0.006
3	4.03±0.021	3	3.18±0.260	3	3.86±0.025
4	4.01±0.019	4	3.05±0.117	4	3.79±0.064
6	4.03±0.017	6	2.75±0.190	6	3.76±0.016
8	4.01±0.005	-	-	8	3.69±0.009
10	3.93±0.001	-	-	10	3.59±0.006
15	3.74±0.028	-	-	15	3.22± 0.108
30	2.96±0.139	-	-	-	-
Rate constant = 0.0383±0.0031		**Rate constant = 0.2370±0.0282**		**Rate constant = 0.0595±0.0046**	
R^2=0.9488		R^2=0.9464		R^2=0.9602	

Table 3: Data of the pseudo-first order phenol formation of dechlorination of chlorinated phenols with activated magnesium reducing systems in ethanol and acetic acid.

Mg		**Mg/C**		**Mg/Pd**	
Time (hr)	**ln (phenol) (μM)**	**Time (hr)**	**ln (phenol) (μM)**	**Time (hr)**	**ln (phenol) (μM)**
-	-	-	-	3	0.4661±0.1136
-	-	-	-	5	1.585±0.1348
-	-	-	-	7	2.225±0.1006
-	-	-	-	10	2.548±0.0181
-	-	-	-	14	2.70±0.0784
-	-	18	0.990±0.0455	18	3.41±0.0483
-	-	24	1.25±0.0102	24	-
48	0.280±0.0725	48	1.71±0.0241	48	-
96	1.27±0.192	96	3.13±0.0544	96	-
144	2.77±0.0909	-	-	144	-
Rate constant = 0.0259±0.0032		**Rate constant = 0.0268±0.0015**		**Rate constant = 0.1652±0.0352**	
R^2=0.985		R^2=0.993		R^2=0.846	

APPENDIX B: SUPPORTING INFORMATION FOR CHAPTER TWO

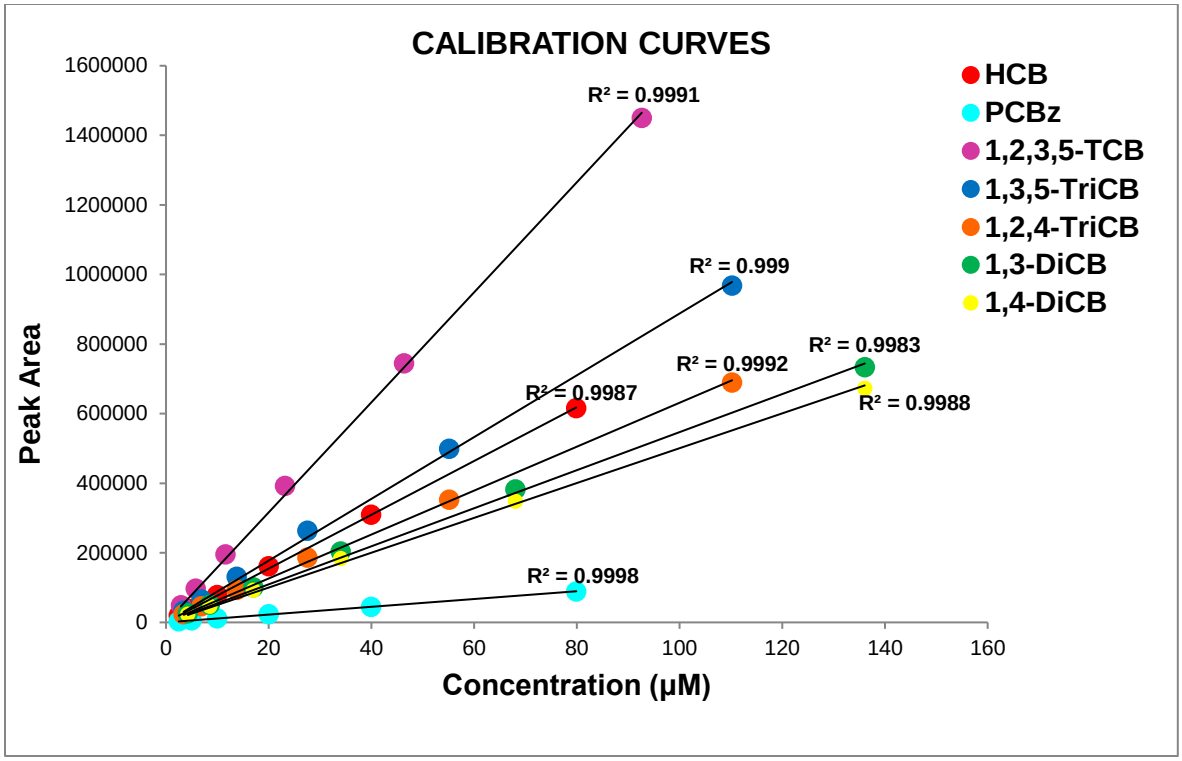

Figure 26: Calibration curves for HCB and its chlorinated byproducts.

Table 4: Mass Spectrometry (MS) Selected Ion Monitoring parameters for the degradation of HCB in 1:1 ethanol/ethyl lactate solvent and acetic acid.

Compound	**Retention Time (min)**	**Molecular Ion (m/z)**	**Fragment Ions (m/z)**
Hexachlorobenzene (HCB)	19.714	284	249, 282
Pentachlorobenzene (PCBz)	17.497	250	215, 248
1,2,4,5-Tetrachlorobenzene (TCB)	14.996	216	179, 214
1,3,4,5-TCB	14.986	-	-
1,2,4-Trichlorobenzene (TriCB)	12.79	182	145, 180
1,3,5-TriCB	12.073	-	-
1,3-Dichlorobenzene (DiCB)	9.933	148	146,147
1,4-DiCB	10.053	-	-
Monochlorobenzene (monoCBz)	6.901	112	77
Benzene (Bz)	3.626	78	51
PCB-153 (Internal Standard)	25.361	360	358,242

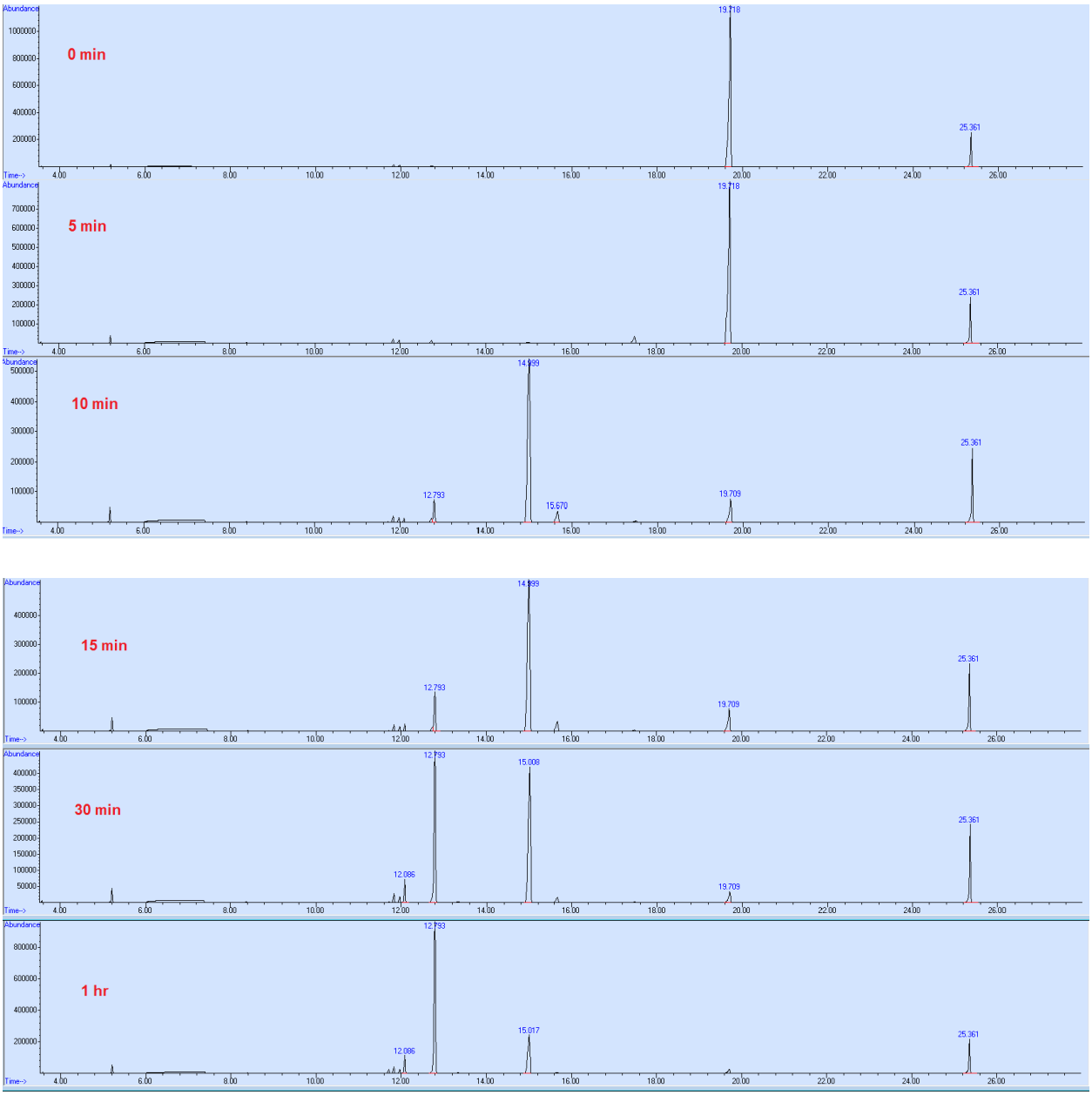

Figure 27: Chromatograms from GCMS of HCB degradation at different time points within 1 hr in 1:1 acidified ethanol/ethyl lactate and Ball-milled ZVMg/C, (19.71 min is HCB peak, 15.67 min is 1,2,3,4-TCB, 14.99 min is 1,2,4,5-TCB, 12.79 min is 1,2,4-TriCB, 12.08 is 1,3,5-TriCB and 25.36 min is PCB-153; internal standard).

Table 5: Data of the pseudo-first order PCP degradation duplicate runs of the reaction of 66.72 μM of PCP with 2.08×106 μM ZVMg in 5 ml acidified ethanol.

Time (min)	**ln (HCB) (μM)**
0	4.19±0.03
5	3.34±0.07
10	2.50±0.03
15	0.76±0.04
Rate constant = 0.22±0.03	
R^2=0.9627	

Table 6: ΔG data of the reaction calculated with Gaussian 09 software with B3LYP method for each chlorinated position in HCB and its degradation products.

x	Reactant	Product	ΔG (kcal/mol)
6	1,2,3,4,5,6-hexachlorobenzene	1,2,3,4,5-pentachlorobenzene	-30.75
5	1,2,3,4,5-pentachlorobenzene	1,2,3,4-tetrachlorobenzene	-27.50
	1,2,3,4,5-pentachlorobenzene	1,2,4,5-tetrachlorobenzene	-30.07
	1,2,3,4,5-pentachlorobenzene	1,3,4,5-tetrachlorobenzene	-29.69
4	1,2,3,4-tetrachlorobenzene	1,2,3-trichlorobenzene	-26.72
	1,2,3,4-tetrachlorobenzene	1,2,4-trichlorobenzene	-26.24
	1,2,4,5-tetrachlorobenzene	1,2,4-trichlorobenzene	-26.68
	1,3,4,5-tetrachlorobenzene	1,2,4-trichlorobenzene	-27.06
	1,3,4,5-tetrachlorobenzene	1,3,5-trichlorobenzene	-29.05
3	1,2,3-trichlorobenzene	1,2-dichlorobenzene	-26.15
	1,2,3-trichlorobenzene	1,3-dichlorobenzene	-28.49
	1,2,4-trichlorobenzene	1,2-dichlorobenzene	-23.63
	1,2,4-trichlorobenzene	1,4-dichlorobenzene	-26.10
	1,3,5-trichlorobenzene	1,3-dichlorobenzene	-23.97
2	1,2-dichlorobenzene	chlorobenzene	-25.18
	1,3-dichlorobenzene	chlorobenzene	-22.84
	1,4-dichlorobenzene	chlorobenzene	-22.71
1	Chlorobenzene	Benzene	-21.61

Table 7: Activation energies data of the reaction calculated with Gaussian 09 software with B3LYP method for each chlorinated position in HCB and its degradation products.

x	Reactant	Product	Ea (kcal/mol)
6	1,2,3,4,5,6-hexachlorobenzene	1,2,3,4,5-pentachlorobenzene	11.123
5	1,2,3,4,5-pentachlorobenzene	1,2,3,4-tetrachlorobenzene	15.72
	1,2,3,4,5-pentachlorobenzene	1,2,4,5-tetrachlorobenzene	12.35
	1,2,3,4,5-pentachlorobenzene	1,3,4,5-tetrachlorobenzene	13.02
4	1,2,3,4-tetrachlorobenzene	1,2,3-trichlorobenzene	17.07
	1,2,3,4-tetrachlorobenzene	1,2,4-trichlorobenzene	14.41
	1,2,4,5-tetrachlorobenzene	1,2,4-trichlorobenzene	17.27
	1,3,4,5-tetrachlorobenzene	1,2,4-trichlorobenzene	16.47
	1,3,4,5-tetrachlorobenzene	1,3,5-trichlorobenzene	14.75
3	1,2,3-trichlorobenzene	1,2-dichlorobenzene	18.48
	1,2,3-trichlorobenzene	1,3-dichlorobenzene	15.67
	1,2,4-trichlorobenzene	1,2-dichlorobenzene	22.55
	1,2,4-trichlorobenzene	1,4-dichlorobenzene	19.39
	1,3,5-trichlorobenzene	1,3-dichlorobenzene	21.46
2	1,2-dichlorobenzene	chlorobenzene	20.82
	1,3-dichlorobenzene	chlorobenzene	24.14
	1,4-dichlorobenzene	chlorobenzene	24.72
1	Chlorobenzene	Benzene	26.22

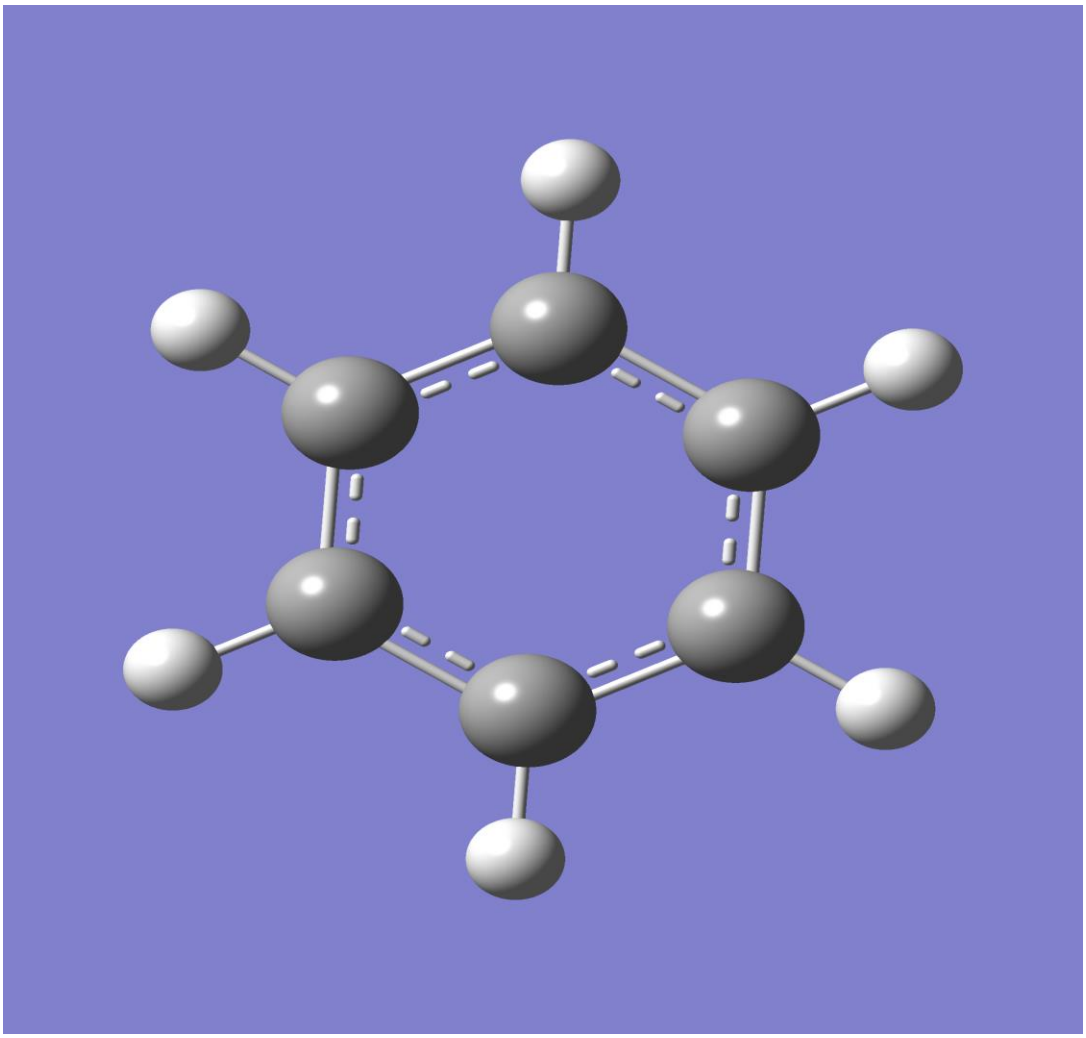

Figure 28: Minimum energy conformation of benzene.

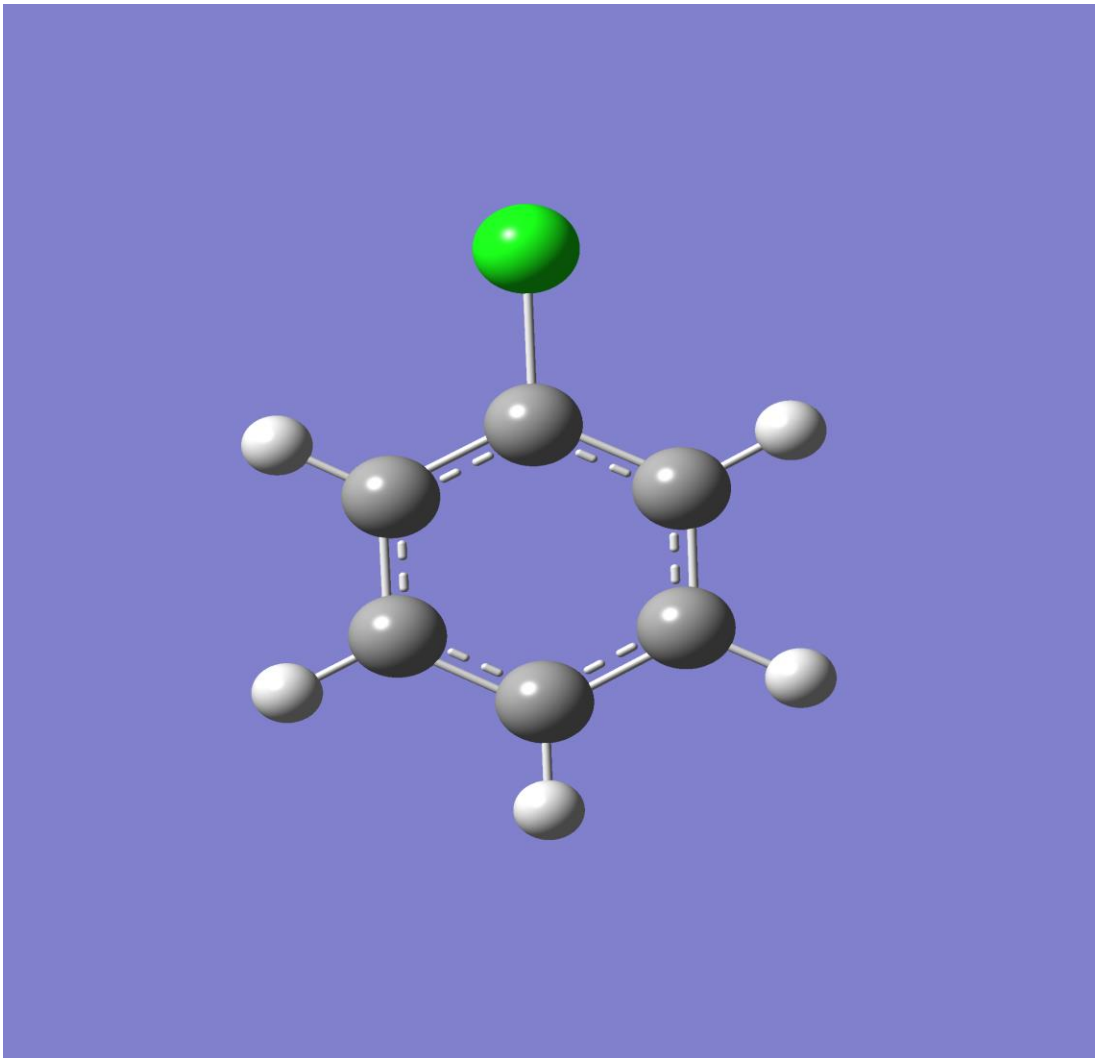

Figure 29: Minimum energy conformation of chlorobenzene.

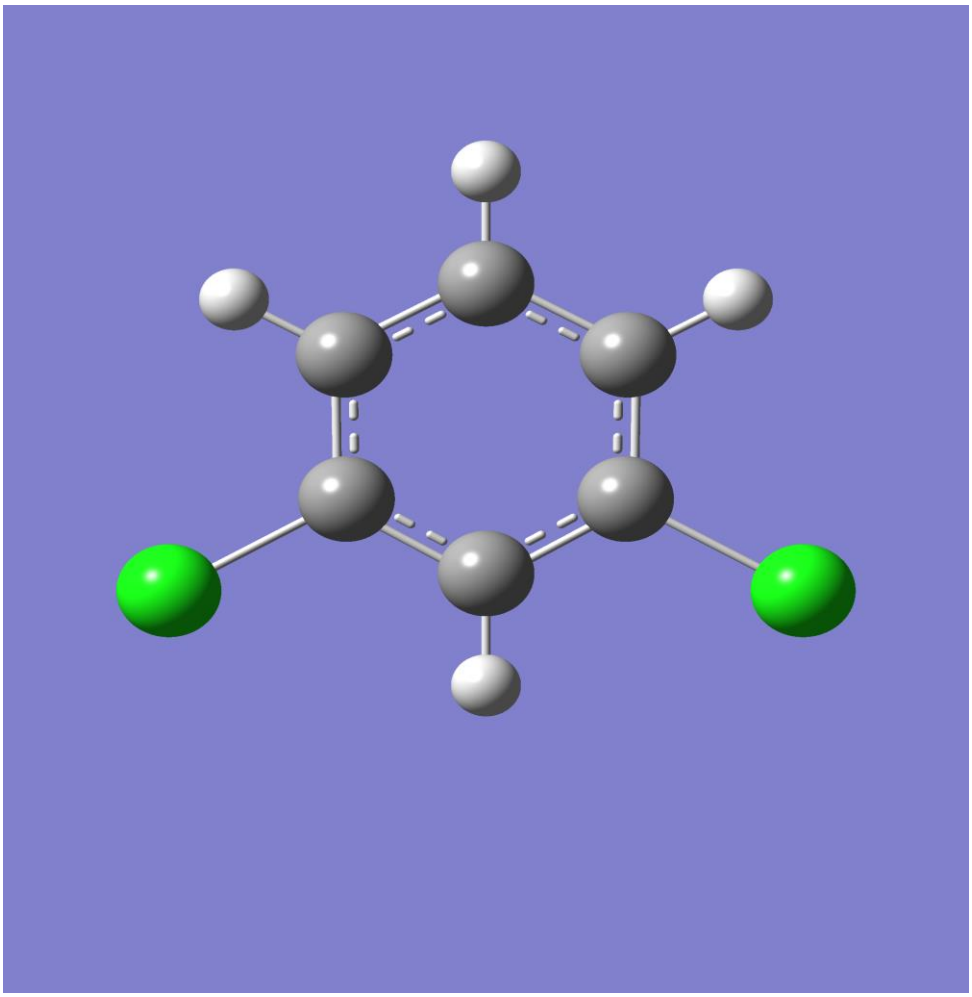

Figure 30: Minimum energy conformation of 1,3-DiCB.

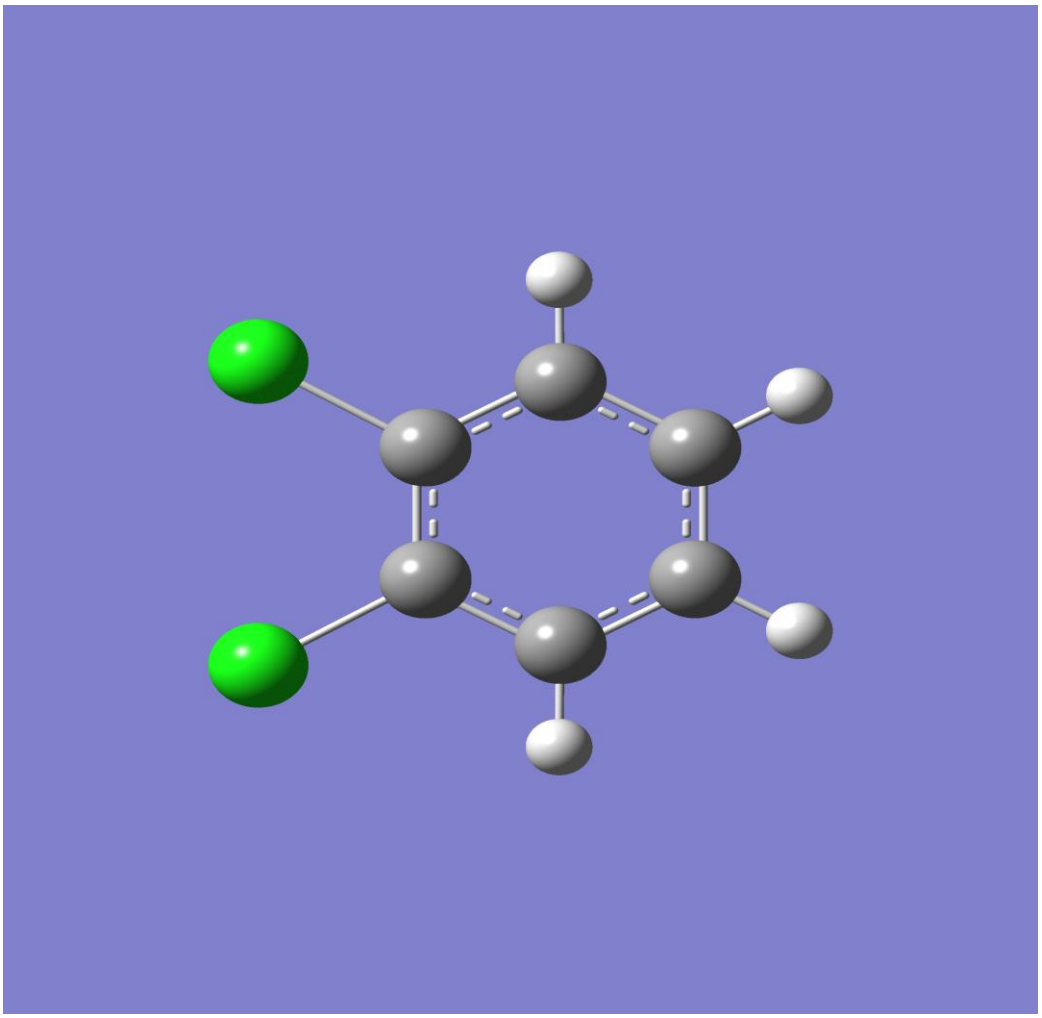

Figure 31: Minimum energy conformation of 1,2-DiCB.

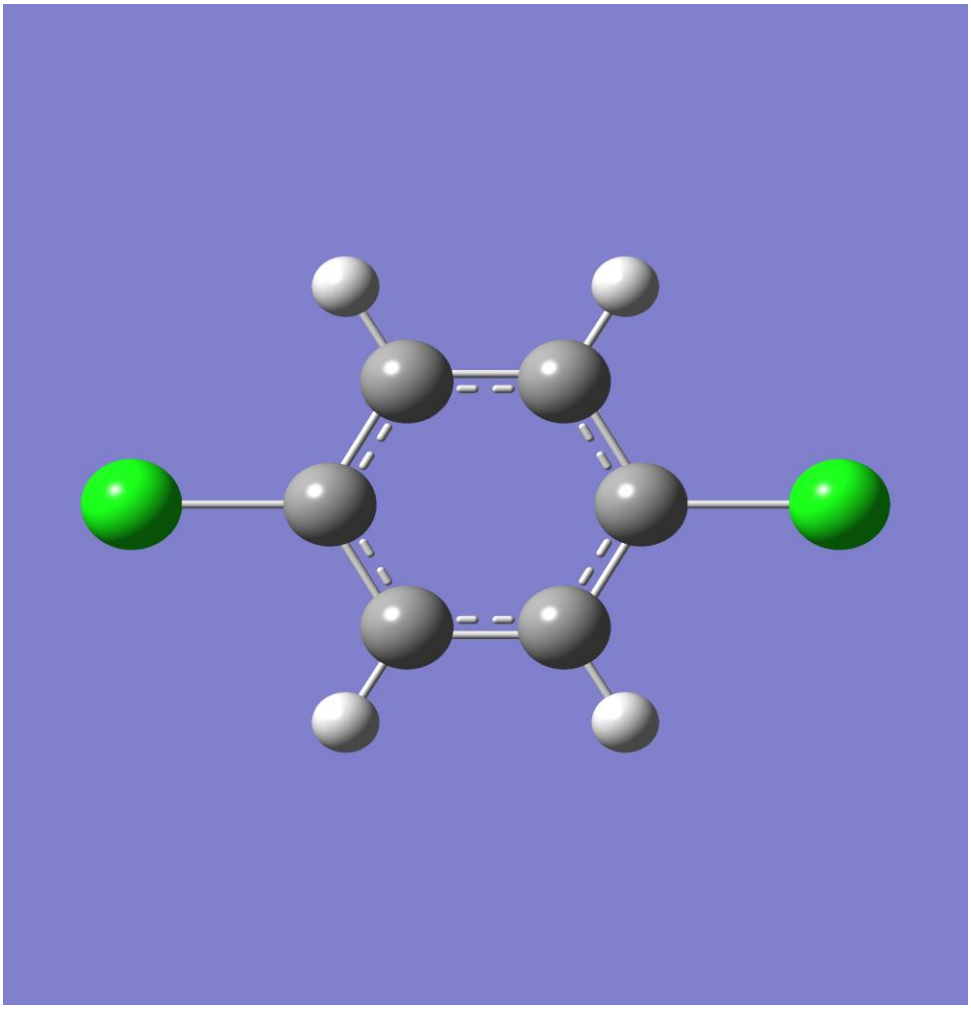

Figure 32: Minimum energy conformation of 1,4-DiCB.

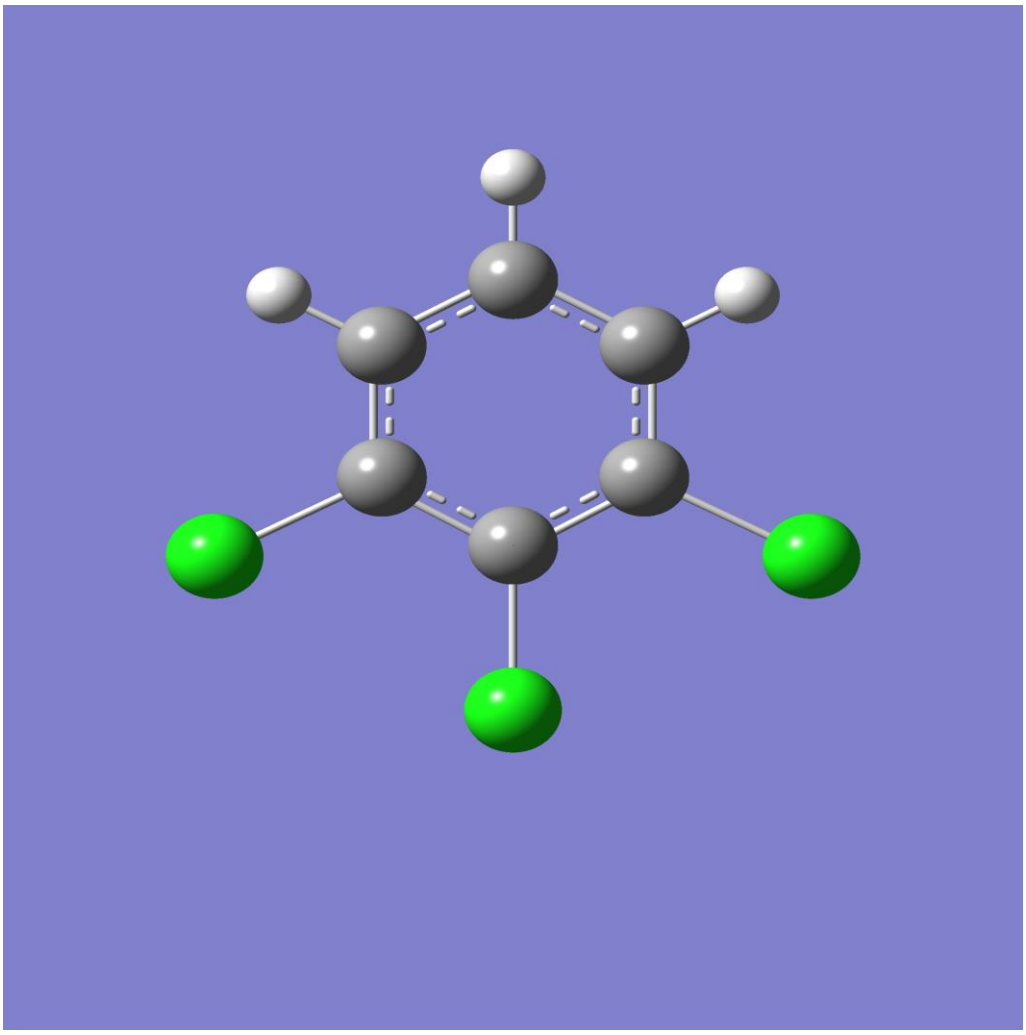

Figure 33: Minimum energy conformation of 1,2,3-TriCB.

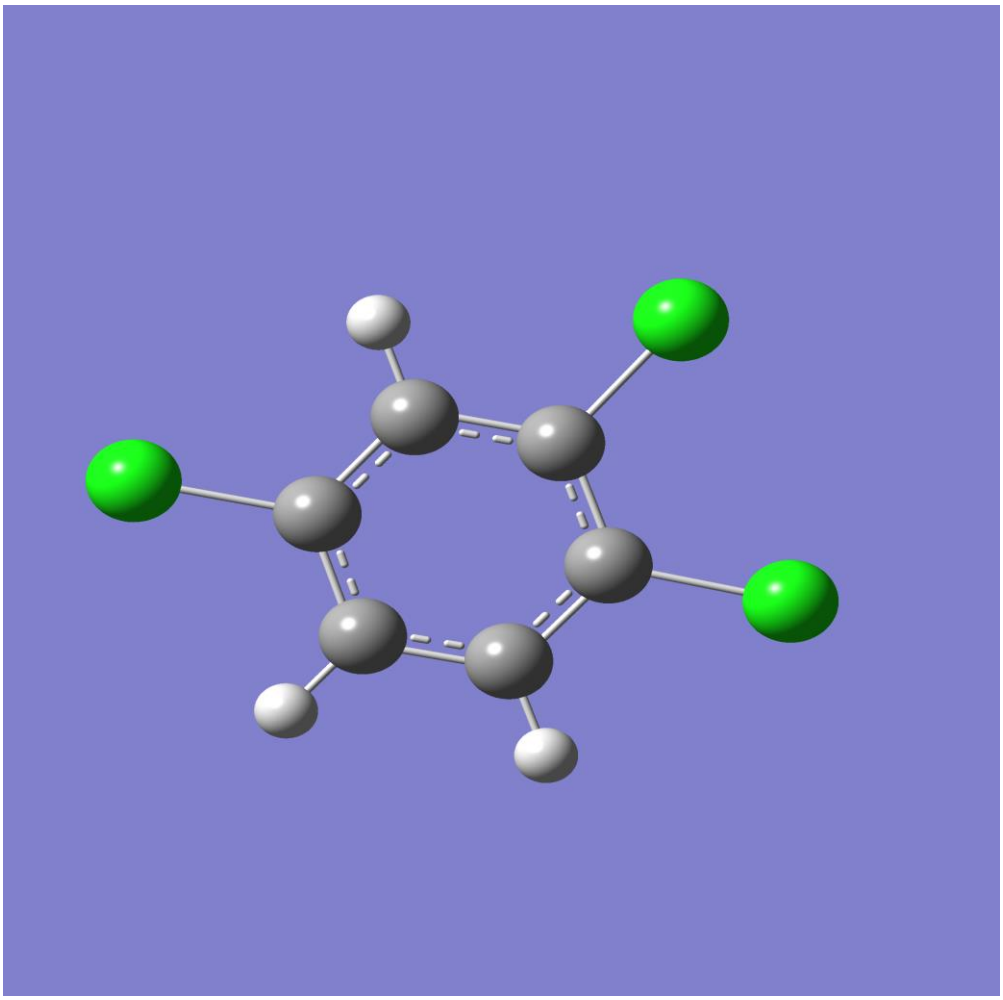

Figure 34: Minimum energy conformation of 1,2,4-TriCB.

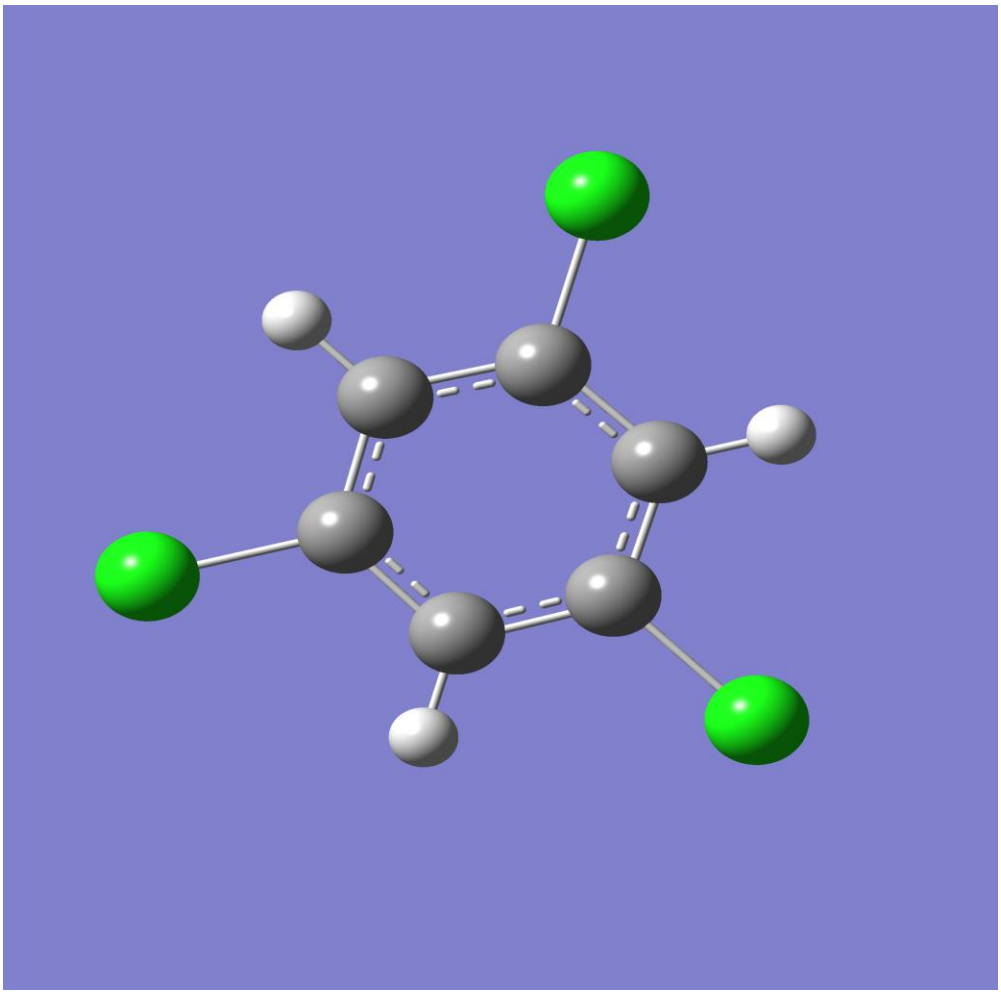

Figure 35: Minimum energy conformation of 1,3,5-TriCB.

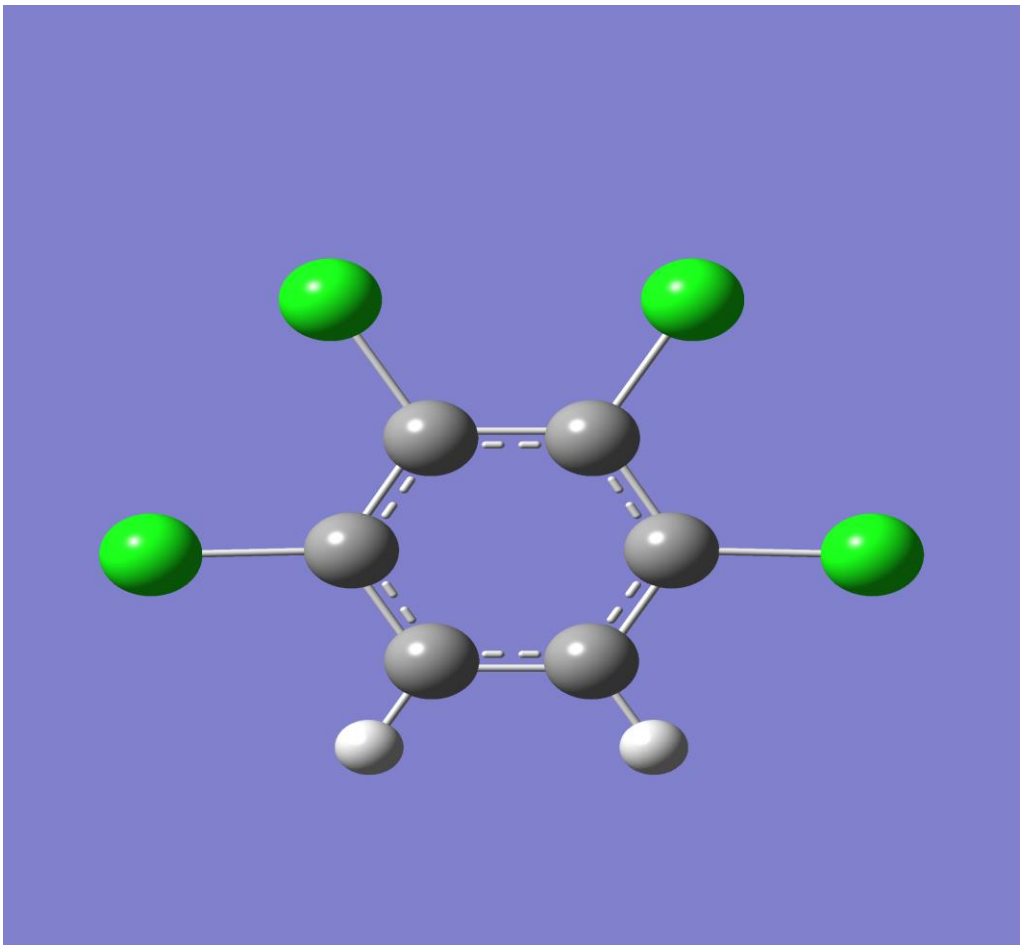

Figure 36: Minimum energy conformation of 1,2,3,4-TCB.

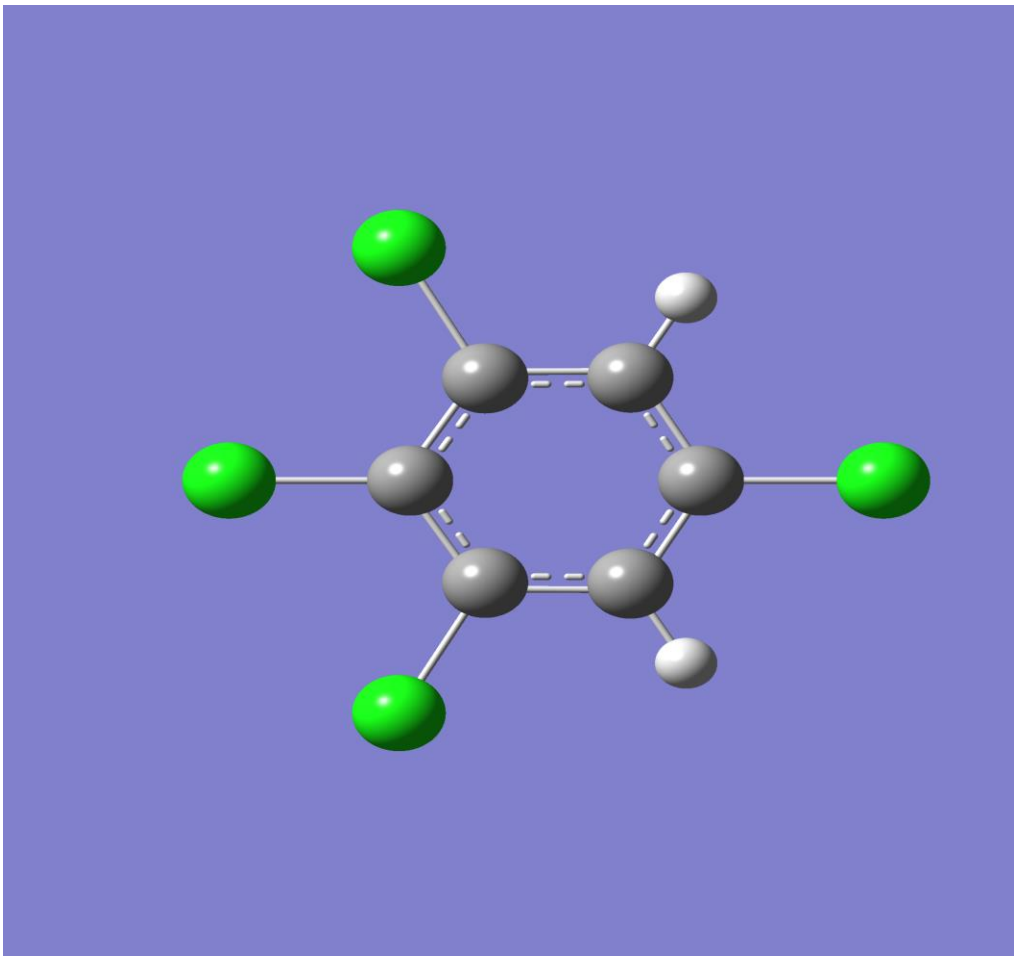

Figure 37: Minimum energy conformation of 1,2,3, 5-TCB.

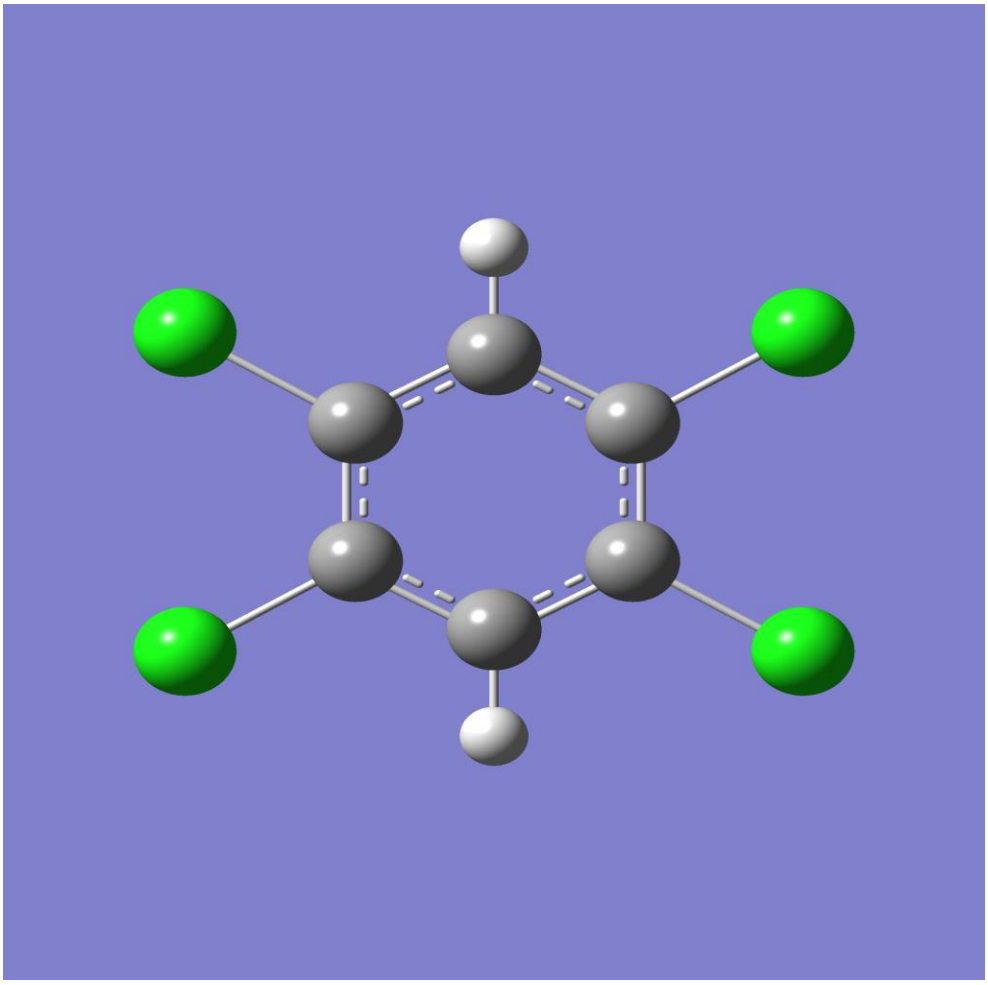

Figure 38: Minimum energy conformation of 1,2,4,5-TCB.

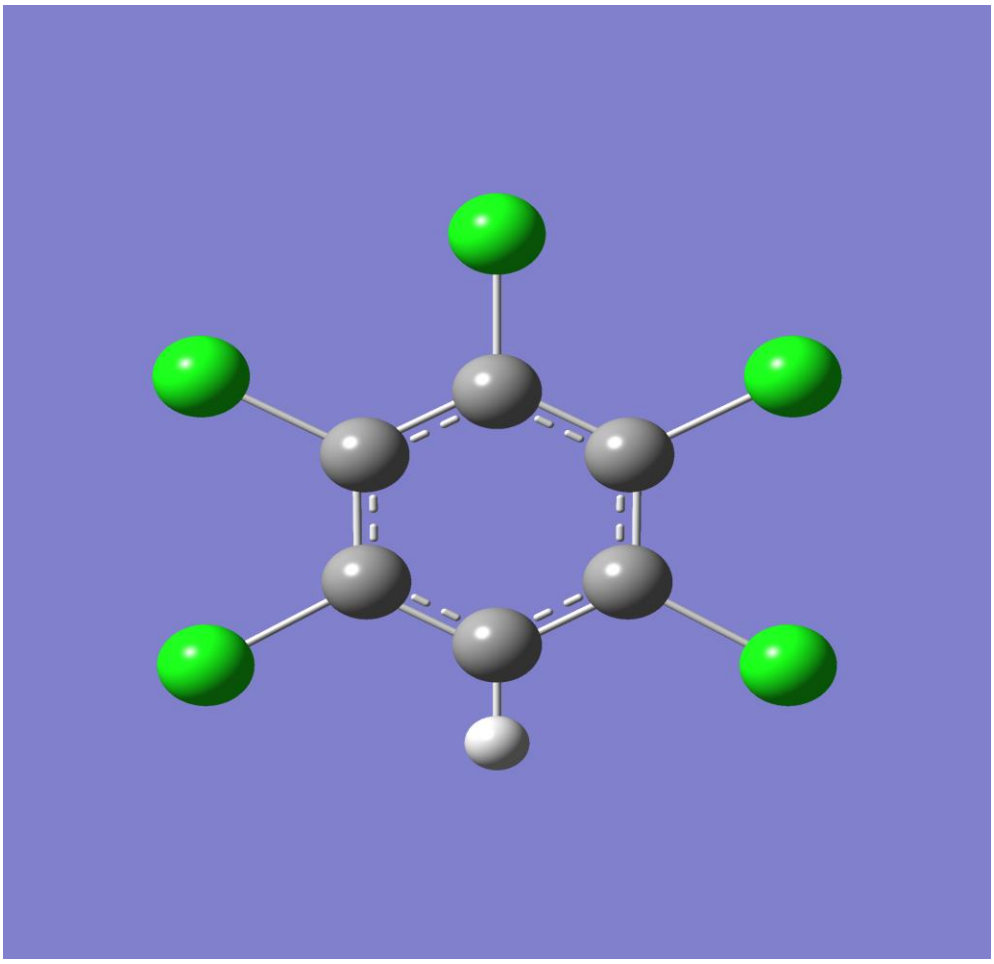

Figure 39: Minimum energy conformation of PCBz.

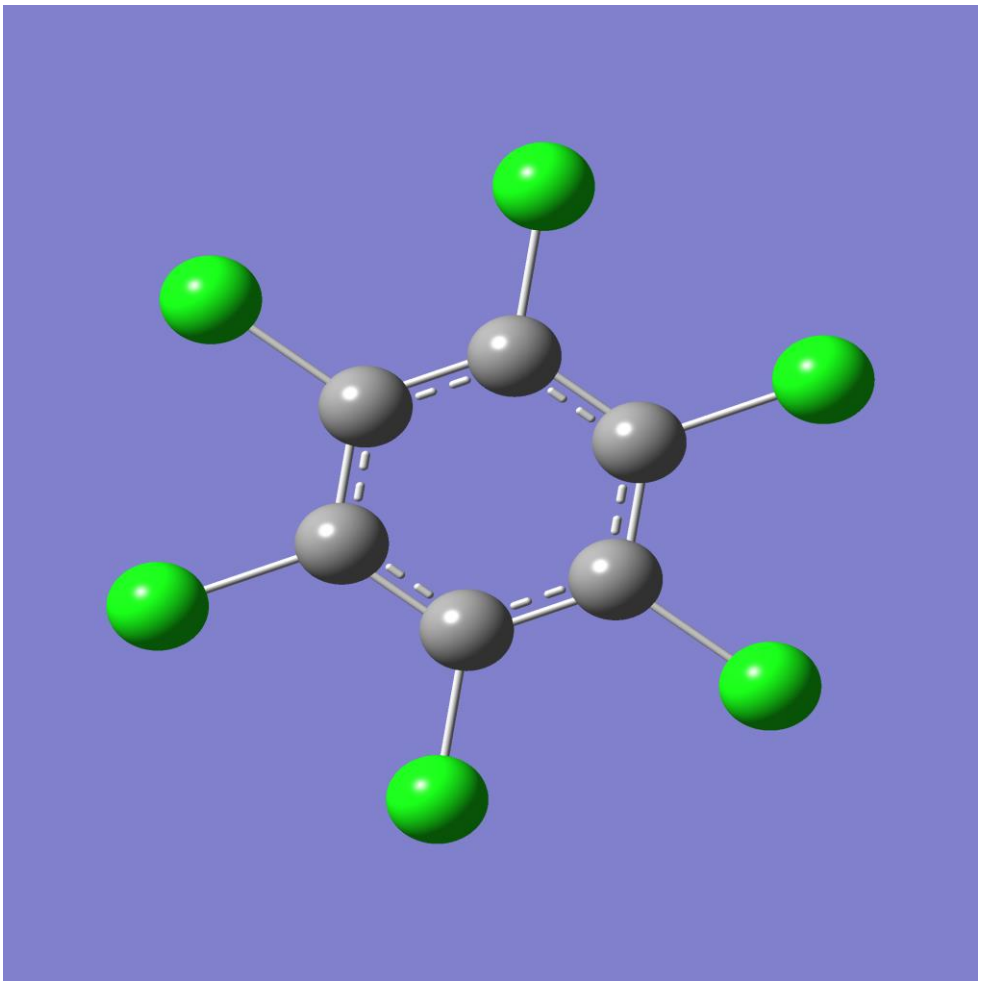

Figure 40: Minimum energy conformation of HCB.

REFERENCES

Bai, X., T. Zhang, H. Li and Z. Yang (2016). "Simultaneous dispersive liquid-liquid microextraction based on a low-density solvent and derivatization followed by gas chromatography for the simultaneous determination of chloroanisoles and the precursor 2,4,6-trichlorophenol in water samples." J. Sep. Sci. **39**(11): 2146-2155.

Beurskens, J. E. M., C. G. C. Dekker, H. van den Heuvel, M. Swart, J. de Wolf and J. Dolfing (1994). "Dechlorination of Chlorinated Benzenes by an Anaerobic Microbial Consortium That Selectively Mediates the Thermodynamic Most Favorable Reactions." Environ. Sci. Technol. **28**(4): 701-706.

Bouaricha, S., J. P. Dodelet, D. Guay, J. Huot and R. Schulz (2001). "Activation of Mg-based hydrogen storage materials modified by graphite and other carbonaceous compounds." J. Mater. Res. **16**(10): 2893-2905.

Brahushi, F., U. Doerfler, R. Schroll and J. C. Munch (2004). "Stimulation of reductive dechlorination of hexachlorobenzene in soil by inducing the native microbial activity." Chemosphere **55**(11): 1477-1484.

Buhr, A., C. Genning and T. Salthammer (2000). "Trace analysis of pentachlorophenol (PCP) in wood and wood-based products -- comparison of sample preparation procedures." Fresenius' J. Anal. Chem. **367**(1): 73-78.

Campoy, S., M. L. Alvarez-Rodriguez, E. Recio, A. Rumbero and J.-J. R. Coque (2009). "Biodegradation of 2,4,6-TCA by the white-rot fungus Phlebia radiata is initiated by a phase I (O-demethylation)-phase II (O-conjugation) reactions system: implications for the chlorine cycle." Environ. Microbiol. **11**(1): 99-110.

Carasek, E., E. Cudjoe and J. Pawliszyn (2007). "Fast and sensitive method to determine chloroanisoles in cork using an internally cooled solid-phase microextraction fiber." J. Chromatogr. A **1138**(1-2): 10-17.

Careri, M., V. Mazzoleni, M. Musci and R. Molteni (2001). "Study of electron beam irradiation effects on 2,4,6-trichloroanisole as a contaminant of cork by gas chromatography-mass spectrometry." Chromatographia **53**(9/10): 553-557.

Cass, Q. B., L. G. Freitas, E. Foresti and M. H. R. Z. Damianovic (2000). "Development of HPLC method for the analysis of chlorophenols in samples from anaerobic reactors for wastewater treatment." J. Liq. Chromatogr. Relat. Technol. **23**(7): 1089-1097.

Chen, K. F., W. Y. Huang, T. Y. Yeh, C. M. Kao and F. Hou (2005). "Biodegradability of 2,4-dichlorophenol under different redox conditions." Pract. Period. Hazard., Toxic, Radioact. Waste Manage. **9**(3): 141-146.

Chen, M.-y., M.-h. Huang and Y.-h. Shih (2007). "Chemical reduction of pentachlorophenol by nanoscale zero-valent iron." Prepr. Ext. Abstr. ACS Natl. Meet., Am. Chem. Soc., Div. Environ. Chem. **47**(2): 158-162.

Chen, W.-f., L. Pan, L.-f. Chen, Q. Wang and C.-c. Yan (2014). "Dechlorination of hexachlorobenzene by nano zero-valent iron/activated carbon composite: iron loading, kinetics and pathway." RSC Adv. **4**(87): 46689-46696.

Chen, W.-F., W. Wang, J. Zhang, X. Zhang and Y. Li (2015). "Effects of co-present cations and anions on hexachlorobenzene removal by activated carbon, nano zerovalent iron and nano zerovalent/activated carbon composite." Desalin. Water Treat.: Ahead of Print.

Cheng, Y., M. Ekker and H. M. Chan (2015). "Relative developmental toxicities of pentachloroanisole and pentachlorophenol in a zebrafish model (Danio rerio)." Ecotoxicol. Environ. Saf. **112**: 7-14.

Coutts, J. L., R. W. Devor, B. Aitken, M. D. Hampton, J. W. Quinn, C. A. Clausen and C. L. Geiger (2011). "The use of mechanical alloying for the preparation of palladized magnesium bimetallic particles for the remediation of PCBs." J. Hazard. Mater. **192**(3): 1380-1387.

Cravotto, G., D. Garella, L. Beltramo, D. Carnaroglio, S. Mantegna and C. M. Roggero (2013). "Enabling technologies for the rapid dechlorination of polychloroarenes and PCBs." Chemosphere **92**(3): 299-303.

Cserjesi, A. J. and E. L. Johnson (1972). "Methylation of pentachlorophenol by Trichoderma virgatum." Can. J. Microbiol. **18**(1): 45-49.

De Vor, R., K. Carvalho-Knighton, B. Aitken, P. Maloney, E. Holland, L. Talalaj, S. Elsheimer, C. A. Clausen and C. L. Geiger (2009). "Mechanism of the degradation of individual PCB congeners using mechanically alloyed Mg/Pd in methanol." Chemosphere **76**(6): 761-766.

DeVor, R., K. Carvalho-Knighton, B. Aitken, P. Maloney, E. Holland, L. Talalaj, R. Fidler, S. Elsheimer, C. A. Clausen and C. L. Geiger (2008). "Dechlorination comparison of mono-substituted PCBs with Mg/Pd in different solvent systems." Chemosphere **73**(6): 896-900.

Doyle, J. G., T. Miles, E. Parker and I. F. Cheng (1998). "Quantification of total polychlorinated biphenyl by dechlorination to biphenyl by Pd/Fe and Pd/Mg bimetallic particles." Microchem. J. **60**(3): 290-295.

Duan, T. H. and L. Adrian (2013). "Enrichment of hexachlorobenzene and 1,3,5-trichlorobenzene transforming bacteria from sediments in Germany and Vietnam." Biodegradation **24**(4): 513-520.

Eker, S. and F. Kargi (2007). "2,4,6 Tri-Chlorophenol Containing Wastewater Treatment Using a Hybrid-Loop Bioreactor System." J. Environ. Eng. (Reston, VA, U. S.) **133**(3): 340-345.

Elie, M. R., C. A. Clausen and C. L. Geiger (2012). "Reduction of benzo[a]pyrene with acid-activated magnesium metal in ethanol: A possible application for environmental remediation." J. Hazard. Mater. **203-204**: 77-85.

Elie, M. R., C. A. Clausen and C. L. Yestrebsky (2013). "Multivariate evaluation and optimization of an activated-magnesium/co-solvent system for the reductive degradation of polycyclic aromatic hydrocarbons." J. Hazard. Mater. **248-249**: 150-158.

Elie, M. R., C. A. Clausen and C. L. Yestrebsky (2013). "Reductive degradation of oxygenated polycyclic aromatic hydrocarbons using an activated magnesium/co-solvent system." Chemosphere **91**(9): 1273-1280.

Engelmann, M. D., J. G. Doyle and I. F. Cheng (2001). "The complete dechlorination of DDT by magnesium/palladium bimetallic particles." Chemosphere **43**(2): 195-198.

Fennell, D. E., I. Nijenhuis, S. F. Wilson, S. H. Zinder and M. M. Haeggblom (2004). "Dehalococcoides ethenogenes Strain 195 Reductively Dechlorinates Diverse Chlorinated Aromatic Pollutants." Environ. Sci. Technol. **38**(7): 2075-2081.

Goswami, M., E. Recio, S. Campoy, J. F. Martin and J.-J. R. Coque (2007). "Environmental significance of O-demethylation of chloroanisoles by soil bacterial isolates as a mechanism that improves the overall biodegradation of chlorophenols." Environ. Microbiol. **9**(10): 2512-2521.

Grittini, C. (1997). Rapid reductive dechlorination of environmentally hazardous aromatic compounds and pesticides (polychlorinated biphenyls, pentachlorophenol, dde, toxaphene, palladized iron). Copyright (C) 2016 American Chemical Society (ACS). All Rights Reserved.

Hadnagy, E., L. M. Rauch and K. H. Gardner (2007). "Dechlorination of polychlorinated biphenyls, naphthalenes and dibenzo-p-dioxins by magnesium/palladium bimetallic particles." J. Environ. Sci. Health, Part A: Toxic/Hazard. Subst. Environ. Eng. **42**(6): 685-695.

Huot, J., G. Liang and R. Schulz (2001). "Mechanically alloyed metal hydride systems." Appl. Phys. A: Mater. Sci. Process. **72**(2): 187-195.

Hwang, H. M., R. E. Hodson and R. F. Lee (1986). "Degradation of phenol and chlorophenols by sunlight and microbes in estuarine water." Environ. Sci. Technol. **20**(10): 1002-1007.

Jiang, L., Q. Wang, H. Liu and J. Yao (2015). "Influence of Degradation Behavior of Coexisting Chlorobenzene Congeners Pentachlorobenzene, 1,2,4,5-Tetrachlorobenzene, and 1,2,4-Trichlorobenzene on the Anaerobic Reductive Dechlorination of Hexachlorobenzene in Dye Plant Contaminated Soil." Water, Air, Soil Pollut. **226**(9): 1-9.

Kengara, F. O., U. Doerfler, G. Welzl, B. Ruth, J. C. Munch and R. Schroll (2013). "Enhanced degradation of 14C-HCB in two tropical clay soils using multiple anaerobic-aerobic cycles." Environ. Pollut. (Oxford, U. K.) **173**: 168-175.

Kim, Y.-H. and E. R. Carraway (2000). "Dechlorination of Pentachlorophenol by Zero Valent Iron and Modified Zero Valent Irons." Environ. Sci. Technol. **34**(10): 2014-2017.

Kim, Y. H. and E. R. Carraway (2003). "Dechlorination of chlorinated phenols by zero valent zinc." Environ. Technol. **24**(12): 1455-1463.

Lamar, R. T. and D. M. Dietrich (1990). "In situ depletion of pentachlorophenol from contaminated soil by Phanerochaete spp." Appl. Environ. Microbiol. **56**(10): 3093-3100.

Li, Y. and K.-C. Loh (2007). "Hybrid-Hollow-Fiber Membrane Bioreactor for Cometabolic Transformation of 4-Chlorophenol in the Presence of Phenol." J. Environ. Eng. (Reston, VA, U. S.) **133**(4): 404-410.

Lin, H. H., P. C. Hung and M. B. Chang (2013). "Effect of NZVI on the pyrolysis of HCB-contaminated soil." Organohalogen Compd. **75**: 894-897.

Loiselle, S., M. Branca, G. Mulas and G. Cocco (1997). "Selective Mechanochemical Dehalogenation of Chlorobenzenes over Calcium Hydride." Environ. Sci. Technol. **31**(1): 261-265.

Lorentzen, J. C., S. A. Juran, M. Nilsson, S. Nordin and G. Johanson (2016). "Chloroanisoles may explain mold odor and represent a major indoor environment problem in Sweden." Indoor Air **26**(2): 207-218.

Maloney, P., R. DeVor, S. Novaes-Card, E. Saitta, J. Quinn, C. A. Clausen and C. L. Geiger (2011). "Dechlorination of polychlorinated biphenyls using magnesium and acidified alcohols." J. Hazard. Mater. **187**(1-3): 235-240.

Marco, J. A. M. and M. A. Kishimba (2007). "Organochlorine pesticides and metabolites in young leaves of Mangifera indica from sites near a point source in Coast region, Tanzania." Chemosphere **68**(5): 832-837.

Merica, S. G., C. E. Banceu, W. Jedral, J. Lipkowski and N. J. Bunce (1998). "Electroreduction of Hexachlorobenzene in Micellar Aqueous Solutions of Triton-SP 175." Environ. Sci. Technol. **32**(10): 1509-1514.

Meylan, W. M. and P. H. Howard (1993). "Computer estimation of the atmospheric gas-phase reaction rate of organic compounds with hydroxyl radicals and ozone." Chemosphere **26**(12): 2293-2299.

Miyoshi, K., T. Nishio, A. Yasuhara, M. Morita and T. Shibamoto (2004). "Detoxification of hexachlorobenzene by dechlorination with potassium-sodium alloy." Chemosphere **55**(11): 1439-1446.

Morales, J., R. Hutcheson and I. F. Cheng (2002). "Dechlorination of chlorinated phenols by catalyzed and uncatalyzed Fe(0) and Mg(0) particles." J. Hazard. Mater. **90**(1): 97-108.

Nie, X., J. Liu, D. Yue, X. Zeng and Y. Nie (2013). "Dechlorination of hexachlorobenzene using lead-iron bimetallic particles." Chemosphere **90**(9): 2403-2407.

Nie, X., J. Liu and X. Zeng (2012). "Effect of Surfactant on HCB Dechlorination by Ag/Fe Bimetal in Polluted Soil Eluent." Procedia Environ. Sci. **16**: 320-326.

Nie, X., J. Liu, X. Zeng and D. Yue (2013). "Rapid degradation of hexachlorobenzene by micron Ag/Fe bimetal particles." J. Environ. Sci. (Beijing, China) **25**(3): 473-478.

Patel, U. D. and S. Suresh (2007). "Dechlorination of chlorophenols using magnesium-palladium bimetallic system." J. Hazard. Mater. **147**(1-2): 431-438.

Pavlostathis, S. G. and M. T. Prytula (2000). "Kinetics of the Sequential Microbial Reductive Dechlorination of Hexachlorobenzene." Environ. Sci. Technol. **34**(18): 4001-4009.

Quint, R. M. (2006). "γ-Radiolysis of aqueous 2-chloroanisole." Radiat. Phys. Chem. **75**(1): 34-41.

Quint, R. M., H. R. Park, P. Krajnik, S. Solar, N. Getoff and K. Sehested (1996). "γ-Radiolysis and pulse radiolysis of aqueous 4-chloroanisole." Radiat. Phys. Chem. **47**(6): 835-845.

Recio, E., M. L. Alvarez-Rodriguez, A. Rumbero, E. Garzon and J. J. R. Coque (2011). "Destruction of chloroanisoles by using a hydrogen peroxide activated method and its application to remove chloroanisoles from cork stoppers." J. Agric. Food Chem. **59**(23): 12589-12597.

Ren, Y., S. Kang and J. Zhu (2015). "Mechanochemical degradation of hexachlorobenzene using Mg/Al2O3 as additive." J. Mater. Cycles Waste Manage. **17**(4): 607-615.

Ren, Y., X. Li, S. Ji, S. Lu, A. Buekens and J. Yan (2014). "Removal of gaseous HxCBz by gliding arc plasma in combination with a catalyst." Chemosphere **117**: 730-736.

Shih, Y.-h., C.-y. Hsu and Y.-f. Su (2010). "Reduction of hexachlorobenzene by nanoscale zero-valent iron: Kinetics, pH effect, and degradation mechanism." Sep. Purif. Technol. **76**(3): 268-274.

Solanki, J. N. and Z. V. P. Murthy (2011). "Reduction of 4-Chlorophenol by Mg and Mg-Ag Bimetallic Nanocatalysts." Ind. Eng. Chem. Res. **50**(24): 14211-14216.

Su, G., Y. Liu, L. Huang, H. Lu, S. Liu, L. Li and M. Zheng (2014). "Synthesis of hierarchical Mg-doped Fe3O4 micro/nano materials for the decomposition of hexachlorobenzene." Chemosphere **99**: 216-223.

Su, G., Y. Liu, L. Huang, Y. Shi, A. Zhang, L. Zhang, W. Liu, L. Gao and M. Zheng (2013). "Synergetic effect of alkaline earth metal oxides and iron oxides on the degradation of hexachlorobenzene and its degradation pathway." Chemosphere **90**(1): 103-111.

Su, Y.-f., C.-Y. Hsu and Y.-h. Shih (2012). "Effects of various ions on the dechlorination kinetics of hexachlorobenzene by nanoscale zero-valent iron." Chemosphere **88**(11): 1346-1352.

Torres, L. G., M. Hernandez, Y. Pica, V. Albiter and E. R. Bandala (2010). "Degradation of di-, tri-, tetra-, and pentachlorophenol mixtures in an aerobic biofilter." Afr. J. Biotechnol. **9**(23): 3396-3403.

Trapido, M., A. Hirvonen, Y. Veressinina, J. Hentunen and R. Munter (1997). "Ozonation, ozone/UV and UV/H2O2 degradation of chlorophenols." Ozone: Sci. Eng. **19**(1): 75-96.

Vorkamp, K. and F. F. Riget (2014). "A review of new and current-use contaminants in the Arctic environment: Evidence of long-range transport and indications of bioaccumulation." Chemosphere **111**: 379-395.

Wang, G.-W. (2013). "Mechanochemical organic synthesis." Chem. Soc. Rev. **42**(18): 7668-7700.

Watanabe, K. and H. Yoshikawa (2008). "Enrichment and isolation of anaerobic microorganisms concerned with reductive degradation of hexachlorobenzene from soils." J. Pestic. Sci. (Tokyo, Jpn.) **33**(2): 166-170.

Wu, Q., C. E. Milliken, G. P. Meier, J. E. M. Watts, K. R. Sowers and H. D. May (2002). "Dechlorination of Chlorobenzenes by a Culture Containing Bacterium DF-1, a PCB Dechlorinating Microorganism." Environ. Sci. Technol. **36**(15): 3290-3294.

Xiao, Y. and J. Jiang (2014). "Base-catalyzed decomposition of hexachlorobenzene: effect on dechlorination efficiency of different hydrogen donors, alkalis and catalysts." RSC Adv. **4**(30): 15713-15719.

Xiao, Y., J. Jiang, Y. Yang and G. Gao (2011). "Base-catalyzed destruction of hexachlorobenzene with zero-valent iron." Chem. Eng. J. (Amsterdam, Neth.) **173**(2): 415-421.

Yamada, S., Y. Naito, M. Takada, S. Nakai and M. Hosomi (2008). "Photodegradation of hexachlorobenzene and theoretical prediction of its degradation pathways using quantum chemical calculation." Chemosphere **70**(4): 731-736.

Yan, D.-Z., L.-Q. Mao, C.-Z. Li and J. Liu (2015). "Biodegradation of hexachlorobenzene by a constructed microbial consortium." World J. Microbiol. Biotechnol. **31**(2): 371-377.

Yin, H., Y. Wada, T. Kitamura and S. Yanagida (2001). "Photoreductive Dehalogenation of Halogenated Benzene Derivatives Using ZnS or CdS Nanocrystallites as Photocatalysts." Environ. Sci. Technol. **35**(1): 227-231.

Yin, K., X. Gao, Y. Sun, L. Zheng and W. Wang (2013). "Thermal degradation of hexachlorobenzene in the presence of calcium oxide at 340-400 °C." Chemosphere **93**(8): 1600-1606.

Yuan, J. H., T. J. Goehl, E. Murrill, R. Moore, J. Clark, L. Hong and R. Irwin (1993). "Toxicokinetics of pentachloroanisole in F344 rats and B6C3F1 mice." Xenobiotica **23**(4): 427-438.

Zacheis, G. A., K. A. Gray and P. V. Kamat (1999). "Radiation-Induced Catalysis on Oxide Surfaces: Degradation of Hexachlorobenzene on γ-Irradiated Alumina Nanoparticles." J. Phys. Chem. B **103**(12): 2142-2150.

Zacheis, G. A., K. A. Gray and P. V. Kamat (2000). "Radiolytic Reduction of Hexachlorobenzene in Surfactant Solutions: A Steady-State and Pulse Radiolysis Study." Environ. Sci. Technol. **34**(16): 3401-3407.

Zhang, J., Z. Zheng, J. Luan, G. Yang, W. Song, Y. Zhong and Z. Xie (2007). "Degradation of hexachlorobenzene by electron beam irradiation." J. Hazard. Mater. **142**(1-2): 431-436.

Zhang, W., H. Wang, H. Jun, M. Yu, F. Wang, L. Zhou and G. Yu (2014). "Acceleration and mechanistic studies of the mechanochemical dechlorination of HCB with iron powder and quartz sand." Chem. Eng. J. (Amsterdam, Neth.) **239**: 185-191.

Zheng, Z., S. Yuan, Y. Liu, X. Lu, J. Wan, X. Wu and J. Chen (2009). "Reductive dechlorination of hexachlorobenzene by Cu/Fe bimetal in the presence of nonionic surfactant." J. Hazard. Mater. **170**(2-3): 895-901.

Zhu, N., H. Luan, S. Yuan, J. Chen, X. Wu and L. Wang (2010). "Effective dechlorination of HCB by nanoscale Cu/Fe particles." J. Hazard. Mater. **176**(1-3): 1101-1105.

Zuin, V. G., F. P. Da Silva Airoldi, N. R. Do Nascimento, M. D. Landgraf and M. O. d. O. Rezende (1999). "Determination of pentachlorophenol and hexachlorobenzene in natural waters affected by industrial chemical residues." J. Braz. Chem. Soc. **10**(1): 25-30.